1-37A

Copy No. _____

Guide for Mechanistic-Empirical Design

OF NEW AND REHABILITATED PAVEMENT STRUCTURES

FINAL REPORT

PART 3. DESIGN ANALYSIS

CHAPTER 3. DESIGN OF NEW AND RECONSTRUCTED FLEXIBLE PAVEMENTS

NCHRP

Prepared for
National Cooperative Highway Research Program
Transportation Research Board
National Research Council

Submitted by
ARA, Inc., ERES Consultants Division
505 West University Avenue
Champaign, Illinois 61820

March 2004

ACKNOWLEDGMENT OF SPONSORSHIP

This work was sponsored by the American Association of State Highway and Transportation Officials, in cooperation with the Federal Highway Administration, and was conducted in the National Cooperative Highway Research Program, which is administered by the Transportation Research Board of the National Research Council.

PART 3—DESIGN ANALYSIS

CHAPTER 3
DESIGN OF NEW AND RECONSTRUCTED FLEXIBLE PAVEMENTS

3.3.1 INTRODUCTION

This chapter describes the mechanistic-empirical design procedures for new and reconstructed flexible pavements. For the purposes of this guide, new and reconstructed flexible pavements are defined as pavement systems having asphalt concrete surfaces. These include the following:

- Conventional flexible pavements—i.e., thin hot-mix asphalt (HMA) layer over granular base/subbase materials.
- Deep strength HMA pavements—i.e., thick HMA layers over granular layers.
- Full-depth HMA pavements—i.e., sections consisting only of HMA layers (HMA surface and HMA stabilized bases).
- "Semi-rigid" pavements—i.e., sections having some type of a chemically stabilized layer as a base layer below the HMA layer.

The allowable pavement cross sections include both conventional layering (decreasing material quality with depth) and sandwich structures (unbound aggregate layer placed between two stabilized layers).

The procedures described in this chapter are most applicable when designing pavements constructed with conventional dense-graded HMA mixtures. The performance models developed are valid for pavement constructed with such mixtures. For flexible pavements constructed with materials such as stone matrix asphalt (SMA) mixtures, polymer modified asphalt (PMA) mixtures, and asphalt mixtures containing recycled asphalt pavement (RAP) materials, the tools described in this chapter could also be used but primarily in the analysis mode in conjunction with level 1 mixture related inputs. Caution should be exercised when drawing design related inferences because the calibrated performance equations included as part of the design guide did not include a significant percentage of pavements sections with such mixtures. Generally speaking, the methodology described in the design guide is applicable for modified mixtures. However, a more comprehensive dataset will be eventually required to develop the necessary calibrated performance models for use in design.

The mechanistic-empirical design of new and reconstructed flexible pavements requires an iterative hands-on approach by the designer. The designer must select a trial design and then analyze the design in detail to determine if it meets the performance criteria established by the designer. The flexible pavement performance measures considered in this guide include permanent deformation (rutting), fatigue cracking (both bottom-up and top-down), thermal cracking, and smoothness (International Roughness Index or IRI). If the trial design does not satisfy the performance criteria, the design is modified and

reanalyzed until the design does satisfy all criteria. The designs that meet the applicable performance criteria are then considered feasible from a structural and functional viewpoint and can be further considered for other evaluations such as life cycle cost analysis.

This chapter provides a detailed description of the design procedure for flexible pavement systems. The contents of this chapter are as follows:

1. Introduction (section 3.3.1).
2. An overview of the design procedure (section 3.3.2).
3. Design inputs for new flexible pavement design (section 3.3.3).
4. Flexible pavement design procedure (section 3.3.4).
5. Special loading considerations (section 3.3.5)
6. Calibration to local conditions (section 3.3.6).

The procedures described in this chapter can be used for design of flexible pavements on new alignments or for reconstruction of existing pavements. There are no fundamental differences in the way pavements are designed for new alignment or reconstruction. However, one practical aspect is that for reconstruction, the potential usage of the materials from the existing pavement structure is an important issue that should be considered. The effects of using the materials recycled from the existing pavement structure in various modified layers of the new pavement can be evaluated using the procedures described in this Guide.

3.3.2 OVERVIEW OF FLEXIBLE PAVEMENT DESIGN PROCESS

The overall iterative design process for asphalt pavements is illustrated in figure 3.3.1. The term “asphalt pavement” refers to any new, reconstructed, or rehabilitated pavement system that has asphalt concrete as the surface layer. The main steps in the design process include the following:

1. Assemble a trial design for specific site conditions—define subgrade support, asphalt concrete and other paving material properties, traffic loads, climate, pavement type and design and construction features.
2. Establish criteria for acceptable pavement performance at the end of the design period (i.e., acceptable levels of rutting, fatigue cracking, thermal cracking, and IRI).
3. Select the desired level of reliability for each of the applicable performance indicators (e.g., select reliability levels for rutting, cracking, and IRI).
4. Process input to obtain monthly values of traffic inputs and seasonal variations of material and climatic inputs needed in the design evaluations for the entire design period.
5. Compute structural responses (stresses and strains) using multilayer elastic theory or finite element based pavement response models for each axle type and load and for each damage-calculation increment throughout the design period.

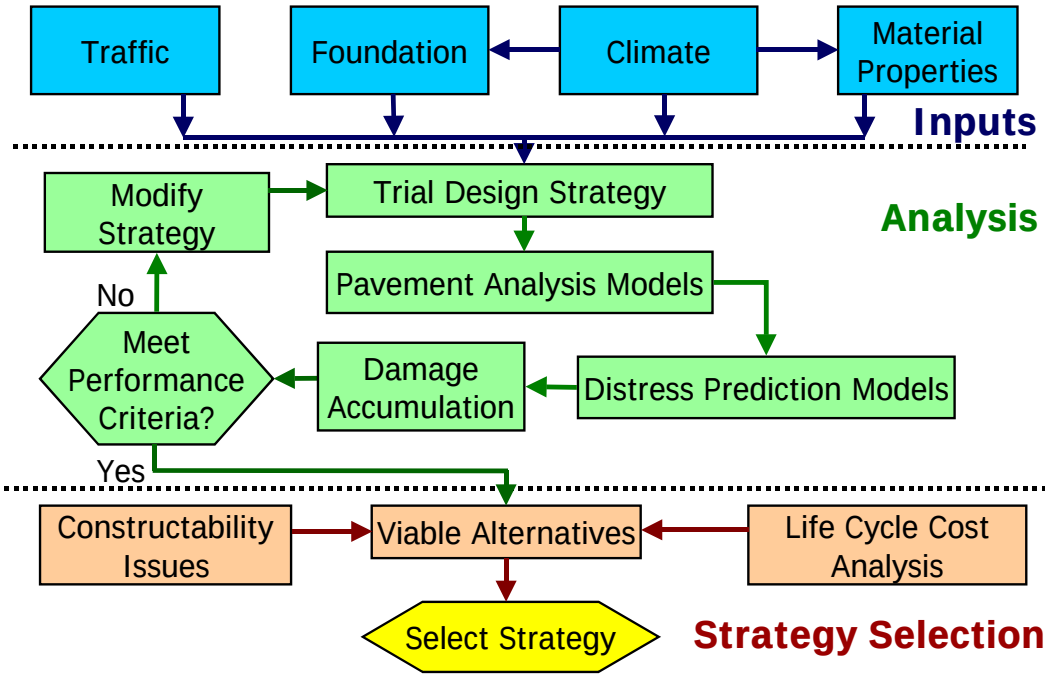

Figure 3.3.1. Overall design process for flexible pavements.

6. Calculate accumulated distress and/or damage at the end of each analysis period for the entire design period.
7. Predict key distresses (rutting, bottom-up/top-down fatigue cracking, thermal cracking) at the end of each analysis period throughout the design life using the calibrated mechanistic-empirical performance models provided in the Guide.
8. Predict smoothness (IRI) as a function of initial IRI, distresses that accumulate over time, and site factors at the end of each analysis increment.
9. Evaluate the expected performance of the trial design at the given reliability level.
10. If the trial design does not meet the performance criteria, modify the design and repeat the steps 4 through 9 above until the design does meet the criteria.

Guidelines on the design process are provided in section 3.3.4. The designs that satisfy performance criteria are considered feasible from a structural and functional viewpoint and can be further considered for other evaluations, such as life cycle cost analysis.

3.3.2.1 Design Inputs

Trial Design Inputs and Site Conditions

The design procedure offers the capability to consider a wide range of structural sections as illustrated in figure 3.3.2. An acceptable design is determined by iteratively analyzing and modifying trial designs until all performance criteria (e.g., rutting, fatigue cracking, thermal cracking, IRI) are satisfied over the analysis period. A trial design includes all details needed to perform design evaluations using the procedures prescribed in this Guide.

Figure 3.3.2. Illustration of possible asphalt pavement layered systems.

In addition to the trial design, the designer must provide inputs for the project site conditions including subgrade properties (including presence of bedrock), traffic, and climatic data. There are also several design inputs related to construction such as the initial smoothness (initial IRI), estimated month of construction, and estimated month that the pavement will be opened to traffic.

A major difficulty in obtaining adequate design inputs is that the desired project specific information is not generally available at the design stage and must often be estimated several years in advance of construction. The actual materials used in a project may not

even be known until a few weeks before construction begins. The designer should obtain as much data as possible on in situ material properties, traffic, and other inputs for use in design to obtain a realistic design. The designers should also conduct a sensitivity analysis to identify key factors that affect pavement performance. Based on sensitivity analysis results, provisions could be made in the contract documents for stringent control of the quality of key material properties (e.g., asphalt concrete stiffness), or the design could be modified to make the pavement performance less sensitive to the input in question.

Design Input Levels

For many of the design inputs, the designer can choose from multiple (generally three) levels of data quality. These are briefly identified below:

1. Level 1—site and/or material specific inputs for the project obtained through direct testing or measurements. Examples of Level 1 data include material properties obtained through laboratory testing and measured traffic volumes and weights at the project site.
2. Level 2—the use of correlations to establish or determine the required inputs. Examples of Level 2 data include the resilient modulus of the subgrade or unbound base materials estimated from CBR or R-values using empirical correlations.
3. Level 3—the use of national or regional default values to define the inputs. Examples of Level 3 input include the use of AASHTO soil classifications to determine a typical resilient modulus value or the use of roadway type and truck type classifications to determine normalized axle weight and truck type distributions.

The input levels can vary from input parameter to input parameter. For example, subgrade resilient modulus can be obtained from a lab test (Level 1) and traffic axle load distribution from regional data (Level 3). The input level selection for a specific parameter depends on several factors, including the following:

- Sensitivity of the pavement performance to a given input.
- The criticality of the project.
- The information available at the time of design.
- The resources and time available to the designer to obtain the inputs.

The input levels are described in PART 2 of this Guide. The level chosen for each input parameter, however, may have a significant effect on project design, costs, and reliability. Sensitivity analysis can be used to determine which parameters should be determined more precisely for a given project.

Processing of Inputs over Design Analysis Period

The raw design inputs have to be processed to obtain seasonal values of the traffic, material, and climatic inputs needed for each analysis increment in the design evaluations. Incremental analysis periods are typically on the order of two weeks for

flexible pavements. Analysis inputs that are required on a seasonal basis consist of the following:

- Average daily number of single, tandem, tridem, and quad axles in each axle weight category for each month.
- Temperatures within the asphalt layer. Average temperature values for the analysis period are used to determine the temperature-dependent asphalt stiffness for rutting and fatigue cracking predictions. Hourly temperature values are needed for thermal cracking prediction. A minimum of 1 year's weather station data is required.
- Average moduli values of all unbound layers (base, subbase, subgrade) for each analysis period.

PART 2, Chapter 4 describes the details of traffic calculation. Temperature and moisture profiles in the various pavement layers can be obtained using the Enhanced Integrated Climatic Model (EICM), which is a part of the Design Guide software and is described in PART 2, Chapter 3 and Appendix DD.

The major material types for flexible pavement design include hot-mix asphalt, asphalt stabilized base, cement stabilized base, other chemically treated materials (e.g., lime-flyash, soil cement, lime-stabilized soils, etc.), unbound aggregate base/subbase, and subgrade soils. PART 2, Chapter 2 describes the materials inputs in detail. PART 2, Chapter 3 describes how each of these materials is affected by seasonally changing temperature and moisture conditions.

Long-term aging and the corresponding change in asphalt concrete stiffness near the surface of the pavement are considered in the flexible design procedure. The asphalt aging model is described in PART 2, Chapter 2 and Appendix CC.

The seasonal input processing is automated in the Design Guide software, and the processed inputs feed directly into the structural response calculation modules that compute critical pavement responses on a period-by-period basis over the entire design period.

3.3.2.2 Pavement Response Models

The purpose of the flexible pavement response model is to determine the structural response of the pavement system due to traffic loads and environmental influences. Environmental influences may be direct (e.g., strains due to thermal expansion and/or contraction) or indirect via effects on material properties (e.g., changes in stiffness due to temperature and/or moisture effects).

The outputs from the pavement response model are the stresses, strains, and displacements within the pavement layers. Of particular interest are the critical response variables required as inputs to the pavement distress models in the mechanistic-empirical design procedure. Examples of critical pavement response variables include:

- Tensile horizontal strain at the bottom/top of the HMA layer (for HMA fatigue cracking)
- Compressive vertical stresses/strains within the HMA layer (for HMA rutting)
- Compressive vertical stresses/strains within the base/subbase layers (for rutting of unbound layers)
- Compressive vertical stresses/strains at the top of the subgrade (for subgrade rutting)

Each pavement response variable must be evaluated at the critical location within the pavement layer where the parameter is at its most extreme value. For a single wheel loading, the critical location can usually be determined by inspection. For example, the critical location for the tensile horizontal strain at the bottom of the HMA layer under a single wheel load is directly beneath the center of the wheel. For multiple wheels and/or axles, the critical location will be a function of the wheel load configuration and the pavement structure. Mixed traffic conditions (single plus multiple wheel/axle vehicle types) further complicates the problem, as the critical location within the pavement structure will not generally be the same over all vehicle types. The pavement response model must search for the critical location for each response parameter in these cases.

Two flexible pavement analysis methods have been implemented in the Design Guide. For cases in which all materials in the pavement structure can realistically be treated as linearly elastic, multilayer elastic theory is used to determine the pavement response. Multilayer elastic theory provides an excellent combination of analysis features, theoretical rigor, and computational speed for linear pavement analyses. In cases where the unbound material nonlinearity is also considered, a nonlinear finite element procedure is used instead for determining the pavement stresses, strains, and displacements. However, caution should be exercised when using the nonlinear finite element code provided with the guide software for routine design. This pavement structural response calculation methods is intended to be used primarily for research purposes. None of the procedures developed and discussed in this guide have been validated or calibrated with this structural response analysis method. Further research will be needed to fully implement nonlinear finite element methods for routine pavement design.

3.3.2.3 Incremental Distress and Damage Accumulation

The trial design is analyzed for adequacy by dividing the target design life into shorter design analysis periods or increments beginning with the traffic opening month. Within each increment (each analysis period), all factors that affect pavement responses and damage are held constant. These include:

- Traffic levels.
- Asphalt concrete modulus.
- Base and subbase moduli.
- Subgrade modulus.

Critical stress and/or strain values for each distress type are determined for each analysis increment. These critical stress and/or strain values are converted to incremental distresses, either in absolute terms (e.g., incremental rut depth) for in terms of a damage index (e.g., fatigue cracking). Incremental distresses and/or damage are summed over all increments and output at the end of each analysis period by the Design Guide software.

3.3.2.4 Distress Prediction

The cumulative distress calculated and accumulated as described in section 3.4.2.3 forms the basis for evaluating the structural adequacy of trial designs formulated. A variety of structural distresses are considered in flexible pavement design and analysis. These include:

- Bottom-up fatigue (or alligator) cracking.
- Surface-down fatigue (or longitudinal) cracking.
- Fatigue in chemically stabilized layers (only considered in semi-rigid pavements).
- Permanent deformation (or rutting).
- Thermal cracking.

Rutting distress is predicted in absolute terms. Therefore the incremental distress computed for each analysis period can be directly accumulated over the entire target design life for the pavement.

Cracking distress (bottom-up/surface-down fatigue cracking, thermal cracking) is predicted in terms of a damage index, which is a mechanistic parameter representing the load associated damage within the pavement structure. When "damage" is very small (e.g., 0.0001) the pavement structure would not be expected to exhibit significant cracking. As computed "damage" increases, visible cracking can be expected to develop in a few locations along the project. The incremental damage is accumulated for each analysis period using Miner's law. The cumulative damage is converted to physical cracking using calibrated models that relate the calculated damage to observable distresses. Calibrated distress prediction models were developed using the LTPP database and other long-term pavement performance data obtained for a wide range of flexible pavement structures located in a variety of climatic conditions and subject to various traffic and environmental loading situations.

More detailed definitions of the various flexible pavement distresses considered in the design guide are presented below.

<u>Bottom-up Fatigue Cracking or Alligator Cracking</u>

This type of fatigue cracking first shows up as short longitudinal cracks in the wheel path that quickly spread and become interconnected to form a chicken wire/alligator cracking pattern. These cracks initiate at the bottom of the HMA layer and propagate to the surface under repeated load applications.

This type of fatigue cracking is a result of the repeated bending of the HMA layer under traffic. Basically, the pavement and HMA layer deflects under wheel loads that result in tensile strains and stresses at the bottom of the layer. With continued bending, the tensile stresses and strains cause cracks to initiate at the bottom of the layer and then propagate to the surface. This mechanism is illustrated in figure 3.3.3 (*1*). The following briefly lists some of the reasons for higher tensile strains and stresses to occur at the bottom of the HMA layer (*1*).

- Relatively thin or weak HMA layers for the magnitude and repetitions of the wheel loads.
- Higher wheel loads and higher tire pressures.
- Soft spots or areas in unbound aggregate base materials or in the subgrade soil.
- Weak aggregate base/subbase layers caused by inadequate compaction or increases in moisture contents and/or extremely high ground water table (GWT).

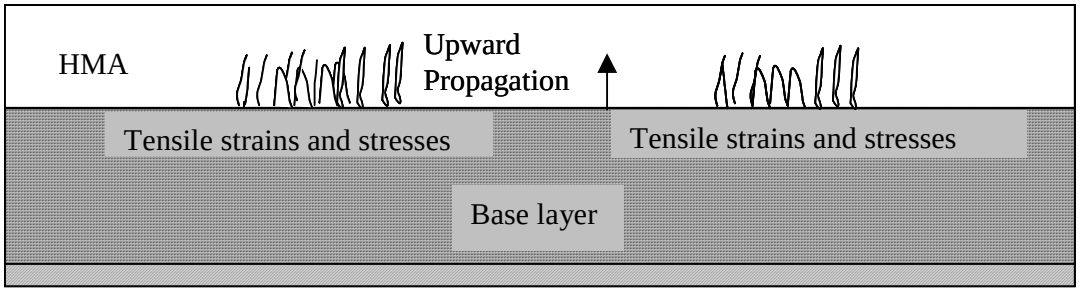

Figure 3.3.3. Bottom-up fatigue cracking.

Surface-down Fatigue Cracking or Longitudinal Cracking

Most fatigue cracks initiate at the bottom of the HMA layer and propagate upward to the surface of the pavement. However, there is increasing evidence that suggests load-related cracks do initiate at the surface and propagate downward. There are various opinions on the mechanisms that cause these types of cracks, but there are no conclusive data to suggest that one is more applicable than the other. Some of the suggested mechanisms are:

- Wheel load induced tensile stresses and strains and strains that occur at the surface and cause cracks to initiate and propagate in tension. Aging of the HMA surface mixture accelerates this crack initiation-propagation process.
- Shearing of the HMA surface mixture caused from radial tires with high contact pressures near the edge of the tire. This leads to cracks to initiate and propagate both in shear and tension.
- Severe aging of the HMA mixture near the surface resulting in high stiffness and when combined with high contact pressures, adjacent to the tire loads, cause the cracks to initiate and propagate.

The downward fatigue cracking mechanism is illustrated in figure 3.3.4. In the approach described in the design guide a preliminary surface-down cracking model has been

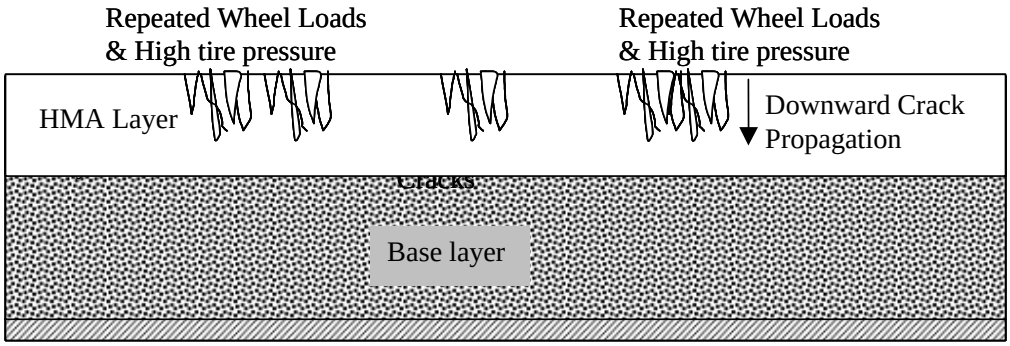

Figure 3.3.4. Top-down fatigue cracking.

incorporated that considers high tensile strains due to load-related effects and the effects of age-hardening of asphalt materials. This theoretical methodology has been calibrated to field longitudinal cracking data (see Appendix II for details).

Permanent Deformation or Rutting

Rutting is a surface depression in the wheel paths caused by inelastic or plastic deformations in any or all of the pavement layers and subgrade (*1*). These plastic deformations are typically the result of: 1) densification or one-dimensional compression and consolidation and 2) lateral movements or plastic flow of materials (HMA, aggregate base, and subgrade soils) from wheel loads. The more severe premature distortion and rutting failures are related to lateral flow and/or inadequate shear strength any pavement layer, rather than one-dimensional densification. Rutting is categorized into two types as defined below.

- *One-dimensional densification or vertical compression.* A rut depth caused by material densification is a depression near the center of the wheel path without an accompanying hump on either side of the depression, as illustrated in figure 3.3.5a. Densification of materials is generally caused by excessive air voids or inadequate compaction for any of the bound or unbound pavement layers. This allows the mat or underlying layers to compact when subjected to traffic loads. This type of rut depth usually results in a low to moderate severity level of rutting (*1*).
- *Lateral flow or plastic movement.* A rut depth caused by the lateral flow (downward and upward) of material is a depression near the center of the wheel path with shear upheavals on either side of the depression, as illustrated in Figure 3-3.5b. This type of rut depth usually results in a moderate to high severity level of rutting. Lateral flow or the plastic movement of materials will occur in those mixtures with inadequate shear strength and/or large shear stress states due to the traffic loads on the specific pavement cross-section used. Over-densification of the HMA layer by heavy wheel loads can also result in bleeding or flushing in the pavement surface. This type of rutting is the most difficult to predict and measure in the laboratory (*1*).

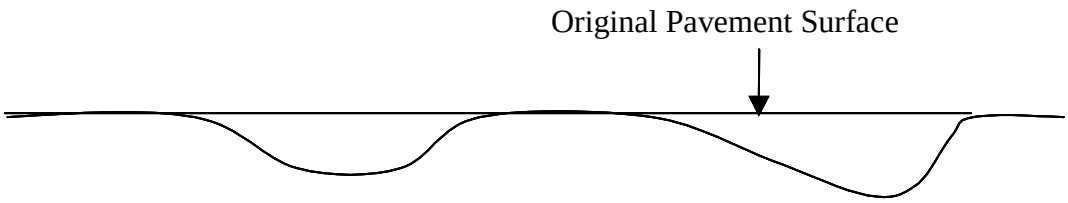

a. One-Dimensional Densification or vertical compression.

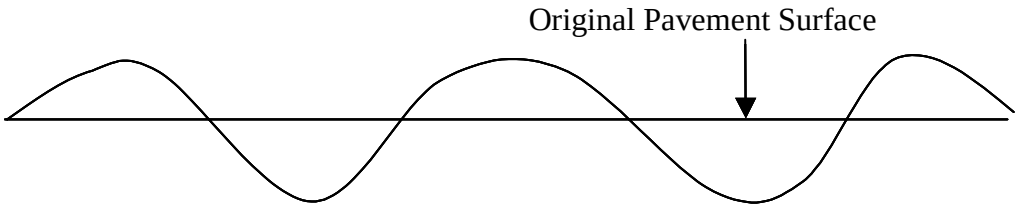

b. Lateral Displacement or Two-Dimensional Plastic Movement

Figure 3.3.5. Types and mechanisms of rutting in flexible pavements (view of transverse profile).

Thermal Cracking

Cracking in flexible pavements due to cold temperatures or temperature cycling is commonly referred to as thermal cracks. Thermal cracks typically appear as transverse cracks on the pavement surface roughly perpendicular to the pavement centerline. These cracks can be caused by shrinkage of the HMA surface due to low temperatures, hardening of the asphalt, and/or daily temperature cycles (*1*).

Cracks that result from the coldest in temperature are referred to as low temperature cracking. Cracking that result from thermal cycling is generally referred to as thermal fatigue cracking. Low temperature cracking is associated with regions of extreme cold whereas thermal fatigue cracking is associated with regions that experience large extremes in daily and seasonal temperatures (*1*).

There are two types of non-load related thermal cracks: transverse cracking and block cracking. Transverse cracks usually occur first and are followed by the occurrence of block cracking as the asphalt ages and becomes more brittle with time. Transverse cracking is the type that is predicted by models in this design guide, while block cracking is handled by material and construction variables (*1*).

Fatigue Fracture in Chemically Stabilized Layers

Apart from the consideration of distresses such as fatigue cracking, permanent deformation, and thermal cracking; an additional distress that needs to be considered in semi-rigid pavements is fatigue fracture in the underlying chemically stabilized base

layers. For the purposes of this guide, chemically stabilized layers are high quality base materials that are treated with materials such as cement, flyash, or lime-flyash. Under repeated applications of loading, microcracks form in these layers leading to a stiffness or modulus reduction and ultimately to fatigue fracture. This process will also have a significant impact on the distress progression in the overlying HMA layers. A good mixture design, structural design, and construction practices need to be followed to minimize fatigue fracture in the chemically stabilized layers.

An important point to note here is that although lime-stabilized subgrades fall within the category of chemically stabilized layers (see PART 2, Chapter 2 for the types of materials that fall under this category), the consideration of fatigue fracture of these layers is optional in the Design Guide procedure. Consequently, additional materials inputs required to characterize these layers for fatigue fracture analysis may not be warranted for certain situations. This is particularly true when these and other relatively weaker chemically stabilized layers are deeper within the pavement structure, i.e., under other base and subbase layers. However, in situations where these layers are higher up in the structure and are expected to carry flexural stresses imposed by the traffic, e.g., low-volume road situations, it may be more important to consider fatigue fracture. However, in all cases, the contribution of these layers in enhancing the pavement performance due to superior stiffness characteristics over in-place natural soils is fully considered in the structural response calculations and performance prediction.

3.3.2.5 Smoothness (IRI) Prediction

The IRI over the design period depends upon the initial as-constructed profile of the pavement from which the initial IRI is computed and upon the subsequent development of distresses over time. These distresses include rutting, bottom-up/top-down fatigue cracking, and thermal cracking for flexible pavements. The IRI model uses the distresses predicted using the models included in this Guide, initial IRI, and site factors to predict smoothness over time. The site factors include subgrade and climatic factors to account for the roughness caused by shrinking or swelling soils and frost heave conditions. IRI is estimated incrementally over the entire design period.

3.3.2.6 Assessment of Performance and Design Modifications

The feasible designs are obtained iteratively in a mechanistic design procedure. The process involves the following steps:

1. Establish performance criteria (e.g., level of rutting, cracking, and smoothness at the end of the design life and the desired level of reliability for each).
2. Assemble a trial design.
3. Predict performance over the design life.
4. Evaluate the predicted performance against the design requirements.
5. If the design criteria are not satisfied, revise design and repeat steps 3 and 4 until the design does satisfy the performance requirements.

3.3.2.7 Design Reliability

A large amount of uncertainty and variability exists in pavement design and construction, as well as in the application of traffic loads and climatic factors over the design life. In the mechanistic-empirical design, the key outputs of interest are the individual distress quantities (e.g., rutting, fatigue cracking, and thermal cracking for flexible pavements). Therefore, the predicted distress is the random variable of interest in reliability design. Quantification of the distribution this variable assumes for all possible estimates of the mean and its associated moments is of interest for reliability estimation. In this Guide, the variability associated with the predicted distress quantity is estimated based on calibration results, after a careful analysis of the differences between the predicted versus actual distresses in the field. For design purposes, the design reliability is established based on knowledge of variation of a given performance around the mean prediction.

Design reliability for the individual pavement distress models (i.e., rutting, bottom-up cracking, top-down cracking, and thermal cracking) are based on the standard error of the estimates of each individual model obtained through the calibration process. These estimates of error include a combined input variability, variability in the construction process, and model or pure error.

The desired level of reliability is specified along with the acceptable level of distress at the end of design life in defining the performance requirements for a pavement design in this Guide. For example, one criterion might be to limit rut depth to 25 mm at a design reliability of 90 percent. Thus, if a designer designed 100 projects, 90 of these projects would exhibit rut depths less than 25 mm at the end of the design life. Different reliability levels may be specified for different distresses in the same design. For example, the designer may choose to specify 95 percent reliability for rutting but 90 percent reliability for thermal cracking and IRI. Of course, the higher the design reliability for a given distress, the higher the initial cost of the pavement; however, the future maintenance cost would be lower for the higher-reliability design.

3.3.2.8 Life Cycle Costs Estimation

After a trial design has passed the structural (distress) and functional (smoothness) requirements, it becomes a technically feasible design alternative. At this point, the pavement can be analyzed for its life cycle costs for comparison with other feasible designs. A general procedure for life cycle costing is provided in Appendix C of this Guide. The predicted distress and IRI of the feasible design alternatives can be used in estimating the mean lives of the design alternatives and their standard deviations, along with a designer-defined maintenance and rehabilitation policy, in conducting a life cycle cost analysis.

3.3.3 INPUTS FOR NEW FLEXIBLE PAVEMENT DESIGN

Input data used for the design of new flexible pavements presented in this chapter are categorized as follows:

- General information.
- Site/Project identification.
- Analysis parameters.
- Traffic.
- Climate.
- Drainage and surface properties.
- Pavement Structure

Several of these inputs, e.g., traffic, climate, etc., are identical to those used for rigid pavement design discussed in PART 3, Chapter 4. However, there are variations in how some these inputs are processed for use in flexible pavement design. The focus of this section is to summarize all the inputs required for the design of flexible pavements using this Guide with appropriate commentary on how they relate to the design process.

Detailed descriptions for several of these inputs were presented in previous chapters of the Guide as indicated below:

- PART 2 – Design Inputs, Chapter 1: Subgrade/Foundation Design Inputs.
- PART 2 – Design Inputs, Chapter 2: Material Characterization.
- PART 2 – Design Inputs, Chapter 3: Environmental Effects.
- PART 2 – Design Inputs, Chapter 4: Traffic.
- PART 3 – Design Analysis, Chapter 1: Drainage.

These chapters should be consulted for more detailed guidelines on the applicable inputs.

3.3.3.1 General Information

The following inputs define the analysis period and type:

- Design life – expected pavement design life (years).
- Base/Subgrade Construction Month – the approximate month in which the base and subgrade are anticipated to be constructed. This input establishes the time t = 0 for the climatic model (see PART 2, Chapter 3 for details). The moisture regime within the unbound layers and subgrade is assumed to be at optimum (see PART 2, Chapter 3) at this time. The progression from optimum moisture to equilibrium moisture starts from this time onward. If this input is completely unknown, the designer should use the month in which most pavement construction will occur in the area.
- Pavement (HMA) construction month – this input defines the time t = 0 for the HMA material aging model (described in PART 2, Chapter 2) and the thermal cracking model (described in a later section of this chapter). If this input is completely unknown, the designer could use the month in which most pavement construction occurs in the area.
- Traffic opening month – the expected month in which the pavement will be opened to traffic. This value defines the climatic conditions at the time of opening to traffic, which affects the temperature and moisture gradients as well as

the layer moduli values, including subgrade. The analysis begins with the month entered (i.e., first day of month is assumed). This input establishes time t = 0 for incremental damage and incremental distress calculations. If this input is completely unknown, the designer should use the month in which most pavement construction was completed at the site.

- Pavement type – Flexible. This input determines the method of design evaluations and the applicable performance models.

3.3.3.2 Site/Project Identification

This group of inputs includes the following:

- Project location.
- Project identification – Project ID, Section ID, begin and end mile posts, and traffic direction
- Functional class of the pavement being designed. The choices under this option include the following:
  - Principal Arterial – Interstate and defense routes.
  - Principal Arterials – others.
  - Minor Arterials.
  - Major Collectors.
  - Minor Collectors.
  - Local Routes and Streets.

The project location defines the climatic conditions for the pavement design. The functional class influences the default design criteria (acceptable level of distress and reliability), helps determine the default (Level 3) vehicle class distribution (see discussion in PART 2, Chapter 4 for more details), and also aids in the selection of the vehicle operating speed input.

3.3.3.3 Analysis Parameters

Initial IRI

The initial IRI defines the as-constructed smoothness of the pavement. This parameter is highly dependent on the project smoothness specifications and has a significant impact on the long-term ride quality of the pavement. Typical values range from 50 to 100 in/mi.

Performance Criteria

The flexible design is based on surface-down and bottom-up fatigue cracking of the asphalt surface, HMA thermal cracking, fatigue cracking in chemically stabilized layers, permanent deformation for both the asphalt layers and the total pavement, and pavement smoothness (IRI). The designer may select some or all of these performance indicators and establish criteria to evaluate a design and make modifications if necessary. The performance criteria for each distress will depend on the individual highway agency's

tolerance for the amount of cracking over the design period. The performance criteria will also depend upon the design reliability level, which in turn will be dependent upon the functional class of the roadway. For example, specifying a high reliability level consistent with an Interstate highway design and a low allowable distress level will result in a very conservative design.

Surface-Down Fatigue Cracking

Surface-down fatigue cracking is manifested as longitudinal cracking at the edge of the wheel paths. Surface-down cracking permits water infiltration into the underlying pavement layers that can cause structural failure of the pavement. Surface-down cracking also contributes to a loss of smoothness.

The performance criterion for surface-down fatigue cracking is defined as the maximum allowable length of longitudinal cracking per mile of pavement that is permitted to occur over the design period. Typical values of allowable surface-down fatigue cracking are on the order of 1000 ft per mile of pavement.

Note that although the calibration of the surface-down fatigue-cracking model was done on the basis of data obtained from 500-foot sections, the results are extrapolated and reported on a per mile basis.

Bottom-Up Fatigue Cracking

Classical bottom-up fatigue cracking is manifested as alligator cracking within the wheel paths. Bottom-up cracking permits water infiltration into the underlying pavement layers that can cause structural failure of the pavement. Bottom-up cracking also contributes directly to a loss of smoothness. Inadequate design to control bottom-up cracking can result in the premature failure of flexible pavements. Latter sections of this chapter discuss the factors affecting this distress mode in more detail.

The performance criterion for bottom-up fatigue cracking is defined as the maximum area of alligator cracking expressed as a percentage of the total lane area that is permitted to occur over the design period. Typical values of allowable bottom-up fatigue cracking are on the order of 25 to 50 percent of the total lane area.

Thermal Cracking

Thermal cracking appears as regularly spaced transverse cracks across the complete pavement surface. Thermal cracking is environmentally induced by sharp and rapid drops in pavement temperature that cause extreme thermal contraction and fracture of the asphalt surface. Thermal cracking permits water infiltration into the underlying pavement layers that can cause structural failure of the pavement. Thermal cracking also contributes directly to a loss of smoothness.

The performance criterion for thermal cracking is defined as the maximum length of transverse cracking per mile of pavement that is permitted to occur over the design

period. Typical values of allowable thermal cracking are on the order of 1000 ft per mile of pavement.

Note that although the calibration of the thermal fatigue cracking model was done on the basis of data obtained from 500-foot sections, the results are extrapolated and reported on a per mile basis.

Fatigue Fracture of Chemically Stabilized Layers

Fatigue cracking in underlying chemically stabilized layers (see PART 2, Chapter 2 the types of materials considered in this category) reduces the support provided to the upper pavement layers. This will accelerate the manifestation of surface distresses, especially surface-down and bottom-up fatigue fracture in the asphalt surface layers. This will lead to a loss of smoothness and can lead to premature failure of the pavement system.

The performance criterion for fatigue cracking in chemically stabilized is defined in terms of a damage index. Typical design damage index values for fatigue cracking in chemically stabilized layers are on the order of 25 percent.

Total Permanent Deformation

Permanent deformation (or rutting) most typically is manifested as ruts within the wheel paths. Total permanent deformation at the surface is the accumulation of the permanent deformation in all of the asphalt and unbound layers in the pavement system.

Rutting is a major contributor to loss of pavement smoothness. It can also create functional problems such as water ponding and consequent vehicle hydroplaning and handling problems for vehicles during lane changes.

The performance criterion for total permanent deformation is defined in terms of the maximum rut depth in the wheel path. Typical maximum rut depths for total permanent deformation are on the order of 0.3 to 0.5 inches. This limiting value is a direct function of the specific policy used by each design agency.

Smoothness

Functional adequacy is quantified most often by pavement smoothness. Rough roads not only lead to user discomfort but also to increased travel times and higher vehicle operating costs. Although the structural performance of a pavement in terms of pavement distress is important the public complaints generated by rough roads often contribute to a large part of the rehabilitation decisions that are made by State highway agencies. In a simplistic way smoothness can be defined as “the variation in surface elevation that induces vibrations in traversing vehicles.” The international roughness index (IRI) is one of the most common ways of measuring smoothness in managing pavements.

As with the structural distresses, the performance criterion for smoothness is defined by the acceptable IRI at the end of design life. Terminal IRI values are chosen by the

designer and should not be exceeded at the design level of reliability. Typically values in the range of 150 to 250 in/mile are used for terminal IRI, depending on the functional class of the roadway and design reliability.

3.3.3.4 Traffic

Traffic data is one of the key data elements required for the analysis and design of pavement structures. The standard traffic option for flexible pavement design is to specify the actual load spectra for single, tandem, tridem, and quad axles. Detailed guidance on traffic inputs is presented in PART 2, Chapter 4.

The second traffic option for flexible pavements is the special axle configuration. This option enables the analysis of pavement performance due to special, heavy, non-conventional off-road vehicle systems that are often subject to special permitting requirements. This is a very important feature of the Guide because it provides the designer information on the amount of damage that could be caused by single or multiple passes of the special vehicle to the pavement structure. A description of the special axle configuration option is given separately in section 3.3.5.

Basic Information

- Annual Average Daily Truck Traffic (AADTT) for base year – the total number of heavy vehicles (classes 4 to 13) in the traffic stream.
- Percent trucks in the design direction (directional distribution factor).
- Percent trucks in the design lane (lane distribution factor).
- Operational speed of vehicles – this input is used in the calculation of moduli of asphalt bound layers.

PART 2, Chapter 4 discusses the recommended procedures to configure these inputs at each of the three hierarchical levels. Default values based on national traffic studies are presented in the Chapter for use at level 3 for the directional and lane distribution factors. Additional discussion on operational speed of vehicles and its relevance to flexible pavement design is presented below.

Vehicle Operational Speed

It is important to discuss the role of the typical operational speed on flexible pavement design. Operational speed is an important input for flexible pavement design as it directly influences the stiffness response of the asphalt concrete layers within the pavement structure. As the traffic moves along the highway, a large number of rapidly applied stress pulses are applied to each element of material within the pavement system. Typically, these stress pulses last for only a short period of time, and the magnitude and duration depend on the vehicle speed, type, and geometry of pavement structure, and the location of the element under consideration.

Figure 3.3.6 shows a typical pavement structure and the stress distribution as a function of the stiffness of the layer. Stiffer layers tend to spread the stresses over a wider area. Considering two elemental points A and B in the asphalt layer, the applied load influences point A whereas point B is outside the influence zone. As the load moves to the right, the stress at point A will increase and reaches a maximum value when the load is directly above point A and will decrease as the load moves away from point A.

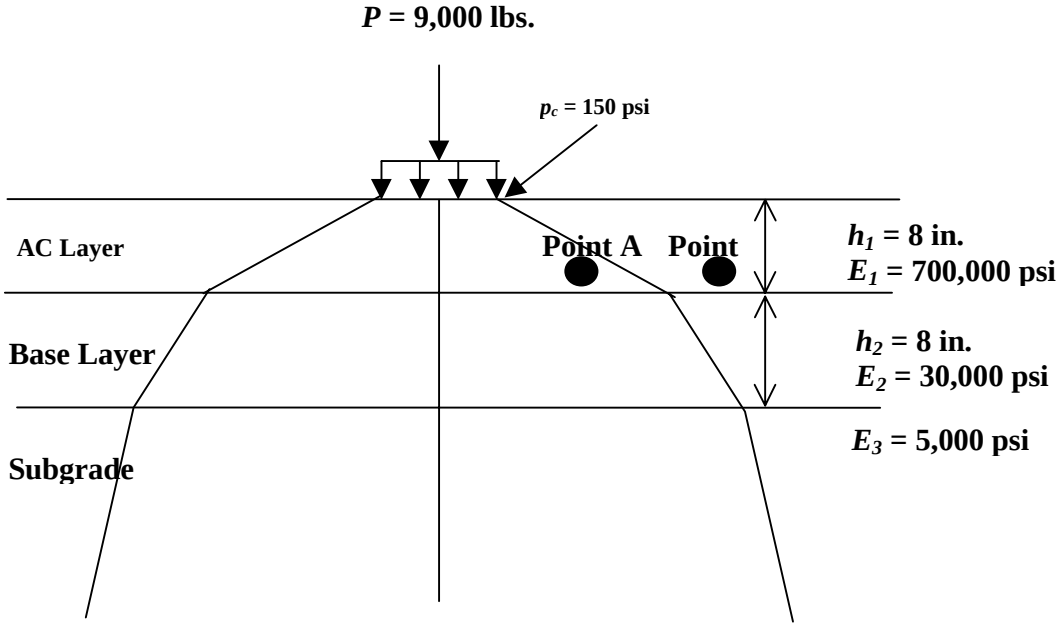

Figure 3.3.6. Stress distribution under wheel load.

Barksdale (*2*) investigated the vertical stress pulse at different points in flexible pavements. Based upon his investigation he concluded that a haversine or a triangular function could approximate the stress pulse under the moving vehicle. After considering the inertia and viscous effect based on vertical stress pulses measured at the AASHO Road Test (*3*), the stress pulse time can be related to the vehicle speed and depth, as shown in figure 3.3.7. A more detailed discussion on vehicle operating speed is provided in Appendix UU.

For the Design Guide, the only material property that will be affected by the load pulse duration is the asphalt stiffness. This includes both asphalt concrete layers and any asphalt treated base layers. Since asphalt layers are usually close to the surface, the depth of the layer may not be a significant factor. However, speed of the vehicle can result in different frequency of load, resulting in different modulus values for asphalt in the analysis.

Table 3.3.1 presents some recommendations for typical vehicle operating speed by roadway facility type. Note that the frequencies corresponding to various speeds are also noted in the table at layer mid-depth locations.

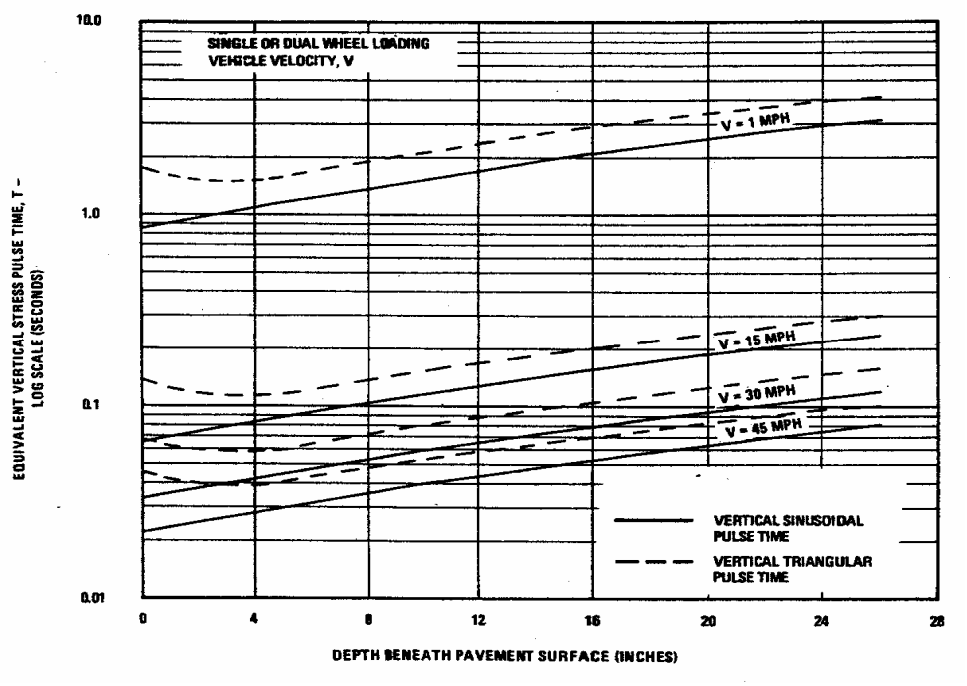

Figure 3.3.7. Variation of equivalent vertical stress pulse time with vehicle velocity and depth (*2*).

Table 3.3.1. Recommendations for selecting vehicle operating speed.

Type of Road Facility	Operating Speed (mph)	Estimated frequency at layer mid-depth (Hz)		
		Representative HMA Layer (4-12 in)	Thin HMA Layer Wearing Surface (1 – 3 in)	Thick HMA Layers Binder/Base (3 – 12 in)
Interstate	60	15-40	45-95	10-25
State Primary	45	10-30	35-70	15-20
Urban Street	15	5-10	10-25	5-10
Intersection	0.5	0.1-0.5	0.5-1.0	0.1-0.25

Traffic Volume Adjustment

Monthly Adjustment Factors

The truck monthly distribution factors are used to determine the monthly variation in truck traffic within the base year. These values are simply the ratio of the monthly truck traffic to the AADTT. Naturally, the average of the ratios for the 12-months of the base year must equal 1.0. PART 2, Chapter 4 discusses the monthly adjustment in more detail. If no information is available, assume even distribution (i.e., 1.0 for all months for all vehicle classes).

Vehicle Class Distribution

The normalized vehicle class distribution represents the percentage of each truck class (classes 4 through 13) within the AADTT for the base year. The sum of the percent

AADTT of all truck classes should equal 100. PART 2, Chapter 4 discusses the procedures to determine this input at each of the input levels. It is important to note that if site specific (level 1) or regional data (level 2) data are not available, truck traffic classification (TTC) can be used in conjunction with the functional class of the roadway to estimate the vehicle class distribution. Each TTC represents a traffic stream with unique truck traffic characteristics, and a default vehicle class distribution was established for each TTC using a national traffic database for use at level 3. The default values are provided in PART 2, Chapter 4 and Appendix AA. They are also a part of the Design Guide software.

Hourly Truck Traffic Distribution

The hourly distribution factors represent the percentage of the AADTT within each hour of the day. These factors are important primarily for rigid pavement analysis. PART 2, Chapter 4 discusses this input in more detail and describes the ways estimate it at each of the three hierarchical input levels.

Traffic Growth Factors

The traffic growth function allows for the growth or decay in truck traffic over time (forecasting or backcasting truck traffic). Three functions are available to estimate future truck traffic volumes:

- No growth.
- Linear growth.
- Compound growth.

Different growth functions may be used for different functional classes. Based on the function chosen, the opening date of the roadway to traffic (excluding construction traffic), and the design life (discussed in *Basic Information* input category), the traffic is projected into the future. The growth functions are presented in PART 2, Chapter 4.

Axle Load Distribution Factors

The axle load distribution factors simply represent the percentage of the total axle applications within each load interval for a specific axle type and vehicle class (classes 4 through 13). This data needs to be provided for each month for each vehicle class. A definition of load intervals for each axle type is provided below:

- Single axles – 3,000 lb to 41,000 lb at 1,000 lb intervals.
- Tandem axles – 6,000 lb to 82,000 lb at 2,000 lb intervals.
- Tridem and Quad axles – 12,000 lb to 102,000 lb at 3,000 lb intervals.

The estimation of axle load distribution factors at different input levels is presented in PART 2, Chapter 4.

General Traffic Inputs

Most of the inputs under this category define the axle load configuration and loading details for calculating pavement responses. The exceptions are "Number of Axle Types per Truck Class" and "Wheelbase" inputs, which are used in the traffic calculations.

Mean Wheel Location

Distance from the outer edge of the wheel to the pavement marking. This input is very important in computing fatigue damage for both JPCP cracking and CRCP punchout predictions but is not used for flexible pavement analyses.

Traffic Wander Standard Deviation

Lateral wander of traffic influences the number of axle load applications over a point for predicting distress and performance. This parameter affects prediction of fatigue and permanent deformation within the pavement system. An increase in wander will result in more fatigue life and less permanent deformation within the pavement system.

It is usually not practical to assess the exact distribution of wander; however, a good approximation is to assume that the wander is normally distributed. The standard deviation for the normal distribution plot represents the wander in inches.

Although wander directly affects the progression of damage for both fatigue and rutting, a slightly different approach is used for each distress. Estimation of fatigue damage is based upon Miner's Law, which states that damage is given by the following relationship.

$$D = \sum_{i=1}^{T} \frac{n_i}{N_i} \qquad (3.3.1)$$

where:

D = damage.
T = total number of periods.
n_i = actual traffic for period i.
N_i = traffic allowed under conditions prevailing in i.

Because Miner's Law is linear with traffic, damage distribution with wander can be computed from the fatigue damage profile obtained that has no wander (wander = 0 inch). This cannot be done when dealing with permanent deformation, because rutting in the pavement is not linearly related to traffic and wander is applied to the pavement response, not the distress. The approach is better explained in figure 3.3.8.

In figure 3.3.8 plot "A" shows the pavement structure with a dual wheel centered at location 1. In this example, 5 points are used to define the damage profile due to wander effect (locations 1, 2, 3, 4, and 5 on the figure); however, within the Design Guide software 11 points are used to define the damage profile. Plot "B" shows the actual damage profile for a wander value of zero predicted by the design program. If no wander is used, the maximum value from this damage will define the fatigue life. Plot "C" in this

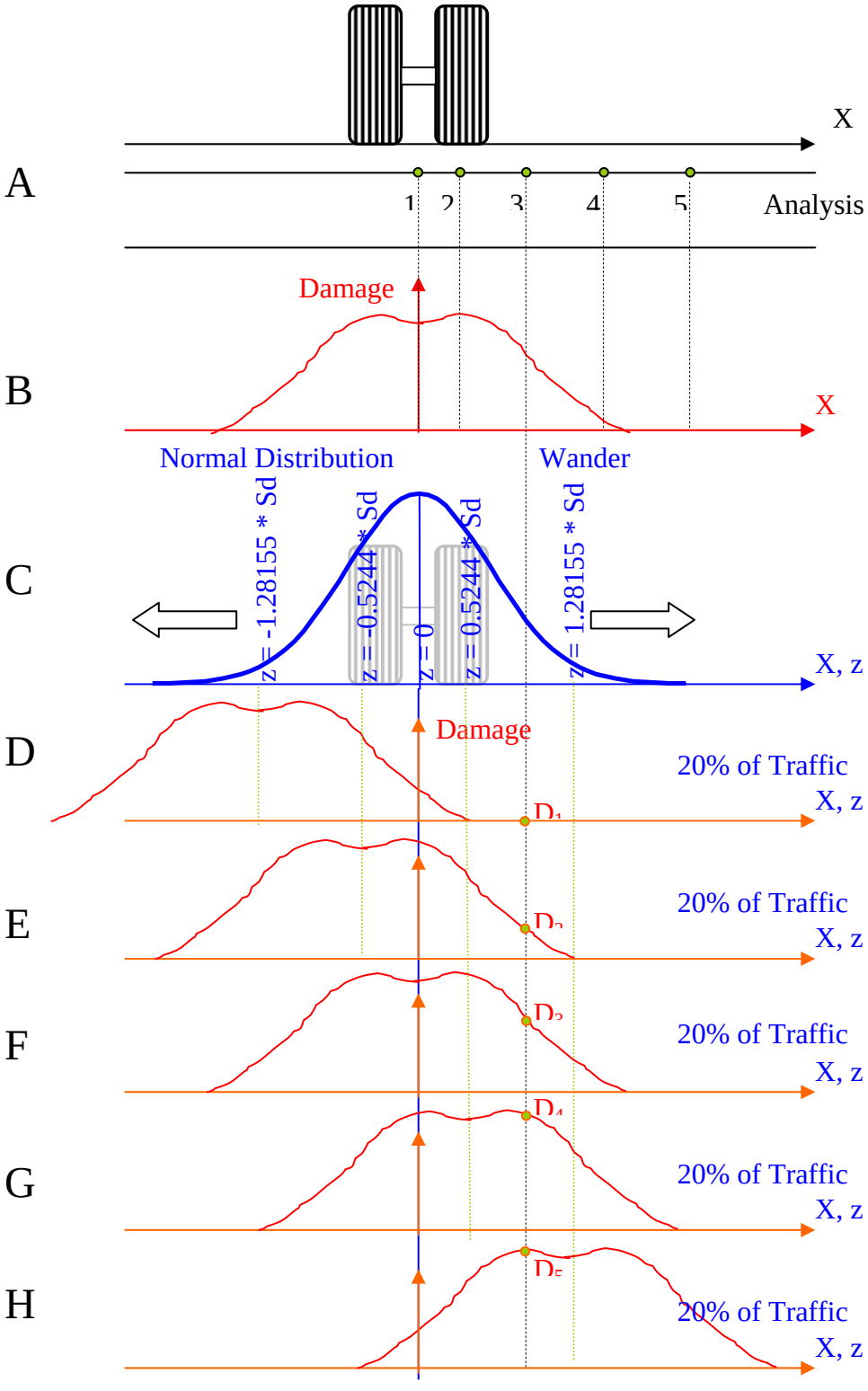

Figure 3.3.8. Fatigue analysis wander approach.

figure shows the wander distribution, assumed to be normally distributed. The spread of the distribution is dependent upon the standard deviation value entered by the user.

A higher standard deviation or higher wander value will result in a larger spread. The area under the normal distribution curve can be divided into five quintiles, each representing 20 percent of the total distribution. For each of these areas, a representative x-coordinate is found by multiplying the standard normal deviate "z" by the wander (standard deviation). Each of the normal deviates will represent accumulated areas equivalent to 10, 30, 50, 70, and 90 percent of the distribution.

Therefore, it is assumed that, for 20 percent of the traffic, the damage distribution will be centered at location equal to $-1.28155\ S_d$, where S_d is the wander standard deviation. For this situation (plot D), damage at location 3 is D_1. Since D_1 is 0 for this case, no fatigue damage occurs at location 3. The next plots (plots E through H) show damage distribution centered at z = -0.5244, 0, 0.5244, and 1.28155. Each represents the situation occurring for 20 percent of the traffic. Damage for cases is D_2, D_3, D_4, and D_5, respectively. Thus, the total damage at location 3 can be computed as:

$$D = 0.2 \times D_1 + 0.2 \times D_2 + 0.2 \times D_3 + 0.2 \times D_4 + 0.2 \times D_5 = 0.2 \times \sum_{i=1}^{5} D_i \qquad (3.3.2)$$

in which the D_i at each analysis location is determined using polynomial or linear interpolation.

The damage approach for wander described above applies only to for fatigue analysis. Rutting distress is not defined in terms of a linear function of damage but is instead computed directly. Therefore, a different and simpler approach is used. For rutting, the Guide software modifies the actual pavement response for the effects of wander and uses this modified response for the calculation of the incremental permanent deformations within each layer.

The estimation of this input at the three input levels is discussed in PART 2, Chapter 4. At level 3, 10 inches may be used for this input unless more accurate information is available. The wander effect is not applicable to the special gear configuration (section 3.3.5). If the user opts to consider a special gear in the analysis, a value of zero wander should be specified.

Design Lane Width

This is the distance between the lane markings on either side of the design lane. It is used primarily for rigid pavement design and has little effect on flexible pavement analyses. The default value for standard-width lanes is 12 ft.

Number of Axle Types per Truck Class

This input represents the average number of axles for each truck class (class 4 to 13) for each axle type (single, tandem, tridem, and quad). The estimation of this input at the

three input levels is discussed in PART 2, Chapter 4. Default values derived from a national traffic database for use at level 3 are provided in PART 2, Chapter 4.

Axle Configuration

A series of data elements are needed to describe the details of the tire and axle loads for use in the pavement response module. Typical values are provided for each of the following elements; however, site-specific values may be used, if available.

- Average Axle-Width – the distance between two outside edges of an axle. For typical trucks, 8.5 ft may be assumed for axle width.
- Dual Tire Spacing – the distance between centers of a dual tire. Typical dual tire spacing for trucks is 12 in.
- Tire Pressure – the hot inflation pressure or the contact pressure of a single tire or a dual tire. For heavy trucks, typical hot inflation pressure is 120 psi.
- Axle Spacing – the distance between the two consecutive axles of a tandem, tridem, or quad. The average axle spacing is 51.6 in for tandem and 49.2 in for tridem axles.

Wheelbase

This information is used primarily for rigid pavement design and has little effect on flexible pavement analyses.

Input Processing

The traffic inputs are further processed to produce the following "processed input" for every month over the entire design period:

- Number of single axles under each load category.
- Number of tandem axles under each load category.
- Number of tridem axles under each load category.
- Number of quad axles under each load category.
- Number of truck tractors (Class 8 and above) under each load category (for top-down cracking).

The hourly traffic distribution factors are applied to the processed traffic input (the traffic counts by axle type for every month of the design period) to obtain hourly traffic at the time of damage calculation for each distress. More discussion on the additional processing of traffic inputs is provided in section 3.3.4 as well as in Appendices GG, II, and MM.

3.3.3.5 Climate

Environmental conditions have a significant effect on the performance of flexible pavements. The interaction of the climatic factors with pavement materials and loading is complex. Factors such as precipitation, temperature, freeze-thaw cycles, and depth to

water table affect pavement and subgrade temperature and moisture content, which, in turn, directly affects the load-carrying capacity of the pavement layers and ultimately pavement performance. Detailed guidance on environmental inputs required for pavement design is presented in PART 2, Chapter 3. This section provides a summary of the climatic inputs required for flexible pavement analysis.

Climatic Inputs

The following weather related information is required to perform flexible pavement design:

- Hourly air temperature over the design period.
- Hourly precipitation over the design period.
- Hourly wind speed over the design period.
- Hourly percentage sunshine over the design period.
- Hourly ambient relative humidity values.
- Seasonal or constant water table depth at the project site.

The first five inputs above can be obtained from weather station data for a given site, if available. For locations within the United States, they can be obtained from the National Climatic Data Center (NCDC) database. The Design Guide software includes an extensive climatic database for over 800 locations in the U.S. and a capability to interpolate between the available sites. At the present time, many locations in the database have data for approximately 60 to 66 months. Note that at least 24 months of weather station data are required for the design guide software to give a reasonable solution.

All of the necessary climatic information at any given location within the U.S., with the exception of the seasonal water table depth, can be generated by simply providing the following inputs:

- Pavement location – latitude and longitude.
- Elevation.

Designers may use data from the closest weather station (called actual weather station [AWS]) or data interpolated from up to six closest weather stations (to create a virtual weather station [VWS]) for design at the specific pavement location. The VWS is the recommended approach, because the data are interpolated to the actual project location and this approach more adequately compensates for missing data from any one weather station.

Input Processing

The climatic inputs are combined with the pavement material properties, layer thicknesses, and drainage-related inputs by the EICM to yield the following information for use in the flexible pavement design analysis:

- Hourly profiles of temperature distribution through the asphalt layers.
- Hourly temperature and moisture profiles (including frost depth calculations) through other pavement layers.
- Monthly or semi-monthly (during frozen or recently frozen periods) predictions of layer moduli for asphalt, unbound base/subbase, and subgrade layers.
- Annual freezing index values.
- Mean annual number of wet days.
- Number of freeze-thaw cycles.

PART 3, Chapter 3 discusses the seasonal temperature and moisture predictions through the pavement profile and the computation of environmental adjustment factors for unbound layer moduli in detail. These are accomplished in the Design Guide software using the EICM.

3.3.3.6 Pavement Structure

Input values for pavement structure properties are organized into the following categories:

- Drainage and surface characteristics.
- Layer properties.
- Distress potential.

Each of these categories is described in turn in the following subsections.

Drainage and Surface Properties

These are general pavement structure properties required for the design analyses. Information required under this category includes the following:

- Pavement surface layer shortwave absorptivity.
- Potential for infiltration.
- Pavement cross slope.
- Length of drainage path.

The first item in the list above is essentially a material property that interacts with the climatic inputs in defining the temperature regime in pavement layers. The remaining three inputs are related to infiltration and drainage. Guidance is not provided in this chapter for any detailed drainage designs or construction methods. The design of drainage components and how the overall pavement drainage is incorporated into structural design is presented in PART 3, Chapter 1. The inputs discussed in this section, however, have a significant impact on the amount of moisture that enters the pavement structure from a given rainfall event and help define some of the other parameters required for drainage calculations.

Pavement Shortwave Absorptivity

The short wave absorptivity of a pavement surface depends on pavement composition, color, and texture. The short wave absorptivity is the ratio of the amount of solar energy absorbed by the pavement surface to the total energy the surface was exposed to, which naturally affects the temperature regime within the pavement structure and the associated structural response. This input ranges from 0 to 1. Generally the lighter and more reflective the surface is, the lower the short wave absorptivity will be. For Level 1 input, this value should be determined through direct testing. The typical values range from 0.8 to 0.9 for weathered asphalt and 0.9 to 0.98 for fresh asphalt . The recommended default value is 0.85 for new pavement design.

Infiltration

This input quantifies the amount of water infiltrating the pavement structure. The calibration of the flexible pavement distress models assumed that no infiltration of moisture occurred throughout the design period. Thus, the flexible pavement design procedure does not allow the designer to choose any level of infiltration at this time. However, adequate consideration to subdrainage should be given when designing flexible pavements. PART 3, Chapter 1 discusses subsurface drainage design in details and presents a methodology for integrating drainage design with pavement design.

Layer Properties

The flexible pavement design procedure allows a wide variety of asphalt, base, and subbase material properties and layer thicknesses as shown in figure 3.3.2. For example, a flexible pavement structure could consist of one or more asphalt concrete surface layers, an asphalt treated base, an aggregate subbase, compacted subgrade, natural subgrade, and bedrock.

The original pavement structure defined by the user usually has 4 to 6 layers. However, the Design Guide software may subdivide the pavement structure into 12 to 15 sublayers for the modeling of temperature and moisture variations. The Design Guide software performs the sublayering internally based on the material type, layer thickness and the location of the layer within the pavement structure. The Design Guide software can analyze a maximum of 19 layers. However, because of the automatic sublayering of certain layers, a maximum of 10 actual input layers is recommended. Figure 3.3.9 shows the criteria upon which the sublayering is based.

A later section titled “Rules of Simulation” provides detailed guidance on the rules and constraints that need to be satisfied in defining flexile pavement structures for design. The following constraints need to be satisfied as a minimum.

- The surface layer in flexible pavement design is always an asphalt concrete layer.
- Full depth asphalt (asphalt concrete on subgrade) is the minimum structure that can be analyzed.

    - Only one unbound granular layer can be placed between two stabilized layers.
- The last two layers in the pavement structure must be unbound layers. (To satisfy this constraint, the Design Guide software automatically sublayers the subgrade into two layers for full depth asphalt pavements where the last bound layer rests directly on the subgrade.)

Defining a trial design involves defining all pavement layers and material properties for each individual layer, including subgrade in accordance with the guidelines provided in the "Rules of Simulation" subsection. Depending on the selected trial design, sub-layering may be necessary for the analysis procedures. The sublayering scheme is discussed for each material type along with a summary of the required layer materials inputs in the following paragraphs. More detailed guidelines on material properties are provided in PART 2, Chapter 2.

Asphalt Concrete and Asphalt Stabilized Layers

The surface asphalt concrete layer is divided into sublayers to account for temperature and aging gradients. Within the program, the user can specify a maximum of three asphalt layers (surface, binder, and base) for new construction. This requires material properties for each individual asphalt layer. Asphalt aging is modeled only for the top sublayer. The largest change in stiffness due to aging occurs only in the top half inch, and the aging gradient for layers other than the top layer is not significant. The top layer is more susceptible to aging since long-term aging is strongly affected by the oxidation process.

Figure 3.3.9 shows a typical original HMA pavement structure. The top asphalt layer is divided into two sub-layers, 0.5 inch and the remainder. In the figure, h_{AC} refers to the original asphalt layer thickness, and h'_{AC} is the second sub-layer within the top asphalt layer. That is, irrespective of the thickness of the top asphalt layer, it is always divided in two sub-layers (0.5 in and the remaining thickness). No sub-layering is carried out for any other asphalt layer in the pavement system.

No sublayering of asphalt-stabilized base layers is performed for design and analysis purposes within the Design Guide software.

The materials inputs required for asphalt concrete layers are grouped under three broad categories – general materials inputs, inputs required to construct the dynamic modulus (E^*) master curve, and inputs required for thermal cracking prediction. These are discussed below:

Maximum Sub-Layering Depth = 8 ft

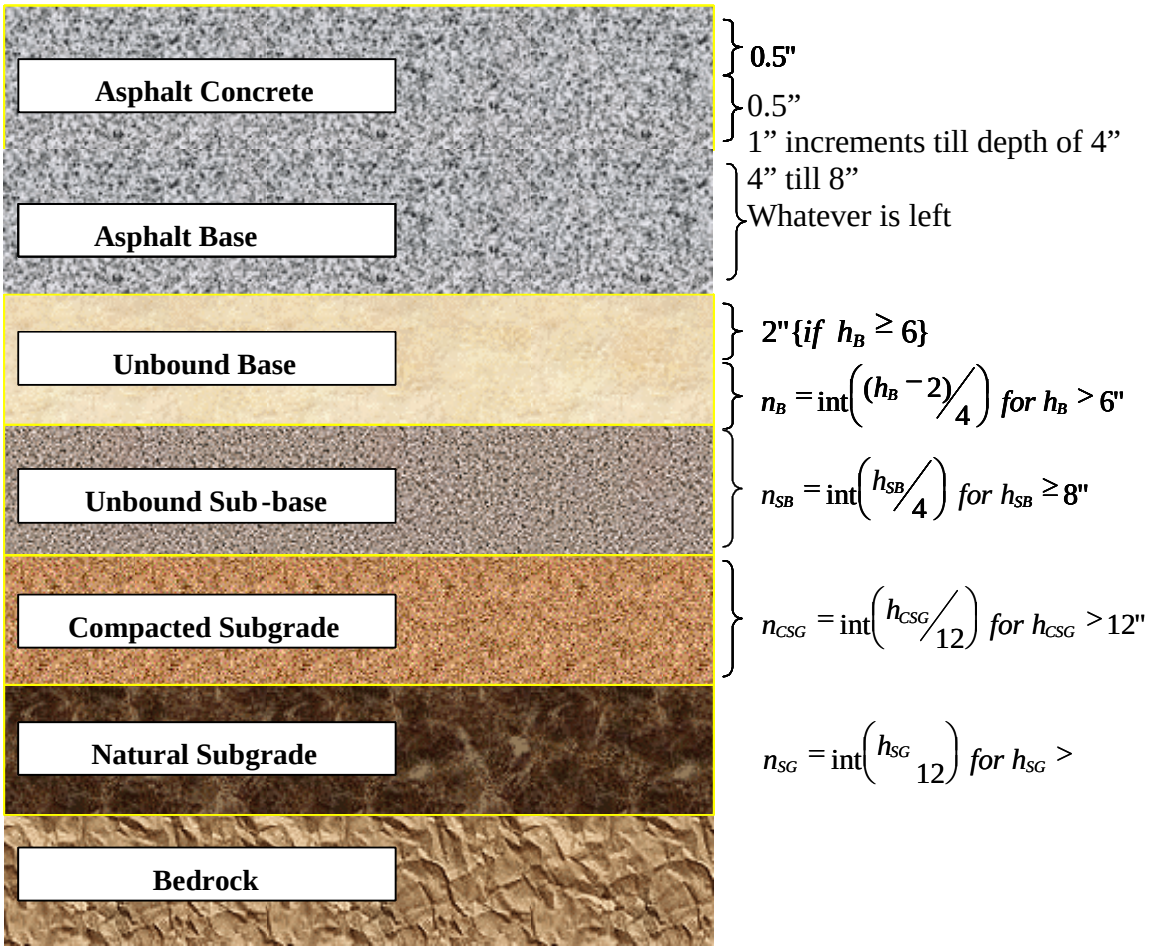

Figure 3.3.9. Layered pavement cross-section for flexible pavement systems (no sub-layering beyond 8 feet).

General Layer Property Inputs

- Layer thickness.
- Poisson’s ratio (see PART 2, Chapter 2).
- Thermal conductivity – the quantity of heat that flows normally across a surface of unit area per unit of time of temperature gradient normal to the surface. The typical value for asphalt-stabilized base material is 0.67 BTU/hr-ft-°F.
- Heat capacity – the heat required to raise the temperature of a unit mass of material by a unit temperature. A typical value for asphalt-stabilized base is 0.23 BTU/lb-°F.
- Total unit weight – typical range for dense-graded hot-mix asphalt is 134 to 148 lb/ft3 (pcf).

Inputs Required to Construct E* Master Curve

The primary material property of interest for asphalt stabilized layers is its dynamic modulus, E^*. For Level 1 input, E*, is determined in the laboratory using standard test protocols (see PART 2, Chapter 2 for details) for various frequencies and rates of loading. A master curve of E* versus reduced time is then derived from this data that defines the behavior of this layer under loading and at various climatic conditions. For input levels 2 and 3, the dynamic modulus prediction equation presented in PART 2, Chapter 2 is used to construct the master curve from the following information:

- Asphalt mixture properties
  - For Level 1 input, – specify the laboratory-measured dynamic modulus values at various temperatures and loading rates.
  - For Level 2 and 3 input – specify the mix properties required for the Witczak dynamic modulus predictive equation:
    - Percent retained on ¾ in sieve – a typical value is 5 to 16 % for dense graded and 30% for permeable.
    - Percent retained on 3/8 in sieve – a typical value is 27 to 49 % for dense graded and 70% for permeable.
    - Percent retained on #4 sieve – a typical value is 38 to 61 % for dense graded and 95% for permeable.
    - Percent passing the #200 sieve – a typical value is 3 to 8% for dense graded and 1% for permeable.
- Asphalt binder
  - For Level 1 input – specify either Superpave or conventional laboratory binder test data
  - For Level 2 input – specify PG grade or Viscosity grade.
  - For Level 3 input – specify PG grade, Viscosity grade, or Penetration Grade.
- Asphalt general
  - Volumetric effective binder content (percent).
  - Air voids (percent).
  - Reference temperature for master curve development (70 °F typical).

More detailed discussion on the determination of dynamic modulus at levels 2 and 3 using the predictive equation is presented in PART 2, Chapter 2.

Inputs Required for Thermal Cracking Prediction

The properties of the asphalt layer specific to the prediction of thermal cracking distress must be specified. These include:

- Average tensile strength at 14^oF.
- Creep compliance data. For Level 1 input, these are mix-specific values measured at three different temperatures (-4^o, 14^o, 32^o F). For Level 2 input, these are mix-

specific values measured at a single temperature (14 ^{o}F). For Level 3 input, these are default material properties based upon the binder performance grade.

- The mix coefficient of thermal contraction. This may be specified directly, or the Guide software can estimate it based upon input values for mix VMA and the thermal contraction coefficient for the aggregates.

PART 2, Chapter 2 discusses the hierarchical inputs As described in section 3.3.5, thermal cracking is predicted using a different pavement response model than for the other load-related distresses. Consequently, no sublayering of the asphalt layer is performed for the thermal cracking analysis.

Chemically Stabilized Layers

No sub-layering is done for any chemically stabilized base or subbase layers. The following inputs are required to define a chemically stabilized layer:

- Maximum design resilient modulus.
- Minimum resilient modulus (after fatigue damage completely propagates the layer).
- Modulus of rupture.
- Unit weight of the material.
- Poisson's ratio.
- Thermal conductivity – the quantity of heat that flows normally across a surface of unit area per unit of time of temperature gradient normal to the surface. A typical value for chemically or chemically stabilized base is 1.0 BTU/hr-ft-°F.
- Heat capacity – the heat required to raise the temperature of a unit mass of material by a unit temperature. A typical value for chemically stabilized base is 0.28 BTU/lb-°F.

Unbound Base/Subbase/Subgrade

Unbound base layers thicker than 6 in and unbound subbase layer thicker than 8 in are sublayered internally within the Guide software for analysis purposes. For the base layer (first unbound layer), the first sub-layer is always 2 in. The remaining thickness of the base layer and any subbase layers that are sub-layered are divided into sublayers with a minimum thickness of 4 in. For compacted and natural subgrades, the minimum sub-layer thickness is 12 in. A pavement structure is sub-layered only to a depth of 8 feet. Any remaining subgrade is treated as an infinite layer. If bedrock is present, the remaining subgrade is treated as one layer beyond 8 feet. Bedrock is not sub-layered and is always treated as an infinite layer. The sublayering scheme for unbound layers within the pavement structure is summarized in figure 3.3.9.

The major inputs required for unbound base/subbase and subgrade layers are:

- Layer thickness (only for base and subbase layers) – for subgrade layers if the lime stabilized (not modified) or compacted subgrades need to be considered separately from the natural subgrade, they can be defined as a structural layer.

- Layer resilient modulus
  - For Level 1 input – specify the nonlinear stress-dependent resilient modulus parameters k_1, k_2, and k_3. It should be noted that level 1 inputs require the use of the nonlinear finite element code for performance prediction which is currently only recommended to be used for research and analysis purposes.
  - For Level 2 input – specify the linearly elastic resilient modulus value directly; alternatively, the resilient modulus value can be determined from empirical relations in terms of other index properties.
  - For Level 3 input – specify a default resilient modulus as a function of the AASHTO or Unified soil classification.
- Poisson's ratio.
- Coefficient of lateral earth pressure, K_o – a typical value for this input is 0.5 for natural or uncompacted materials.

Seasonal Analysis

The designer has the choice of including or not including seasonal analysis for the unbound base materials and soils. The following options are available for seasonal analysis for Level 1 and 2 unbound material inputs:

1. Enter a representative design resilient modulus (M_r) at the optimum moisture content (either k_1, k_2, and k_3 for Level 1 inputs or M_r for Levels 2 and 3) or other allowable soil strength/stiffness parameters (CBR, R-value, AASHTO structural layer coefficient, or PI and gradation) and use the EICM module embedded in the Design Guide software to estimate seasonal variations based on changing moisture and temperature profiles through the pavement structure. The additional inputs for EICM include plasticity index, percent passing No. 4 and No. 200 sieves, and the effective grain size corresponding to 60 percent passing by weight (D_{60}) for the layer under consideration. Using these inputs, EICM estimates the unit weight, the specific gravity of solids, saturated hydraulic conductivity of the pavement layer, optimum gravimetric moisture content, degree of layer saturation, and the soil water characteristic curve parameters. These computed quantities may be substituted with direct inputs.
2. In lieu of using the EICM, the seasonal moduli (either k_1, k_2, and k_3 for Level 1 inputs or M_r for Levels 2 and 3), CBR, R-value, or other values may be entered directly. For direct input, 12 monthly laboratory estimated M_r values (or other allowable soil tests) are required.
3. Seasonal variation in stiffness of unbound materials may be ignored. In this case, a representative design modulus value (or other test value) is required.

For Level 3, the required input is the layer resilient modulus at optimum water content (default value based on AASHTO or Unified soil class), and the EICM performs the seasonal adjustment. If seasonal analysis is not desired, a single resilient modulus is entered that is held constant throughout the entire year (no moisture content is entered).

Bedrock

The presence of bedrock within 10 ft of the pavement surface influences the structural response of pavement layers. The inputs for this layer include the following:

- Layer thickness (infinite if it is the last layer).
- Unit weight.
- Poisson's ratio.
- Layer modulus.

Input levels 1 and 2 do not apply for bedrock. Typical modulus values for bedrock in various conditions (e.g., solid, or highly fractured and weathered) are provided in PART 2, Chapter 2.

Distress Potential

These supplementary properties are required for the smoothness (IRI) prediction models. They are used with empirical relations to predict the development of additional distresses affecting smoothness that are not mechanistically considered by the Guide. The two distress potential properties required are:

- Block cracking (at all severity levels as defined by the LTPP Distress Identification Manual), defined as a percent of total lane area.
- Sealed longitudinal cracks outside of wheel path, defined in terms of feet per mile (at medium and high severity as defined by the LTPP Distress Identification Manual).

Appendix OO presents a discussion on the estimation of these input quantities for design purposes.

Rules of Simulation

The following provides some general rules of simulation or guidance for the creating the flexible pavement structure to be analyzed using the Design Guide software. Note that these rules are mere suggestions and the designer has the choice of using local experience in actually modeling the structure to be analyzed.

To get started, the designer should simulate the pavement structure and foundation as detailed as possible, and then begin to combine layers, as needed. As noted earlier, the software takes the structure defined by the designer and further divides those layers into sublayers to more accurately calculate the responses throughout the pavement structure. The number of sublayers that the program creates depends on the number of layers and the thickness of those layers. Figure 3.3.9 graphically illustrates the sublayers that are created by the program. The greater the number of layers, the greater the number of sublayers and the more time that will be required to calculate the various pavement responses for analyzing the structure and predicting distress using the Guide software.

The number of sublayers cannot exceed 20 or the number of evaluation points cannot exceed 26 otherwise the Design Guide software will not execute. The maximum number of sublayers is more likely to be exceeded in simulations using thick non-frost susceptible granular base materials to prevent frost penetration or the use of thick HMA layers with aggregate base layers on heavily traveled roadways. This section of the guide provides guidance on simulating the pavement structure so that the maximum number of sublayers will not exceed 20 while still maintaining the original intent of designer as much as possible.

General Notes

- The designer should try to combine the lower layers first and treat the upper layers in more detail, if at all possible. The discussion and guidance that follows, however, starts with the foundation layers and proceeds up to the surface layers.
- Thin non-structural layers should be combined with other layers. Any layer that is less than 1-inch in thickness should be combined with the supporting layer. As an example, an HMA open-graded friction course should be combined with the supporting HMA layer.
- Similar materials of adjacent layers should be combined into one layer. Similar is defined as materials or layers with both similar structural response properties and physical properties that are needed for the climatic model.

Subgrade Layers

- The designer should divide the subgrade or foundation soils into two layers especially when bedrock and other hard soils are not encountered. The lower layer will be the natural soil, while the upper layer is to be the compacted soils just beneath the pavement materials. If the designer elects not to use two subgrade layers, the program will create an additional layer for the EICM computations.
- Bedrock or other hard soils (such as hard pan, shale, sandstone, etc.) that are encountered more than about twenty feet below the surface will have an insignificant effect on the calculated pavement responses for predicting various distresses. Many back-calculation programs, however, will provide better results if that hard layer is encountered within 600 inches to the surface. Thus, the bedrock or hard layer can be ignored when that depth exceeds 20 feet for pavement design, but not for back-calculation of layer modulus.
- Filter fabrics used for drainage purposes between a fine-grained soil and aggregate base material cannot be simulated in the pavement structure and should be ignored in the structural design section analyzed.

Unbound Aggregate Materials

- In most cases, the number of unbound granular base and subbase layers should not exceed two, especially when one of those layers is thick (more than 18 inches in thickness). Sand and other soil-aggregate materials should be simulated separately from crushed stone or crushed aggregate base materials.

- If thick, unbound aggregate materials (exceeding 18 inches) are used, this layer can be treated as the upper subgrade layer without compromising the quality of the solution (since this change in nomenclature only affect sublayering within the Design Guide software and not the response calculation). Thick granular layers are typically used in northern climates as non-frost susceptible materials. When these layers are treated as the upper subgrade, only one subgrade layer is needed.
- Conversely, if a thin aggregate base layer is used between two thick unbound materials, the thin layer should be combined with the weaker or lower layer. As an example, a 6-inch sand subbase layer placed between the subgrade soil and 15-inch crushed stone base can be combined with the upper subgrade layer. If the designer believes that the 20 sublayer limit will not be exceeded, the 6-inch sand subbase layer could be simulated by itself.
- When similar aggregate base and subbase materials are used, those materials can be combined into one layer, especially when the combined thickness of the layers exceeds 18 inches. The material properties used for that layer should be those from the thicker layer. Averaging the material properties is not recommended. When similar materials have about the same thickness, the material with the lower modulus value should be used.
- Geo-grids and other reinforcing materials used in unbound aggregate layers can not be simulated in the structural response program.
- When unbound layers are present in the pavement structure, care should be taken to ensure that the modular ratio of adjacent layers, i.e., M_r of upper unbound layer divided by M_r of lower unbound layer (including subgrade layers), does not exceed a value of 3 to avoid decompaction and the build up of tensile stresses in these layers (*4*).

Treated and Stabilized Materials

- Asphalt treated or stabilized base layers sometimes referred to as “blackbase” should be treated as a separate layer and not combined with dense-graded HMA base mixtures. Typically, these are crushed stone base materials that have a small amount of asphalt and/or emulsion that can be produced at a plant or mixed in-place. If needed, the asphalt treated base mixture should be combined with the crushed stone base materials or considered as an unbound aggregate mixture. However, asphalt treated base materials that are designed using the gyratory compactor or other compaction device and produced through a production facility should be treated or considered as an HMA base material and combined with that mixture or layer.
- Cement treated and other pozzolanic stabilized materials that are used as a base layer for structural support should be treated as a separate layer. In cases a small portion of cement, lime, or flyash may be added to granular base materials to improve the strength and/or lower the plasticity index of those materials for constructability issues. If these materials are not “engineered” to provide long-term strength and durability, they should be considered as an unbound material, and combined with those unbound layers, if necessary. On the other hand, if

these layers are engineered to provided structural support, they can be treated as chemically stabilized structural layers.

- Lime and/or lime-flyash stabilized subgrade soils should also be treated as separate layer, if at all possible. In some cases, a small amount of lime or lime-flyash is added to soils in the upper subgrade to lower the plasticity index and from a constructability standpoint. For these cases, the lime or lime-flyash stabilized soil should be treated as the subgrade and not as a structural layer in the pavement. If these materials are not "engineered" to provide long-term strength and durability, they should be considered as an unbound material, and combined with those unbound layers, if necessary. On the other hand, if these layers are engineered to provided structural support, they can be treated as moisture insensitive, constant modulus structural layers or chemically stabilized layers (see PART 2, Chapter 2 for more discussion).

Drainage Layers/Materials

- Asphalt treated base drainage layers should be treated as a separate layer and not combined with dense-graded HMA layers or asphalt treated base layers. If the error message noting that the number of sublayers exceeds 20 continually shows up, the OGDL can be combined with the lower layer.

HMA Mixtures and Materials

- The number of HMA layers should not exceed three, in any case. However, it may be necessary to limit the number of HMA layers to two when thick HMA layers and thick unbound aggregate layers are used.
- Similar HMA materials could be combined into one layer. As an example an HMA wearing surface or mix and an HMA binder layer can be combined into one layer without affecting the accuracy of the predictions if the gradations and binder contents are relatively close. The material properties entered into the software, if measured or determined for both layers should be those for the thicker layer or those for the upper or surface layer when the layers have similar thickness.
- Thin HMA layers can be combined with an adjacent HMA layer. Thin is defined as less than 1.5 inches in thickness.
- Thin HMA leveling courses or for the condition when the thickness of the leveling course is highly variable along the roadway can be ignored without affecting the overall accuracy of the results.

3.3.4 FLEXIBLE PAVEMENT DESIGN PROCEDURE

This section presents a detailed description of the overall performance prediction methodology for new and reconstructed flexible pavements. The term "flexible pavement" refers herein to any new, reconstructed, or rehabilitated pavement system that has an asphalt concrete mixture for the surface. The design methodology used is based upon mechanistic-empirical approaches to predict a variety of distress types:

- Asphalt fatigue fracture (top down and bottom up).
- Permanent deformation (HMA layer, unbound layer, subgrade, total).
- HMA thermal fracture (environmental induced).
- Chemically stabilized load associated fatigue fracture.

While the Design Guide addresses the vast majority of common distress types encountered in asphalt-surfaced pavements, it is important to recognize that not all important material durability issues (e.g., moisture sensitivity, stripping, etc.) are directly considered in the design process. Thus, the designer must still rely upon current technology and material specifications to address potential distress types not directly considered in the Guide. More importantly, the Guide does not contain any mechanistic-empirical methodology to address the issue of reflective cracking. This is certainly a much greater limitation for the rehabilitation design than for the new and reconstructed pavement designs discussed in this chapter. Nevertheless, even in new and reconstructed pavement design, reflective cracking in chemically stabilized layers (semi-rigid pavement sections) is a primary factor in dictating the degree of cracking that may eventually occur in the asphalt surface layer.

Distress predictions developed from the mechanistic-empirical approach are also linked to estimates of the IRI (International Roughness Index) as a functional performance criterion (along with specific distress predictions) that can be employed in the design process. Both deterministic and reliability-based solutions are available in the Guide.

3.3.4.1 Trial Design Parameters

A wide variety of flexible pavement types can be designed using the Guide procedures. Specific types of flexible pavement systems that can be analyzed include: (1) conventional flexible sections, consisting of relatively thin HMA surfacing and thick aggregate base/subbase layers, (2) "deep strength" asphalt sections having thicker layers of asphalt mixtures, (3) full-depth HMA sections, where the asphalt layer is placed directly on the subgrade, and (4) "semi-rigid" systems having a chemically stabilized (pozzolanic) layer. It is important to note that the layering of these materials can be in the conventional manner of decreasing layer quality with depth (i.e., HMA over aggregate over subgrade or HMA over chemically stabilized over aggregate over subgrade) or in an inverted (sandwich) type order in which a stiff layer (either HMA or chemically stabilized) is placed between an unbound aggregate layer and the subgrade layer. Figure 3.3.2 schematically shows some of the different pavement types considered in the Design Guide.

The designer must first select an initial trial pavement structure for design using guidance provided in the “Rules of Simulation” subsection (see Section 3.3.3.4). The designer must identify the pavement cross section and specify the layer material types and layer thicknesses for the initial pavement section to be analyzed.

The designer must next decide whether a seasonal analysis is required. If a seasonal analysis is not selected, all non-HMA layers will be assumed to have constant values of E_i and μ_i (modulus and Poisson's ratio) throughout the entire analysis period. However, the effects of seasonal variations in temperature and aging on the stiffness of the asphalt concrete materials will still be considered even if the seasonal analysis option is not selected. The following options are available for a seasonal analysis:

- EICM predictions.
- Monthly seasonal values.

If the EICM option is selected, the program internally generates environmental adjustment factors for the resilient modulus values entered by the user to estimate the seasonal material variation on monthly or semi-monthly intervals. Monthly intervals are used during non-frost seasons. If frost is predicted at the pavement location, the analysis period is reduced to two weeks to more accurately account for the stiffening effects of frost and the detrimental weakening during the thaw recovery period.

For the monthly seasonal values option, the designer must enter modulus and moisture values for each month for the entire year. The input modulus values are used directly in the pavement response model. The moisture content is required for the unbound permanent deformation model. The monthly values entered by the user are repeated for each year throughout the analysis period.

The next important decision is the selection of the design performance criteria for each distress type. The specific information required for the design performance criteria depends upon whether a deterministic or reliability design analysis has been selected. In a deterministic analysis, only two pieces of information are needed for the pavement analysis: the limiting design value for the distress (or IRI), and the design life. A performance criterion would thus be expressed for example, as the "design should not exceed an HMA rutting level of 0.4 inches within a 25-year period." Figure 3.3.10a shows schematically the increase in rut depth as a function of time for three different asphalt mixes having stiffness values A, B, and C. The stiffer mixes will result in less rutting as compared to the softer mixes. As shown in the figure, mix A will rut to 0.4 inch in 10 years, whereas mix C will reach the same rutting after 30 years. Consequently, for the stated performance criterion of 0.4 inches of rutting after 25 years, the optimum stiffness is between mix A and mix C. Figure 3.3.10b shows the effect of mix stiffness on the design life for a rut depth of 0.4 inches; mix stiffness D is the optimum for achieving a design life of 25 years with the rut depth not exceeding 0.4 inch.

In contrast to the deterministic analysis, the reliability approach requires three pieces of information: the limiting design value for the distress (or IRI), the design life, and the desired reliability level. A performance criterion would thus be expressed for example, as the "design should have a 90% probability of not exceeding an HMA rutting level of 0.4 inches within a 25-year period."

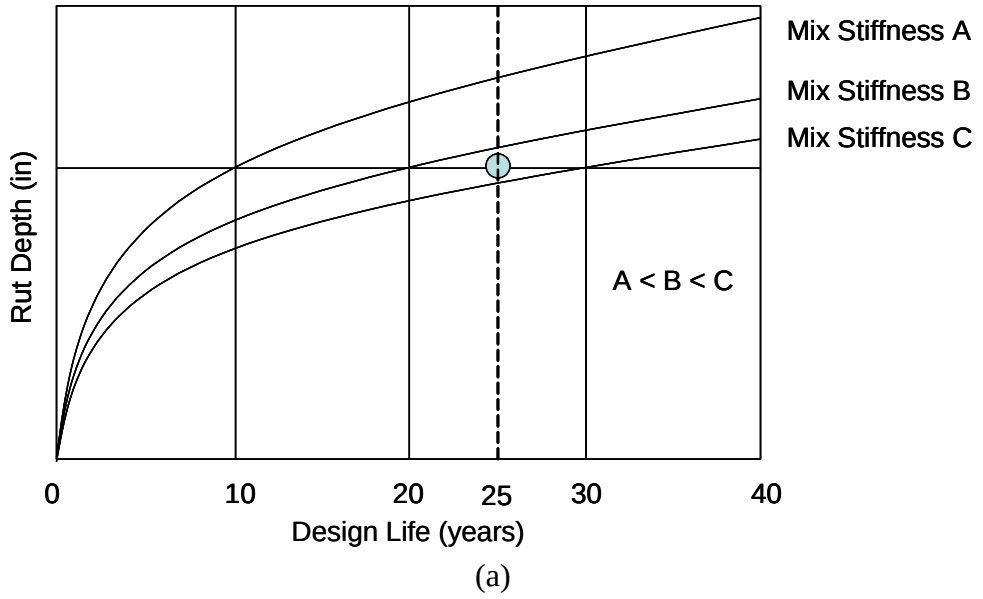

(a)

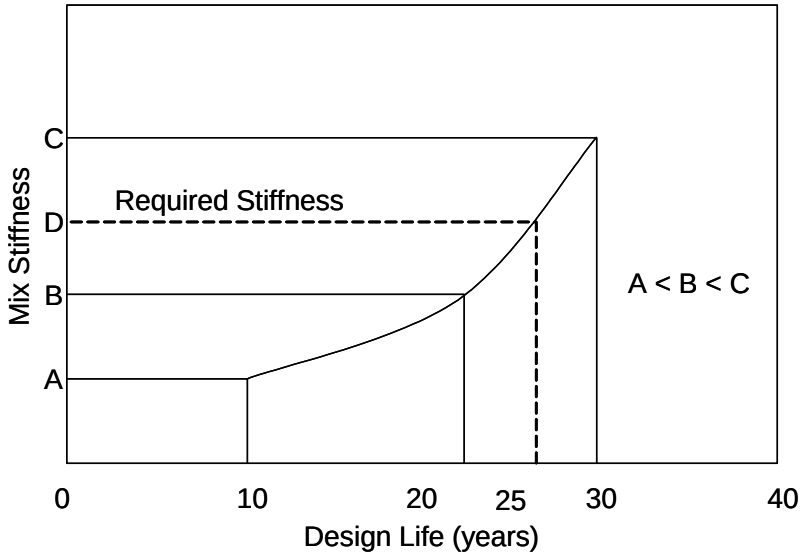

(b)

Figure 3.3.10. Deterministic approach used in the design guide for performance prediction.

Figure 3.3.11 shows schematically the results of the reliability analyses for the three different example mixes. Mix A is the softest and most susceptible to rutting, whereas mix C is the stiffest and, hence, least susceptible to rutting. The normal distribution on each plot represents the rut depth prediction variation. This variability in rut depth may be attributed to the variability in traffic levels, material properties, construction quality, and other variables that contribute to rutting. As shown in Figure 3.3.11a, the softest mix (mix A) provides only 10 percent confidence that the rutting will be less than 0.4 inches at the end of 25 years. Mix B provides intermediate performance, while mix C provides a 95% reliability level that exceeds the required 90% criterion.

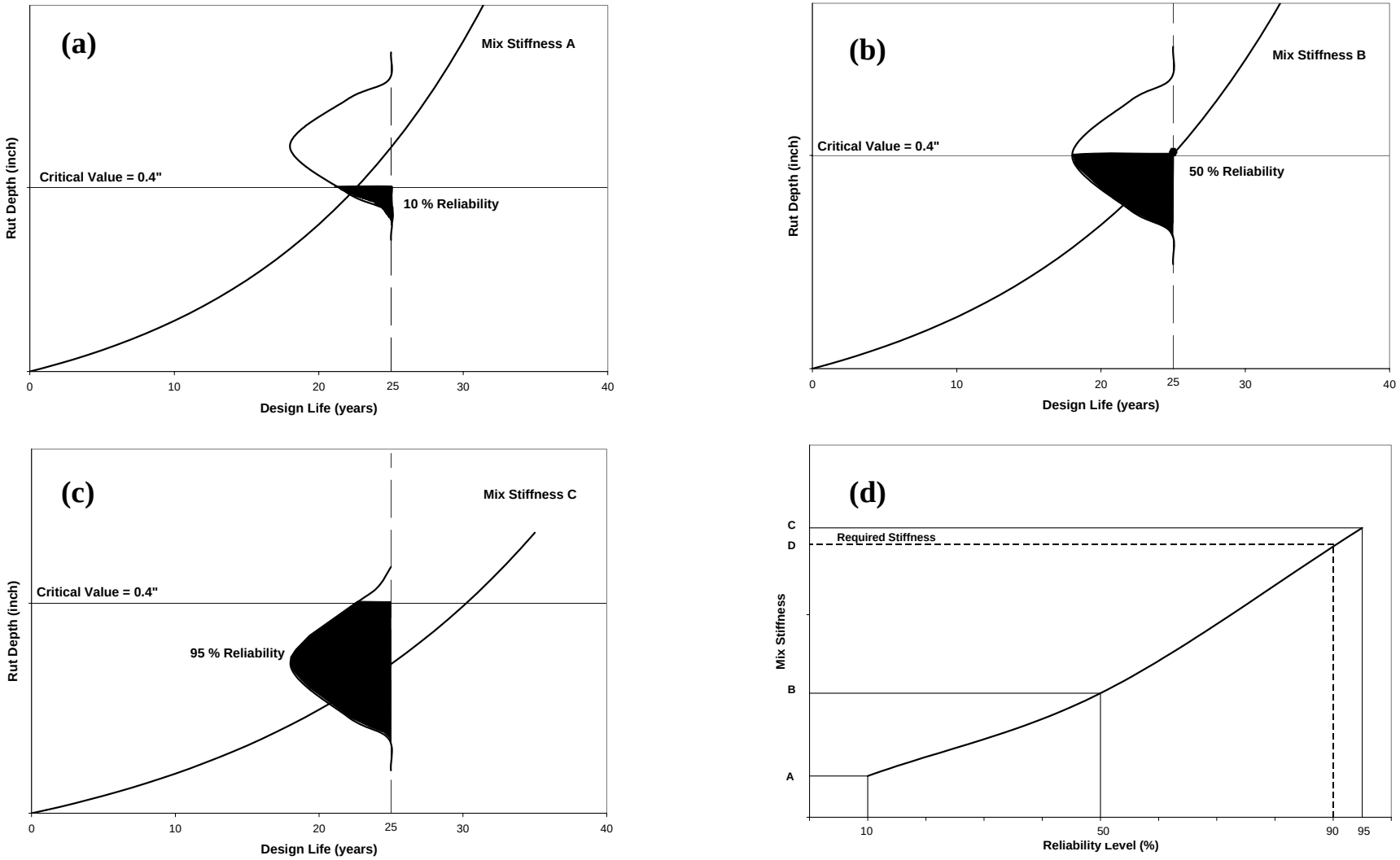

3.3.41

Figure 3.3.11. Probabilistic approach used in the Design Guide for performance prediction

.

Figure 3.3.11d can be developed to obtain the required stiffness (point D) that will exactly provide a 90 percent reliability level. In addition, figure 3.3.11c shows the performance curve intersecting the critical rut depth value at around a 30-year design life. That is, mix stiffness C will provide 50 percent reliability that the pavement will have less than 0.4 inch rutting at the end of 30 years of service life.

Additional information on the reliability analysis procedures implemented in the Design Guide can be found in Appendices BB, GG, HH, II, and MM.

3.3.4.2 Pavement Response Models

Analysis Models

The purpose of the pavement response model is to determine the structural response of the pavement system due to traffic loads and environmental influences. Environmental influences may be direct (e.g., strains due to thermal expansion and/or contraction) or indirect via effects on material properties (e.g., changes in stiffness due to temperature and/or moisture effects).

Inputs to the flexible pavement response models include:

1. Pavement geometry
    a. Layer thickness.
2. Environment
    a. Temperature vs. depth for each season.
    b. Moisture vs. depth for each season.
3. Material properties (adjusted for environmental and other effects, as necessary)
    a. Elastic properties.
    b. Nonlinear properties (where appropriate).
4. Traffic
    a. Load spectrum—i.e., frequencies of vehicle types and loads within each vehicle type.
    b. Tire contract pressure distributions and areas.

The outputs from the pavement response model are the stresses, strains, and displacements within the pavement layers. Of particular interest are the critical response variables required as inputs to the pavement distress models in the mechanistic-empirical design procedure. Examples of critical pavement response variables include:

- Tensile horizontal strain at the bottom of the HMA layer (for HMA fatigue cracking)
- Compressive vertical stresses/strains within the HMA layer (for HMA rutting)
- Compressive vertical stresses/strains within the base/subbase layers (for rutting of unbound layers)
- Compressive vertical stresses/strains at the top of the subgrade (for subgrade rutting)

Many techniques are available for determining the stresses, strains, and deformations in flexible pavement systems. Two flexible pavement analysis methods have been implemented in the Design Guide. For cases in which all materials in the pavement structure can realistically be treated as linearly elastic, the JULEA multilayer elastic theory program is used to determine the pavement response. JULEA provides an excellent combination of analysis features, theoretical rigor, and computational speed for linear pavement analyses. In cases where the unbound material nonlinearity is also considered, the DSC2D nonlinear finite element code is used instead for determining the pavement stresses, strains, and displacements.

A major advantage of MLET solutions is very quick computation times. Solutions for multiple wheel loads can be constructed from the fundamental axisymmetric single wheel solutions via superposition automatically by the computer program.

The principal disadvantage of MLET solutions is the restriction to linearly elastic material behavior. Real pavement materials, and the unbound materials in particular, often exhibit stress-dependent stiffness. The materials may even reach a failure condition in some locations, such as in tension at the bottom of the unbound base layer in some pavement structures. These nonlinearities vary both through the thickness of the layer and horizontally within the layer. Some attempts have been made to incorporate these material nonlinearity effects into MLET solutions in an approximate way (*5,6*), but the fundamental axisymmetric MLET formulation makes it impossible to include the spatial variation of stiffness in a realistic manner.

Some of the limitations of MLET solutions are the strengths of FE analysis. In particular, finite element methods can simulate a wide variety of nonlinear material behavior; the underlying finite element formulation is not constrained to linear elasticity, as is the case with MLET. Stress-dependent stiffness and no-tension conditions for unbound materials can all be treated within the finite element framework.

Analysis Locations

Each pavement response variable must be evaluated at the critical location within the pavement layer where the parameter is at its most extreme value. For a single wheel loading, the critical location can usually be determined by inspection. For example, the critical location for the tensile horizontal strain at the bottom of the HMA layer under a single wheel load is directly beneath the center of the wheel. For multiple wheels and/or axles, the critical location will be a function of the wheel load configuration and the pavement structure. Mixed traffic conditions (single plus multiple wheel/axle vehicle types) further complicates the problem, as the critical location within the pavement structure will not generally be the same over all vehicle types. The pavement response model must search for the critical location for each response parameter in these cases.

For performance prediction, it is important to identify the locations in the pavement system that will result in the maximum damage over the entire analysis period. However, for mixed traffic conditions it is not possible to specify in advance the maximum damage location. To overcome this problem, the Guide software defines the analysis locations

where the maximum damage is most likely to occur under mixed traffic. Figure 3.3.12 shows the analysis locations for the four axle types (single, dual, tridem, tandem) in the standard or general traffic condition. Damage is calculated at all these locations, and the performance prediction is based on conditions at the location producing the maximum damage.

The analysis locations defined in figure 3.3.12 are applicable both for the layer elastic analysis (JULEA) and for the FEM approach. The "X" and "Y" locations shown in plan view in figure 3.3.12 are given below:

X-Axis Locations:

X1 = 0.0 {center of dual tires/tire spacing}
X2 = $((T_{spacing}/2) - T_{radius})/2$ {$T_{spacing}$ = tire spacing; T_{radius} = tire contact radius}
X3 = $(T_{spacing}/2) - T_{radius}$X4 = $T_{spacing}/2$
X5 = $(T_{spacing}/2) + T_{radius}$
X6 = $(T_{spacing}/2) + T_{radius}$ + 4 in
X7 = $(T_{spacing}/2) + T_{radius}$ + 8 in
X8 = $(T_{spacing}/2) + T_{radius}$ + 16 in
X9 = $(T_{spacing}/2) + T_{radius}$ + 24 in
X10 = $(T_{spacing}/2) + T_{radius}$ + 32 in

Y-Axis Locations:

Y1: y = 0.0 {center of dual tires/tire spacing}
Y2: y = S_{tandem} {tandem axle spacing}
Y3: y = $S_{tandem}/2$
Y4: y = S_{tridem} {tridem/quad axle spacing)
Y5: y = $S_{tridem}/2$
Y6: y = $S_{tridem}3/2$
Y7: y = $S_{tridem}4/2$

The above discussion only related to the analysis locations in the x-y or plan view plane. Critical responses are determined at several depth locations beneath each of these locations, depending upon the distress type. The following depth locations are evaluated in the analyses:

Fatigue Depth Locations:

1. Surface of the pavement (z=0),
2. 0.5 inches from the surface (z=0.5),
3. Bottom of each bound or stabilized layer.

Rutting Depth Locations:

1. Mid-depth of each structural layer/sub-layer,

2. Top of the subgrade,
3. Six inches below the top of the subgrade.

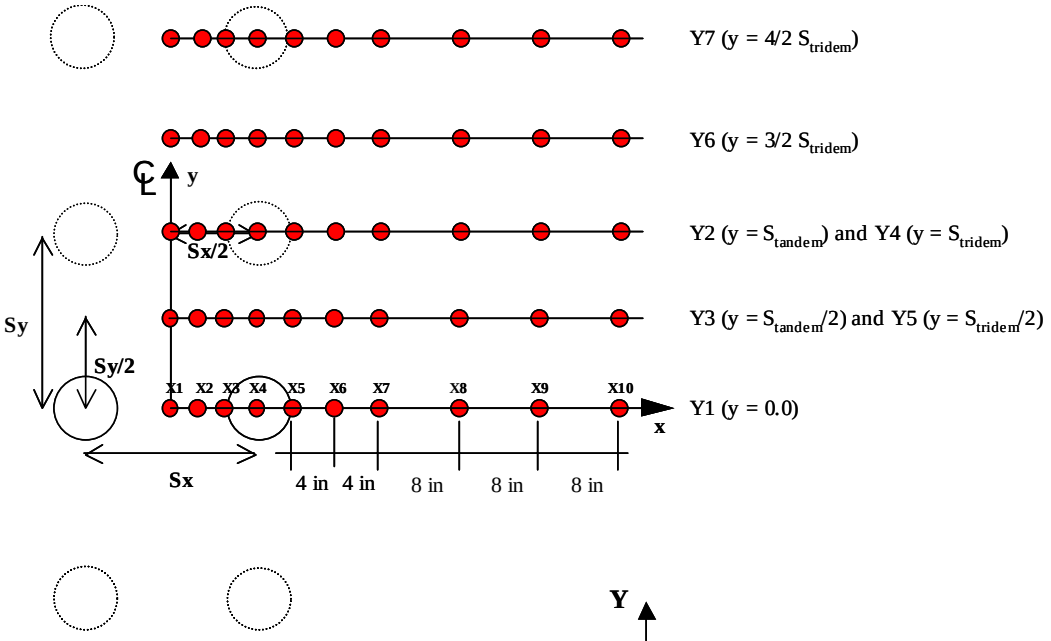

Computed Responses

- Single
  - Response 1 = Y1
- Tandem
  - Response 1 = Y1 + Y2
  - Response 2 = 2 * Y3
- Tridem
  - Response 1 = Y1 + 2 * Y4
  - Response 2 = 2 * Y5 + Y6
- Quad
  - Response 1 = Y1 + 2 * Y4 + Y7
  - Response 2 = 2 * Y5 + 2 * Y6

Figure 3.3.12. Schematics for horizontal analysis locations regular traffic.

3.3.4.3 Performance Prediction

The design and analysis of a given pavement structure is based upon the accumulation of damage as function of time and traffic. The primary distresses considered in the design guide for flexible pavements are:

- Permanent deformation (rutting).
- Fatigue cracking (bottom-up and top-down).

- Thermal cracking.

In addition, pavement smoothness (IRI) is predicted based on these primary distresses and other factors.
The Design Guide methodology is based upon an incremental damage approach. Distress or damage is estimated and accumulated for each analysis interval. An analysis interval of one month is defined as the basic unit for estimating the damage. However, the analysis interval reduces to semi-monthly during freeze and thaw periods because of the rapid change in the modulus under these conditions. The change in temperature and moisture conditions directly affects the material response and hence the performance.

The models used for the prediction of each distress are described in more detail in the following sections.

Permanent Deformation

Permanent deformation is one of the most important types of load-associated distresses occurring in flexible pavement systems. It is associated with rutting in the wheel path, which develops gradually as the number of load repetitions accumulate. Rutting normally appears as longitudinal depressions in the wheel paths accompanied by small upheavals to the sides. The width and depth of the rutting profile is highly dependent upon the pavement structure (layer thickness and quality), traffic matrix and quantity as well as the environment at the design site.
In general, the design engineer is concerned with the total deformation of the pavement structure and how it affects the lateral and longitudinal profiles at the surface, as this may be a significant safety concern. Major problems can be associated with changes in these profiles due to differential consolidation altering the surface level. In the transverse profile, rutting along the wheel path modifies drainage characteristics and reduces runoff capability. Water can accumulate in traffic lanes, creating conditions for aquaplaning of vehicles, reduced skid resistance of the surface course, and unsafe traffic conditions. Also, in colder environments, snow and ice removal is impeded because the surface is not flat. In the longitudinal profile, differential permanent deformations due to variability of materials and/or construction increase roughness and reduce the overall serviceability of the road.

For many years it has been common practice in several mechanistic-empirical pavement design approaches to associate permanent deformation to excessive vertical strains on top of the subgrade. It was assumed that if the pavement was well designed and the quality of pavement materials above the subgrade were well controlled, rutting could be reduced to tolerable levels by limiting the vertical strain on the subgrade. This approach mirrored the historic design approach for flexible pavements by assuming that structural design was merely a procedure to decrease the shear stresses in the controlling subgrade layer. Nevertheless, with time and enhanced technical capabilities and knowledge; it became quite clear to design engineers that the total permanent deformation was a product of cumulative ruts occurring in all layers of the pavement system.

One major objective of the permanent deformation subsystem developed in the Design Guide is to insure that mixture design of the asphaltic mixtures is definitely linked to the structural design process.

For the Design Guide, a predictive rutting system is available to evaluate the permanent deformation within all rut susceptible layers (generally asphaltic and all unbound material layers) in the pavement within the analysis period. Individual layer rut depths are predicted for each layer as a function of time and traffic repetition.

Regardless of the material type considered, there are generally three distinct stages for the permanent deformation behavior of pavement materials under a given set of material, load and environmental conditions. Figure 3.3.13 illustrates the three stages, which can be described as follows:

- *Primary Stage*: high initial level of rutting, with a decreasing rate of plastic deformations, predominantly associated with volumetric change.
- *Secondary Stage*: small rate of rutting exhibiting a constant rate of change of rutting that is also associated with volumetric changes; however, shear deformations increase at increasing rate.
- *Tertiary Stage*: high level of rutting predominantly associated with plastic (shear) deformations under no volume change conditions.

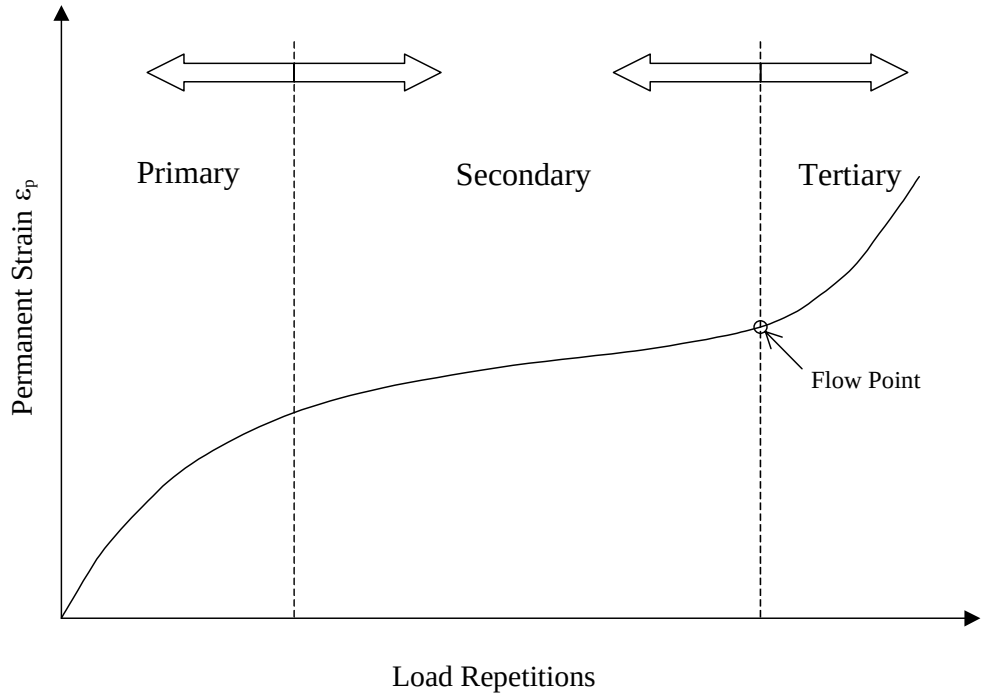

Figure 3.3.13. Typical repeated load permanent deformation behavior of pavement materials.

The Design Guide utilizes an approach that models both the primary and secondary stages, with the primary stage modeled using an extrapolation of the secondary stage trend. The tertiary stage, though also very important, is not taken into account explicitly in the Design Guide methodology. Permanent deformation tests to reach this stage are extremely time consuming, difficult to perform, and lack a prediction methodology for implementation. However, major research studies are currently in progress to analytically treat this type of deformation. It should be understood that true plastic shear deformations are not modeled within the system (in fact, few, if any, rutting prediction models incorporate this stage).

In addition to the above-mentioned limitation, it should be recognized that no permanent deformation is assumed to occur for chemically stabilized materials, bedrock, and PCC fractured slab materials. These materials are assumed to have no contribution to the total permanent deformation of the pavement system.

As previously mentioned earlier, the approach presented in the Design Guide is based upon incremental damage. The damage or rutting is estimated for each subseason at the mid-depth of each sublayer within the pavement system. To estimate the permanent deformation of each individual sublayer, the system verifies the type of layer, applies the model corresponding to the material type of the sublayer, and computes the plastic strain accumulated at the end of each subseason. The overall permanent deformation for a given season is the sum of permanent deformation for each individual layer and is mathematically expressed as:

$$RD = \sum_{i=1}^{nsublayers} \varepsilon_p^i h^i \tag{3.3.3}$$

where:

RD	=	Pavement permanent deformation
$nsublayers$	=	Number of sublayers
ε_p^i	=	Total plastic strain in sublayer i
h^i	=	Thickness of sublayer i

The process is repeated for each load level, subseason, and month of the analysis period. Within the Design Guide the permanent deformation is only estimated for the asphalt bound and unbound layers. No permanent deformation is estimated for chemically stabilized materials. The estimation of permanent deformation for asphalt bound and unbound layers is discussed in the following paragraphs.

Permanent Deformation in Asphalt Mixtures

Permanent deformation (rutting) of asphalt mixtures is one of the most important distress types in flexible pavement systems. The constitutive relationship used in the Guide to predict rutting in the asphalt mixtures is based upon a field calibrated statistical analysis of laboratory repeated load permanent deformation tests. This laboratory model form selected is:

$$\frac{\varepsilon_p}{\varepsilon_r} = a_1 T^{a_2} N^{a_3} \tag{3.3.4}$$

where:

ε_p = Accumulated plastic strain at N repetitions of load (in/in)
ε_r = Resilient strain of the asphalt material as a function of mix properties, temperature and time rate of loading (in/in)
N = Number of load repetitions
T = Temperature (deg F)
a_i = Non-linear regression coefficients

While statistical relationships evaluated from laboratory repeated load tests on asphalt mixtures, were found to be reasonable; field calibration factors, β_{ri}, were necessary to ascertain the final field distress model. The final asphalt rutting equation implemented in the Design Guide is thus of the form:

$$\frac{\varepsilon_p}{\varepsilon_r} = \beta_{r1} a_1 T^{a_2 \beta_{r2}} N^{a_3 \beta_{r3}} \qquad (3.3.5)$$

It is a relatively simple equation to use in the implementation process. The final lab expression that was initially selected for the field calibration / validation process was:

$$\frac{\varepsilon_p}{\varepsilon_r} = 10^{-3.15552} T^{1.734} N^{0.39937} \qquad (3.3.6)$$

R^2 = 0.644
N = 3476 observations
S_e = 0.321
S_e/S_y = 0.597

This model shown in equation 3.3.6 was based on extensive research work conducted by Leahy (*7*), Ayers (*8*), and Kaloush (NCHRP 9-19: "Superpave Models" [*9*]). Appendix GG-1 contains more details related to the model selection and development.

The national field calibrated model used in the Design Guide was determined by numerical optimization and other modes of comparison to result in national calibration factors of:

β_{r1} = 0.509
β_{r2} = 0.9
β_{r3} = 1.2

This resulted in the final model shown below:

$$\frac{\varepsilon_p}{\varepsilon_r} = k_1 * 10^{-3.4488} T^{1.5606} N^{0.479244} \qquad (3.3.7)$$

In this equation it can be observed that a depth parameter "k_1"has been introduced to provide as accurate a rut depth prediction model as possible. This analysis was completed by utilizing trench studies from the MnRoad test site.

$$k_1 = (C_1 + C_2 * depth) * 0.328196^{depth} \quad (3.3.8a)$$

$$C_1 = -0.1039 * h_{ac}^2 + 2.4868 * h_{ac} - 17.342 \quad (3.3.8b)$$

$$C_2 = 0.0172 * h_{ac}^2 - 1.7331 * h_{ac} + 27.428 \quad (3.3.8c)$$

where,

k_1 = function of total asphalt layers thickness (h_{ac}, in) and depth (*depth*, in) to computational point, to correct for the confining pressure at different depths

R^2 = 0.648
N = 387 observations
S_e = 0.063 in
S_e/S_y = 0.574

The rutting model for new pavement systems has been partially calibrated based on 88 LTPP new sections located in 28 states. Time-series data were available for many of the sections, making the total number of field rutting observations 387. Appendix GG-1 contains a detailed explanation of the calibration process and data used for the calibration of the asphalt-rutting model.

Figure 3.3.14 shows the plot of the predicted versus the estimated measured asphalt rutting. The observed rutting in the LTPP sections were reported as the average total rutting of the measured at the surface in the left and right lanes. However, to obtain the rutting in individual layers, the percentage from the predicted sublayer rutting was multiplied by the average total rutting to approximate the rutting in each layer. This approach is applicable to the rutting in the granular and subgrade layers. This critical assumption was necessary in the rutting model development because trench (layer rut depth) data were not available.

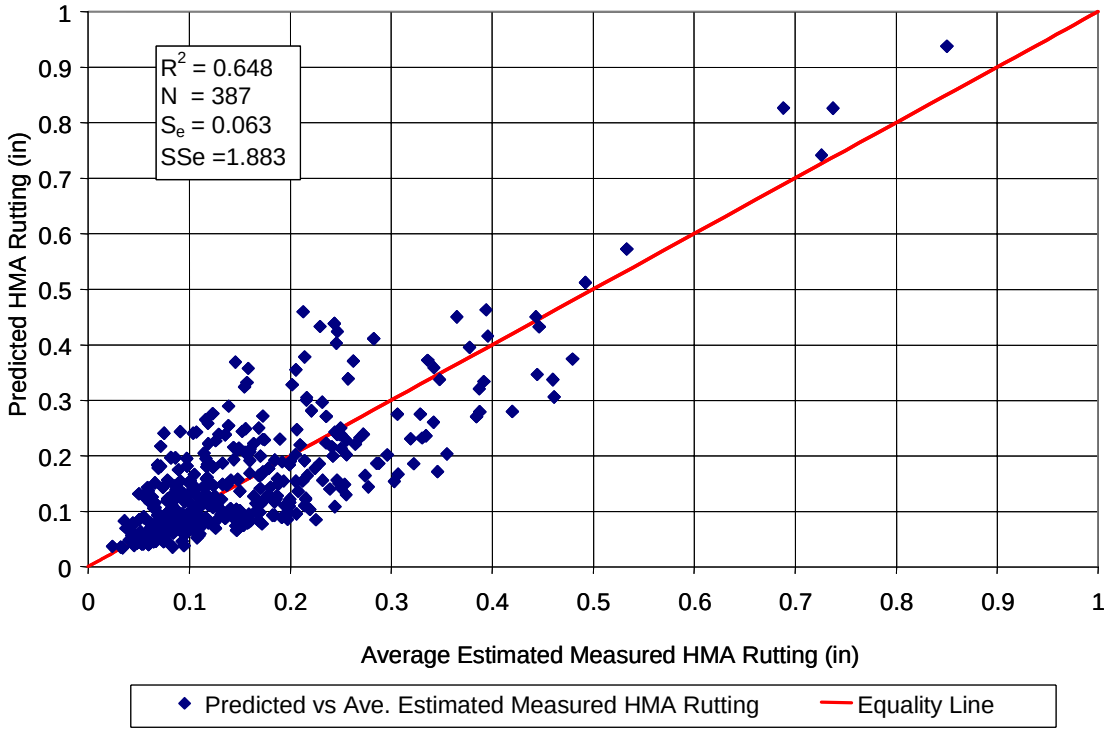

Figure 3.3.14. Nationally calibrated predicted versus estimated measured asphalt rutting.

Permanent Deformation in Unbound Materials

The initial model framework used to predict the permanent deformation in unbound material layers was that proposed by Tseng and Lytton (*10*). The basic relationship is:

$$\delta_a(N) = \beta_1 \left(\frac{\varepsilon_0}{\varepsilon_r} \right) e^{-\left(\frac{\rho}{N}\right)^{\beta}} \varepsilon_v \, h \qquad (3.3.9)$$

where:

δ_a = Permanent deformation for the layer/sublayer (in).
N = Number of traffic repetitions.
ε_o, β, and ρ = Material properties.
ε_r = Resilient strain imposed in laboratory test to obtain the above listed material properties, ε_o, β, and ρ (in/in).
ε_v = Average vertical resilient strain in the layer/sublayer as obtained from the primary response model (in /in)
h = Thickness of the layer/sublayer (in).
β_1 = calibration factor for the unbound granular and subgrade materials

During the development process and field calibration studies, numerous modifications were necessary to determine a final reasonable calibrated relationship. Detailed explanations of the modifications made are included in Appendix GG-1. Changes leading

to the elimination of the stress term in the model, major simplifications to the "β" and "ρ" equations and an eventual combination of all unbound granular and subgrade materials into one model were accomplished. The modified models developed are:

$$\log \beta = -0.61119 - 0.017638\, W_c \tag{3.3.10a}$$

$$\log\left(\frac{\varepsilon_0}{\varepsilon_r}\right) = \frac{(e^{(\rho)^\beta} * a_1 E_r^{b_1}) + (e^{(\rho/10^9)^\beta} * a_9 E_r^{b_9})}{2} \tag{3.3.10b}$$

$$C_o = \ln\left[\frac{(a_1 E_r^{b_1})}{(a_9 E_r^{b_9})}\right] \tag{3.3.10c}$$

$$\rho = 10^9\left[\frac{C_o}{\left(1-(10^9)^\beta\right)}\right]^{\frac{1}{\beta}} \tag{3.3.10d}$$

$$W_c = 51.712\left[\left(\frac{E_r}{2555}\right)^{\frac{1}{0.64}}\right]^{-0.3586*GWT^{0.1192}} \tag{3.3.10e}$$

where:

W_c = Water content (%).
E_r = Resilient modulus of the layer/sublayer (psi).
GWT = Ground water table depth (ft).
a1 = 0.15
b1 = 0.0
a9 = 20.0
b9 = 0.0

The final calibrated model for the unbound granular base is as follows:

$$\delta_a(N) = \beta_{GB}\left(\frac{\varepsilon_0}{\varepsilon_r}\right) e^{-\left(\frac{\rho}{N}\right)^\beta}\, \varepsilon_v\, h \tag{3.3.11}$$

with the national calibration factor of β_{GB} = 1.673 being determined.

R^2 = 0.677
N = 387 observations
S_e = 0.023 in
S_e/S_y = 0.524

Figure 3.3.15 shows the plot of the predicted versus the estimated measured granular base rutting. The model statistics are shown in the graph.

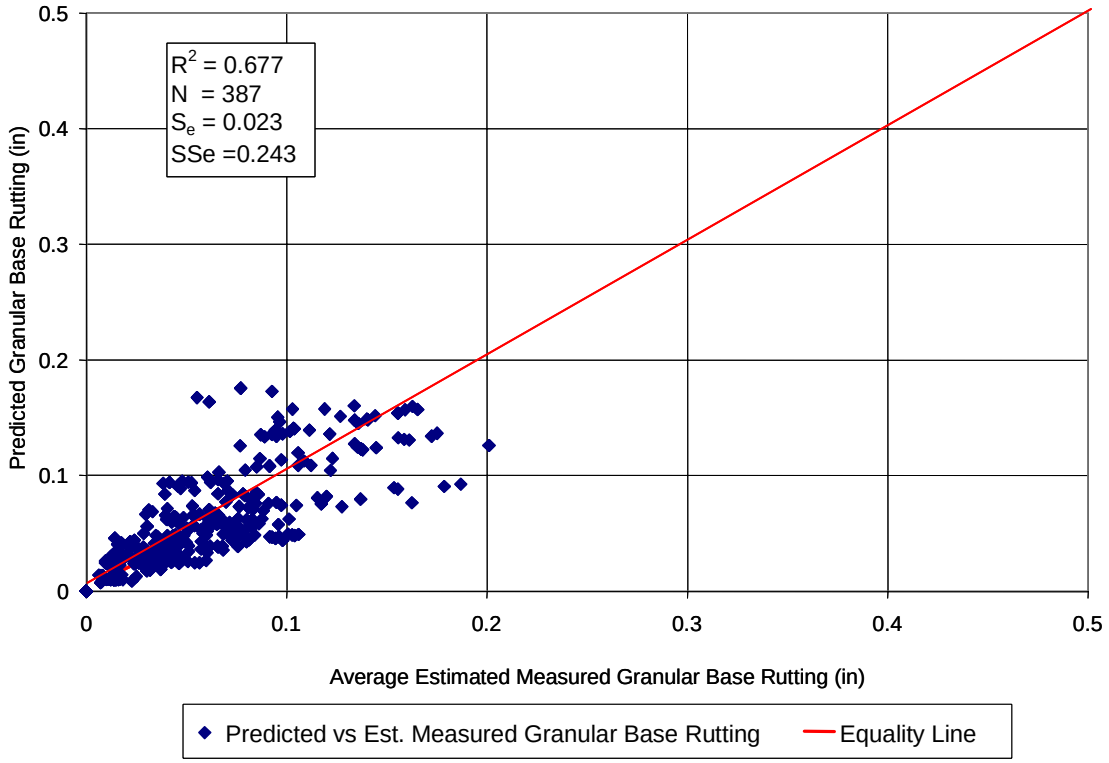

Figure 3.3.15. National calibrated predicted versus estimated measured granular base rutting.

The final calibrated model for all subgrade soils is as follows:

$$\delta_a(N) = \beta_{SG}\left(\frac{\varepsilon_0}{\varepsilon_r}\right)e^{-\left(\frac{\rho}{N}\right)^{\beta}}\varepsilon_v\, h \qquad (3.3.12)$$

with the national calibration factor of β_{GB} = 1.35 being determined.

R^2 = 0.136
N = 387 observations
Se = 0.045 in
Se/Sy = 0.850

Both rutting models were calibrated based on 88 LTPP new sections located in 28 states. Time-series data were available for many of the sections, making the total number of field rutting observations 387. In addition, comparative studies involving general comparisons of unbound rutting levels for AASHTO Design Guide (current) pavement structures also, provided valuable insight into the final selection. Appendix GG-1 contains detailed explanation of the calibration process and data used for the calibration

of the rutting model. Figure 3.3.16 shows the plot of the predicted versus the estimated measured subgrade rutting. The model statistics are shown in the graph.

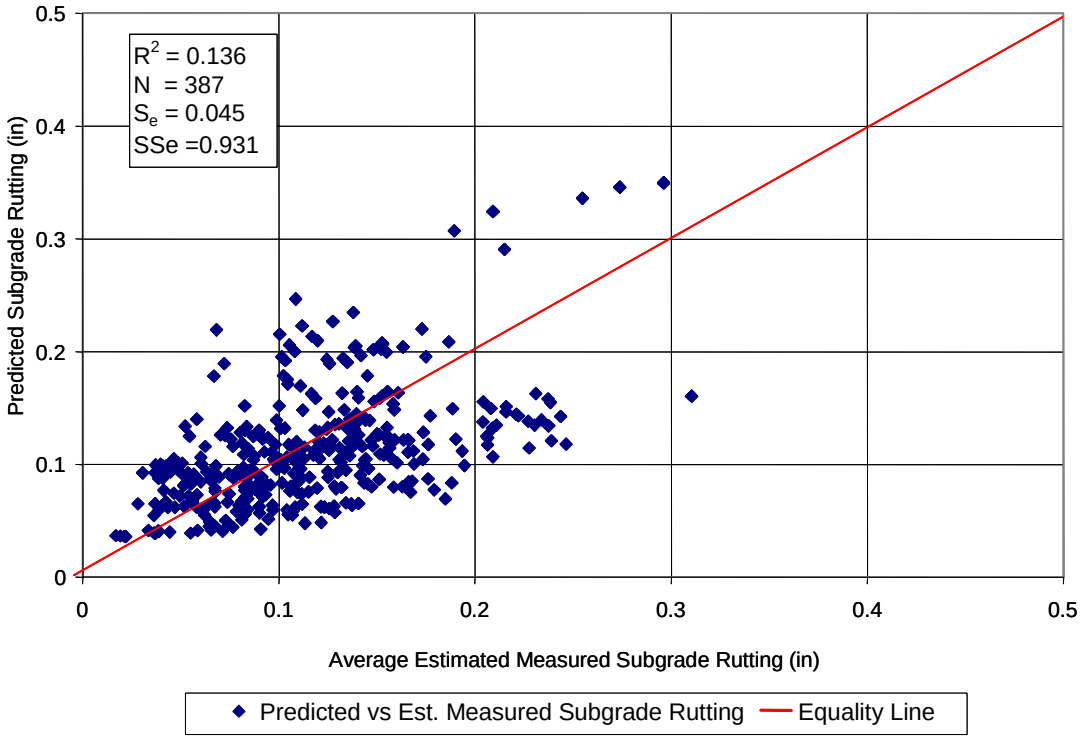

Figure 3.3.16. National calibrated predicted versus estimated measured subgrade rutting.

Permanent Déformation of Total Pavement Structure

The total rutting in the pavement structure is equal to the summation of the individual layer permanent deformation for each season. The total rutting can be expressed by the following equation:

$$RD_{Total} = RD_{AC} + RD_{GB} + RD_{SG} \qquad (3.3.13)$$

The statistical summary of the comparison between the total rut depth predicted and the total rut depth measured is as follows:

R^2 = 0.399
N = 387 observations
Se = 0.121 in
Se/Sy = 0.822

The permanent deformation in the asphalt, granular base / subbase, and subgrade layers are shown in equations 3.3.7, 3.3.11, and 3.3.12, respectively. The rutting model was calibrated based on 88 LTPP sections located in 28 States.

Appendix GG-1 contains detailed explanation of the calibration process and data used for the calibration of the total pavement-rutting model. Figure 3.3.17 shows the plot of the predicted versus the measured total rutting with the model statistics shown on the graph.

Factors Affecting Permanent Deformation in Flexible Pavements

Many factors affect the permanent deformation in the pavement layers. Some of these factors can be controlled or modified, while the rest are external factors that cannot be controlled. The following factors affect the amount of the permanent deformation in different layers of the pavement structure:

- HMA layer thickness
- HMA layer dynamic modulus
- Binder grade in the HMA mixture
- Air voids in the asphalt layers

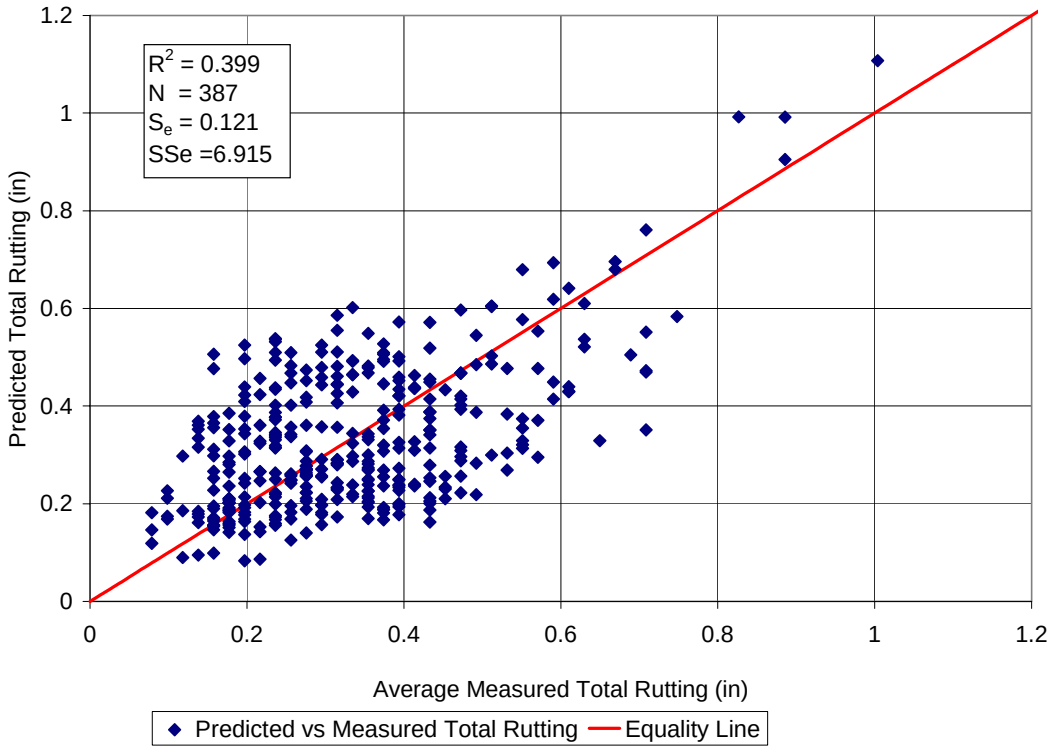

Figure 3.3.17. National calibrated predicted versus average measured total rutting.

- Effective binder content in the asphalt layers
- Base type
- Base thickness
- Base stiffness
- Traffic load, contact area and tire pressure
- Traffic operating speed

- Traffic wander
- Temperature and environmental conditions

While many of the parameters above remain constant throughout the design period (e.g., layer thickness), others vary seasonally, monthly, hourly, or with pavement age. For accurate results, all cases that produce significantly different stresses must be evaluated separately. The rut accumulation defined in this Guide was determined to account for those cases as follows:

Pavement age – accounts for the changes in HMA dynamic modulus and hardening of the asphalt binder.

Month – accounts for monthly variations in surface and pavement temperatures, which affects the HMA dynamic modulus, as well as, the moisture variation in the subgrade and base layers. It can be a semi-monthly period if freezing and thawing exists.

Traffic speed (loading frequency) – affect on the dynamic modulus of the HMA mixture.

Load configuration -Single, tandem, tridem, and quad
Load level –

- Single axles – 3,000 to 41,000 lb in 1,000-lb increments.
- Tandem axles – 6,000 to 82,000 lb in 2,000-lb increments.
- Tridem axles – 12,000 to 102,000 lb in 3,000-lb increments.
- Quad axles – 12,000 to 102,000 lb in 3,000-lb increments.

Traffic Wander – Contained traffic to a fixed path causes the load to be concentrated at a certain location, which leads to higher rutting at this location. However, the use of a general wheel wander width will reduce the load concentration and hence, reduce the layer rutting.

Temperature and environmental conditions –

- Temperature is an important factor affecting the asphalt stiffness and consequently the dynamic modulus of asphalt concrete mixes. Because the modulus of the asphalt layers within the pavement structure affect the overall pavement response, it is important to properly account for the temperature as a function of time and depth.
- Environmental conditions are represented by the moisture change in the subgrade and granular soil. The moisture content change is the most important factor for the amount of rutting for a given type of unbound materials. This is due to the fact that increasing the moisture content in an unbound layer will lead to a decrease in the resilient modulus of the layer. For all conditions remaining the same, this will lead to a greater elastic (resilient) strain and therefore more rutting. During the freezing season, the moisture will freeze and the layer greatly

increases in stiffness. This will result in (for all practical purpose) no rutting to occur.

Permanent Deformation Prediction Procedure

To predict rutting for flexible pavements certain steps are needed to be followed, these steps are summarized below:

1. Tabulate input data – summarize all inputs needed for predicting rutting.
2. Process traffic data – the processed traffic data needs to be further processed to determine equivalent number of single, tandem, and tridem axles produced by each passing of tandem, tridem, and quad axles.
3. Process pavement temperature profile data – the hourly pavement temperature profiles generated using EICM (nonlinear distribution) need to be converted to distribution of equivalent linear temperature differences by calendar month.
4. Process monthly moisture conditions data – the effects of seasonal changes in moisture conditions on base subgrade modulus.
5. Calculate stress and strain states – calculate stress corresponding to each load, load level, load position, and temperature difference for each month within the design period at the mid depth of each layer. Using material modulus and Poisson's ratio; determine the elastic strains at each computational point.
6. Calculate permanent deformation – calculate rutting for each sub-season and sum to determine accumulated rutting in each layer.

Step 1: Tabulate input data

All input data required for the prediction of permanent deformation is explained in details in PART 2, Chapter 2 Material characterization.

Step 2: Process traffic data

The traffic inputs are first processed to determine the expected number of single, tandem, tridem, and quad axles in each month within the design period. This procedure is described in detail in PART 2, Chapter 4.

Step 3: Process temperature profile data

A base unit of one month is typically used for damage computations. In situations where the pavement is exposed to freezing and thawing cycles, the base unit of one month is changed to 15-days (half month) duration to account for rapid changes in the pavement material properties during frost/thaw period. While damage computations are based on a two-week or monthly average temperature; the influence of extreme temperatures, above and below the average, are directly accounted for in the design analysis. In order to include the extreme temperatures during a given month (or during 15 days for freeze/thaw period), the following approach had been used in the analysis scheme.

The solution sequence from the EICM provides temperature data at intervals of 0.1 hours (6 minutes) over the analysis period. This temperature distribution for a given month (or

15-days) can be represented by a normal distribution with a certain mean value (μ) and the standard deviation (σ), $N(\mu,\sigma)$ as shown in Figure 3.3.18.

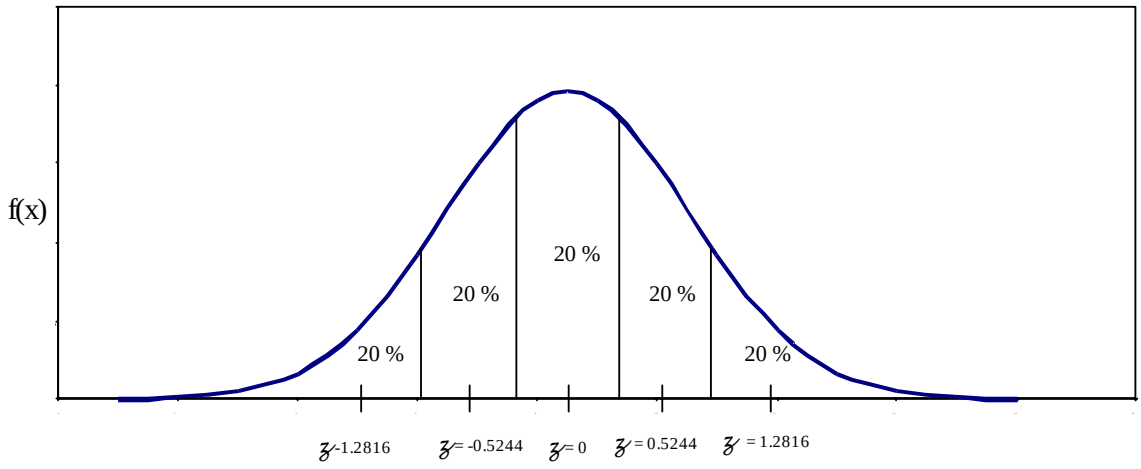

Figure 3.3.18. Temperature distribution for a given analysis period

The frequency distribution of temperature data obtained using EICM is assumed to be normally distributed as depicted in figure 3.3.18. The frequency diagram obtained from the EICM represents the distribution at a specific depth and time. Temperatures in a given month (or bi-monthly for frost/thaw) may have extreme temperatures (even at a low frequency of occurrence) that could be significant for rutting.

Using the average temperature value will not capture the damage caused by these extreme temperatures. In order to account for the extreme temperature, the temperatures over a given interval are divided into five different sub-seasons. For each sub-season the sub-layer temperature is defined by a temperature that represents 20 % of the frequency distribution of the pavement temperature. This sub-season will also represent those conditions when 20% of the monthly traffic will occur. This is accomplished by computing pavement temperatures corresponding to standard normal deviates of -1.2816, -0.5244, 0, 0.5244 and 1.2816. These values correspond to accumulated frequencies of 10, 30, 50, 70 and 90 % within a given month.

Step 4: Process monthly moisture conditions data

EICM calculates the moisture content and corrects for the moisture change in the unbound layer. Refer to PART 2, Chapter 3 for detailed explanation of the method used to correct the unbound layer modulus.

Step 5: Calculate stress

It is necessary to use the pavement response model for the layered pavement structure to calculate stresses (strains) for all cases that needs to be analyzed. The number of cases depends on the damage increment. The following increments are considered:

- Pavement age – by year.

- Season – by month or semi-month.
- Load configuration – axle type.
- Load level – discrete load levels in 1,000 to 3,000 lb increments, depending on axle type.
- Temperature – pavement temperature for the HMA dynamic modulus.

The damage increments and stress calculation are discussed in the following section.

Given a particular layered pavement cross section, the vertical resilient strain at any given depth (along a vertical axis, defined in the *x*, *y* plane) is defined by knowledge of the three-dimensional stress state and the elastic properties (modulus and Poisson's ratio) of the HMA layer in question from:

$$\varepsilon_{rz} = \frac{1}{E^*}(\sigma_z - \mu\sigma_x - \mu\sigma_y) \qquad (3.3.14)$$

The complex moduli of asphalt mixtures are employed in the Design Guide via a master curve. Thus, E^* is expressed as a function of the mix properties, temperature, and time of the load pulse.

Knowledge of the predicted vertical resilient strain at any point, along with the ε_p relationship, allows for the direct calculation of the plastic strain, ε_p, at any given point within the asphalt layer, after N repetitions of load, to be computed.

The incremental rut depth for each sublayer in the HMA layer can be found from:

$$\Delta RD_i = \varepsilon_{p_i} . \Delta h_i \qquad (3.3.15)$$

Finally, by simply summing all incremental ΔRD_i through the entire layer, one can obtain the total layer rut depth from:

$$RD = \sum_{i=1}^{n} \Delta RD_i \qquad (3.3.16)$$

Step 6: Calculate permanent deformation

Models for permanent deformation in the Design Guide provide the plastic strain under specific pavement conditions for a total number of load repetitions. Because conditions vary from one season to another (e.g., temperature, resilient strain, moisture) and it is necessary to account for the total plastic deformation up to the specific season *i*, it is necessary to use a special approach called the strain hardening approach, to incorporate these variable parameters in a cumulative deformation subsystem.

For the general solution, permanent deformation is estimated for each layer at each computational location using pavement responses calculated at the mid-depth of each sublayer.

Computations of permanent deformations are done at locations defined by the analysis module for regular traffic. Alternatively, for special wheel configurations, the user is allowed to select the location points of interest for evaluation. In the following model description, the equivalent number of load cycles for each subseason is found by solving the permanent deformation model for *N* with the deformation accumulated up to the current subseason and the material properties and load conditions prevailing in the current subseason.

The approach is illustrated in figure 3.3.19 for a model of the form:

$$\varepsilon_p = f(\varepsilon_r, T, N) \tag{3.3.17}$$

where:

ε_p = Total plastic strain (in/in).
ε_r = Resilient strain which is related to the dynamic modulus (E*) of the mix and other mixture properties (in/in).
T = Temperature (deg. F).
N = Total number of load cycles (given axle type and load).

The total plastic strain $\varepsilon_{p,i-1}$ at the end of subseason *i-1* corresponds to a total number of traffic repetitions Nt_{i-1} (point A). In the next subseason *i*, the layer temperature is T_1 and resilient strain for load and material conditions prevailing in *i* is $\varepsilon_{r,i}$.

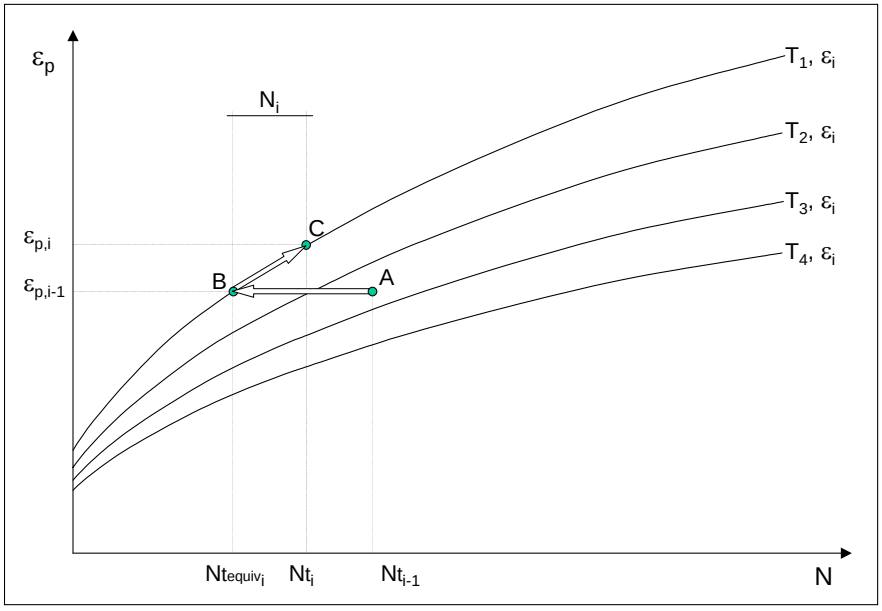

Figure 3.3.19. Permanent deformation approach.

At the beginning of the next subseason *i* (point B), there is an equivalent number of traffic repetitions $Nteq_i$ that is associated with the total deformation at the end of subseason *i-1* but under conditions prevailing in the new sub-season (T_1, $\varepsilon_{r,i}$). The

approach is necessary because models for permanent deformation provide an estimate of the total deformation rather than the increment in plastic strain due to seasonal traffic.

By adding the number of traffic repetitions at season *i* (N_i) to the total equivalent number of repetitions $Nteq_i$, using the specific material model, it is possible to estimate point C, which corresponds to the total plastic strain at the end of sub-season *i*.

For subgrade layers, the approach presented must be adjusted to account for layers with very large depths and, sometimes, for practical purposes, a layer with an infinite depth. Therefore, in many cases, it would not be feasible to divide a thick subgrade into sublayers and compute plastic strains at middepth of each sublayer in order to estimate the total subgrade permanent deformation, due to the huge computational effort involved.

An alternative approach was suggested by Ayres (*8,11*) to evaluate the plastic strain for an infinite layer. Pavement responses at three different horizontal locations for various depths from the top of the subgrade, ranging from 0 to 150 inches, were obtained for several pavement structures. Overburden stresses resulting from the materials above the computational points were added to the load-induced stresses.

Using the model for subgrade materials provided by Tseng and Lytton, plastic strains were calculated for the computational locations within the subgrade. The plastic strain trend along each of the three vertical axes previously selected was evaluated using numerical optimization techniques. This analysis indicated that the following model structure provides an R^2 exceeding 97 percent:

$$\varepsilon_p(z) = (\varepsilon_{p,z=0})\, e^{-k\,z} \qquad (3.3.18)$$

where:

$\varepsilon_p(z)$	=	Plastic vertical strain at depth z (measured from the top of the subgrade).
$\varepsilon_{p,z=0}$	=	Plastic vertical strain at the top of the subgrade (z = 0)
z	=	Depth measured from the top of the subgrade.
k	=	Constant obtained from regression.

Using this assumption, the procedure to estimate the total permanent deformation of the subgrade follows the procedure described below:

- Compute pavement response at the top of the subgrade and at a depth of 6 inches from the top of the subgrade (resilient strain and deviator stress)
- Using the models already described for subgrade materials, compute parameters $\left(\frac{\varepsilon_o}{\varepsilon_r}\right)$, β and ρ at the two depths, z = 0 and z = 6 in.
- Using the parameters previously computed, estimate the plastic strain for both depths as:

$$\varepsilon_p = \left(\frac{\varepsilon_o}{\varepsilon_r}\right) e^{-\left(\frac{\rho}{N}\right)^{\beta}} \varepsilon_v \tag{3.3.19}$$

- Using the model structure described and the two data points, solve for k:

$$k = \frac{1}{6}\ln\left(\frac{\varepsilon_{p,z=0}}{\varepsilon_{p,z=6}}\right) \tag{3.3.20}$$

  In the above equation, the assumption is made that the strains at the top of the subgrade are larger than the strains at 6 inches below the subgrade. However, this is not true in all situations, and the reverse happens in some situations, invalidating the assumption resulting in a negative k value. This will result in increased permanent strain with depth resulting in inaccurate permanent deformation predictions for the subgrade. This can happen because of the overlapping stresses because of multiple wheel configurations.

  To overcome this problem, a limiting value of k equal to 0.000001 has been used in the program. This assumption will not cause any significant error in the results since the subgrade is divided into several sub-layers and the contribution for the lower sub-layer should be negligible. This approach is only used for the last subgrade layer, which is 8 feet below the surface, as explained in section 3.3.3.6.

- The plastic deformation of the subgrade is given by the following relationship:

$$d\delta = \varepsilon_p(z)\, dz \tag{3.3.21}$$

- The total permanent deformation is found by solving the following integral:

$$\delta = \int_0^{h_{bedrock}} \varepsilon_p(z)\, dz \tag{3.3.22}$$

or:

$$\delta = \varepsilon_{p,z=0} \int_0^{h_{bedrock}} e^{-k\,z}\, dz = \left(\frac{1 - e^{-k h_{bedrock}}}{k}\right) \varepsilon_{p,z=0} \tag{3.3.23}$$

where:

δ = Total plastic deformation of the subgrade, in.
$h_{bedrock}$ = Depth to bedrock, feet (z=0 represents top of subgrade)

The stresses and strains computed by the pavement response model, combined with the overburden stresses calculated by the program, are used in the permanent deformation models available. Vertical resilient strain at the mid-depth of the layer are required.

The stresses and strains are always computed at the mid depth location of each layer/sublayer of the pavement structure, except for the subgrade. Subgrade response is estimated at the interface between subgrade and lowermost pavement layer and also at a depth of 6 inches from this interface, as previously described.

Finally, there is one consideration for predicting rutting within near surface HMA sublayers. For linear elastic analysis using the JULEA multilayer elastic program, the program also estimates the vertical strains for sublayers that are too close to the surface for multi-layer elastic analysis. This occurs when the layer mid-depth location is between the surface and a depth not exceeding 20 percent of the tire contact area radius. The process for obtaining these strains at shallow depths is to interpolate linearly between this response at the surface and at the depth corresponding to this minimum value.

Permanent Deformation Reliability

The reliability design is obtained by determining the predicted rutting at the desired level of reliability as follows:

$$RD\_P = \sum_i \left(\overline{RD}_i\right) + \left(\sqrt{Se_{RDAC}{}^2 + Se_{RDGB}{}^2 + Se_{RDSG}{}^2}\right) * Z_p \quad (3.3.24)$$

where,

RD_P = predicted rutting at the reliability level P, inch.
RD_i = predicted rutting based on mean inputs (corresponding to 50% reliability), inch.
Se_{RDi} = standard error of rutting at the predicted level of mean rutting
Z_P = standard normal deviate (one-tailed distribution).
i = *layer type, HMA, base, or subgrade.*

$$Se_{RDAC} = 0.1587\ RD_{ac}{}^{0.4579} \quad (3.3.25a)$$

$$Se_{RDGB} = 0.1169\ RD_{GB}{}^{0.5303} \quad (3.3.25b)$$

$$Se_{RDSG} = 0.1724\ RD_{SG}{}^{0.5516} \quad (3.3.25c)$$

Appendix BB includes details of the reliability and the standard error computations.

Modification of Flexible Design to Reduce Permanent deformation

If the predicted rutting is greater than the design requirements, the trial design must be modified to increase structural capacity and for the quality of materials used in all layers. Different design parameters have a different impact on different performance measures.

The first thing that the engineer needs to accomplish is to critically evaluate the initial predicted rut depth quantities by layer material type in the first (trial) design run. This is an extremely important step as the design option (modifications) must be consistent with the layer(s) having the greatest rut depth predictions. For practical purposes, the discussion that follows is based upon which material layer is yielding the greatest percentage of the total pavement rut depth.

HMA Layer Rutting

If the major source of rutting occurs in the HMA asphalt layer; one major design consideration would be to increase the quality of the HMA layer being placed. In the Design Guide approach, the direct factor that can be controlled is to increase the HMA mixture stiffness (modulus) by increasing the mix Master Curve location. This can be accomplished by using a stiffer grade of binder, using less asphalt and insuring that field compaction specifications are fully complied with. In addition, all of the known, historic factors that tend to enhance the stability of a HMA mixture must also be considered in the mix design phase (i.e. crushed particles, nominal maximum aggregate size etc…). If this is accomplished, it will be very important to insure that all other HMA related distresses, such as fatigue and thermal fracture, are not increased to the point where they exceed their own distress target criteria.

Another important consideration that the Engineer should recognize is the fact that the majority of all rutting in the HMA layer will generally occur within the top 3- to 5-in. Thus, if a poor quality HMA mixture is being used, increasing the thickness of this poor quality layer will not decrease the rutting in the HMA layer. In fact, in all likelihood, the rutting will be increased. Thus, increasing the thickness of a HMA layer, of poor quality, will provide absolutely no benefit to having the total pavement rut depth decreased.

Finally, if the engineer is convinced that the HMA mix design is adequate, increases in the HMA layer thickness may be evaluated to ascertain to what degree, the potential HMA layer rut can be decreased. In general, this decrease may not be significant. However, as will be explained in the next section, increasing the HMA thickness will definitely provide benefits to decreasing the layer rut depth in the unbound base, subbase and particularly, the subgrade layer.

Unbound Base / Subbase Rutting

As a general rule, the prediction of rutting within unbound bases and subbases will typically not be a major problem when current material and construction specifications are adhered to in the design. If rutting is above typical desired target values, the engineer should increase (improve) the quality (CBR or R-value) of the unbound layer in question. The use a CSM (chemically stabilized layer) will tend to eliminate the rutting problem within the base / subbase layer. This action will also tend to decrease the potential for rutting within sublayers (subgrade) below the base / subbase system. As a general rule, if any of the layers within the base / subbase are of poor quality; increasing the thickness of the poor layer will only tend to increase the rutting, not decrease it. Finally, the presence of excess moisture in any base / subbase layer (particularly, as the layer material has ab

increasing level of fines) is a very direct way to decrease the modulus value of the layer material. As the modulus is decreased, the resilient strain is significantly increased and as a consequence, the rutting is greatly increased. This magnifies the need to have highly drainable base / subbase systems present in any design.

Unbound Subgrade Rutting

For all practical purposes, it may be reasonable to anticipate that the initial trial deign analysis will lead to larger than tolerable rut depths within the foundation (subgrade) levels. In order to reduce the rutting magnitude in the subgrade layers; the engineer should understand and recognize that all factors that tend to increase the overall stiffness and rigidity of the entire pavement structure that lies over the subgrade, will tend to reduce the rutting in the subgrade layers. This is to say, that any design modifications that will increase the layer stiffness and / or layer thickness of any layers above the subgrade layers will have a tendency to reduce the resilient strain, and hence plastic strain, in the subgrade layers. The net effect of this action will be to have a reduced subgrade rut depth prediction.

In general, the use of added HMA layers accomplishes two significant factors. First, the increased modulus of the thicker layer will result in a significant increase in the layer "relative stiffness". This will cause a reduction in the stress and strain states in the subgrade, which will reduce the rut depth magnitude. As previously noted, the use of CSM layers will accomplish the same impact as increasing the thickness of the HMA layer. Finally, an effective way in which the rutting in the subgrade can be reduced is to increase the thickness of the unbound subbase layer. This effectively, reduces the stress (strain) states in the subgrade layers that lead to a reduced rut depth magnitude in the subgrade.

Finally, while all of the previous design considerations have focused on changes in the overlying pavement layer structure to reduce the resulting subgrade strain; the final design considerations by the engineer should focus upon all design activities that will increase the stiffness (modulus) of the subgrade layer(s) itself. By far, the most important consideration in increasing the subgrade modulus relates to the ability to protect this critical layer from the detrimental effects of moisture. Increasing the in-situ moisture, by only a few percent, can lead to very significant changes in the subgrade strength (modulus). Design options that are available to consider to minimize (eliminate) excessive subgrade rutting are: the use of treated subgrade with lime, cement etc; efficient utilization of subsurface drainage systems; goetextile fabrics; impenetrable moisture barrier wraps and even consideration of increasing the road grade elevation to increase the distance of the GWT (ground water table) to the surface of the subgrade itself.

Fatigue Cracking

Load-associated fatigue cracking is one of the major distress types occurring in flexible pavement systems. The action of repeated traffic loads induces tensile and shear stresses in the bound layers, which eventually lead to a loss in the structural integrity of a

stabilized layer. Repeated load or fatigue initiates cracks at points where the critical tensile strains and stresses occur. The location of the critical strain/stress is dependent upon several factors. The most important is the stiffness of the layer and the load configuration. In addition, it should be realized that the maximum tensile strain developed within the pavement system might not be the most critical or damaging value. This is because the critical strain is a function of the stiffness of the mix. Since the stiffness of an asphalt mix in a layered pavement system varies with depth, these changes will eventually effect the location of the critical strain that causes fatigue damage. Once the damage initiates at the critical location, the continued action of traffic eventually causes these cracks to propagate through the entire bound layer.

Propagation of the cracks throughout the entire layer thickness will allow water to seep into the lower unbound layers, weakening the pavement structure and reducing the overall performance. This will result in a significant loss in smoothness causing a decrease in pavement rideability (adapted after *12*). This phenomenon of crack initiation and then propagation through the entire layer occurs not only in the surface layer but also in all the stabilized layers underneath. Cracking in the underlying layer, such as the cement stabilized, reduces the overall structural capacity and may induce reflective cracking in the upper layers.

Over the last 3 to 4 decades of pavement technology, it has been common to assume that fatigue cracking normally initiates at the bottom of the asphalt layer and propagates to the surface (bottom-up cracking). This is due to the bending action of the pavement layer that results in flexural stresses to develop at the bottom of the bound layer. However, numerous recent worldwide studies have also clearly demonstrated that fatigue cracking may also be initiated from the top and propagates down (top-down cracking). This type of fatigue is not as well defined from a mechanistic viewpoint as the more classical "bottom-up" fatigue. In general, it is probably due to critical tensile and/or shear stresses developed at the surface and caused by extremely large contact pressures at the tire edges-pavement interface; coupled with highly aged (stiff) thin surface layer that have become oxidized.

The Design Guide utilizes an approach that models both the top-down and bottom-up cracking. The approach is based on calculating the fatigue damage at the surface for the top-down cracking and at the bottom of each asphalt layer for the bottom up cracking. The fatigue damage is then correlated using calibration data to the fatigue cracking.

Estimation of fatigue damage is based upon Miner's Law, which states that damage is given by the following relationship.

$$D = \sum_{i=1}^{T} \frac{n_i}{N_i} \qquad (3.3.26)$$

where:

D = damage.
T = total number of periods.
n_i = actual traffic for period i.

N_i = traffic allowed under conditions prevailing in *i*.

The estimation of the fatigue damage and fatigue cracking for both the top-down and bottom-up cracking is discussed in the following paragraphs.

Fatigue Cracking in Asphalt Mixtures

To characterize the fatigue damage in asphalt layer, numerous model forms can be found in the existing literature. The most commonly used model form to predict the number of load repetitions to fatigue cracking is a function of the tensile strain and mix stiffness (modulus). The critical locations may either be at the surface and result in top-down cracking or at the bottom of the asphaltic layer and result in bottom-up cracking.

Most of relationships available have a common basic structure and are function of the stiffness of the mix and the tensile strain. The commonly used mathematical relationship used for fatigue characterization is of the following form:

$$N_f = Ck_1\left(\frac{1}{\varepsilon_t}\right)^{k_2}\left(\frac{1}{E}\right)^{k_3}$$
$$= \beta_{f1}k_1(\varepsilon_t)^{-\beta_{f2}k_2}(E)^{-\beta_{f3}k_3} \qquad (3.3.27)$$

where:

N_f	= number of repetitions to fatigue cracking.
ε_t	= tensile strain at the critical location.
E	= stiffness of the material.
k_1, k_2, k_3	= laboratory regression coefficients.
β_{f1}, β_{f2}, β_{f3}	= calibration parameters.
C	= laboratory to field adjustment factor.

The final relationship used for the prediction of the number of repetitions to fatigue cracking is the Asphalt Institute model (*13*), which is based on constant stress criterion and can be expressed as

$$N_f = 0.00432C\left(\frac{1}{\varepsilon_t}\right)^{3.291}\left(\frac{1}{E}\right)^{0.854}$$
$$C = 10^M$$
$$M = 4.84\left(\frac{V_b}{V_a + V_b} - 0.69\right) \qquad (3.3.28)$$

where:

V_b	=	effective binder content (%).
V_a	=	air voids (%).

The national field calibrated model used in the Design Guide was determined by numerical optimization and other modes of comparison to result in national calibration factors of

$\beta_{f1} = k_1^{'} * \beta'_{f1}$
$\beta'_{f1} = 1.0$
$\beta_{f2} = 1.2$
$\beta_{f3} = 1.5$

This resulted in the following final model:

$$N_f = 0.00432 * k'_1 * C \left(\frac{1}{\varepsilon_t}\right)^{3.9492} \left(\frac{1}{E}\right)^{1.281} \quad (3.3.29)$$

In this equation the parameter "$k_1^{'}$" has been introduced to provide a correction for different asphalt layer thickness (h_{ac}) effects.

a. For the bottom-up cracking

$$k'_1 = \frac{1}{0.000398 + \frac{0.003602}{1 + e^{(11.02-3.49*hac)}}} \quad (3.3.30a)$$

b. For the top-down cracking

$$k'_1 = \frac{1}{0.01 + \frac{12.00}{1 + e^{(15.676-2.8186*hac)}}} \quad (3.3.30b)$$

where:

h_{ac} = Total thickness of the asphalt layers, in.

The final transfer function to calculate the fatigue cracking from the fatigue damage is expressed as:

a. For bottom-up cracking (% of total lane area)

$$FC_{bottom} = \left(\frac{6000}{1 + e^{(C_1*C'_1 + C_2*C'_2*\log10(D*100))}}\right) * \left(\frac{1}{60}\right) \quad (3.3.31a)$$

where:

FC_{bottom} = bottom-up fatigue cracking, percent lane area
D = bottom-up fatigue damage
C_1 = 1.0
$C_1^{'}$ = $-2 * C_2^{'}$
$C_2^{'}$ = 1.0
$C'_2 = -2.40874 - 39.748 * (1 + h_{ac})^{-2.856}$

N = 461 observations
S_e = 6.2 percent

S_e/S_y = 0.947

b. For top-down cracking (feet/mile)

$$FC_{top} = \left(\frac{1000}{1 + e^{(7.0-3.5*\log10(D*100))}} \right) * (10.56) \qquad (3.3.31b)$$

where:

FC_{top} = top-down fatigue cracking, ft/mile
D = top-down fatigue damage

N = 414 observations
S_e = 1242.25 ft/mile
S_e/S_y = 0.977

The fatigue-cracking model for the asphalt concrete mixtures has been calibrated based on 82 LTPP sections located in 24 States. Time series data were available for many of the sections, resulting in 441 observations for alligator cracking and 408 data points for longitudinal cracking. Appendix II-1 contains a detailed explanation of the calibration process and data used for the calibration of the HMA fatigue cracking models. Figures 3.3.20 and 3.3.21 show the plots of the relationship of both the measured and predicted cracking as a function of the fatigue damage in the asphalt layers. The bottom-up cracking is calculated as a percentage of the total lane area. While, the longitudinal cracking is calculated as linear feet in a mile. The measured cracking used in the calibration is the total summation of the high, medium and low severity cracking.

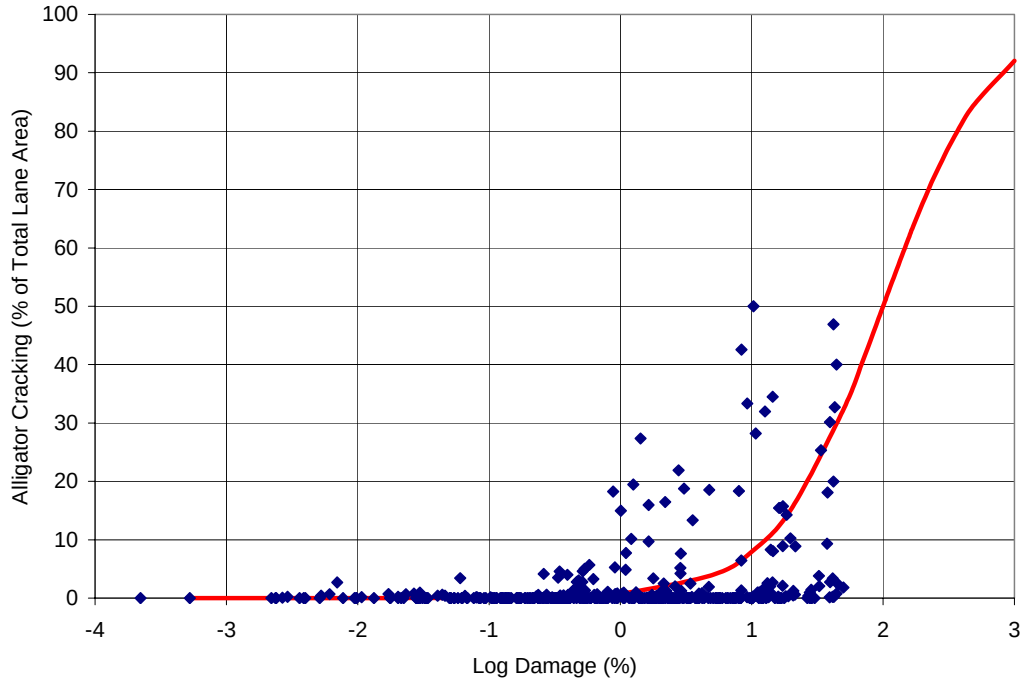

Figure 3.3.20. Bottom-up cracking versus fatigue damage at bottom of HMA layer.

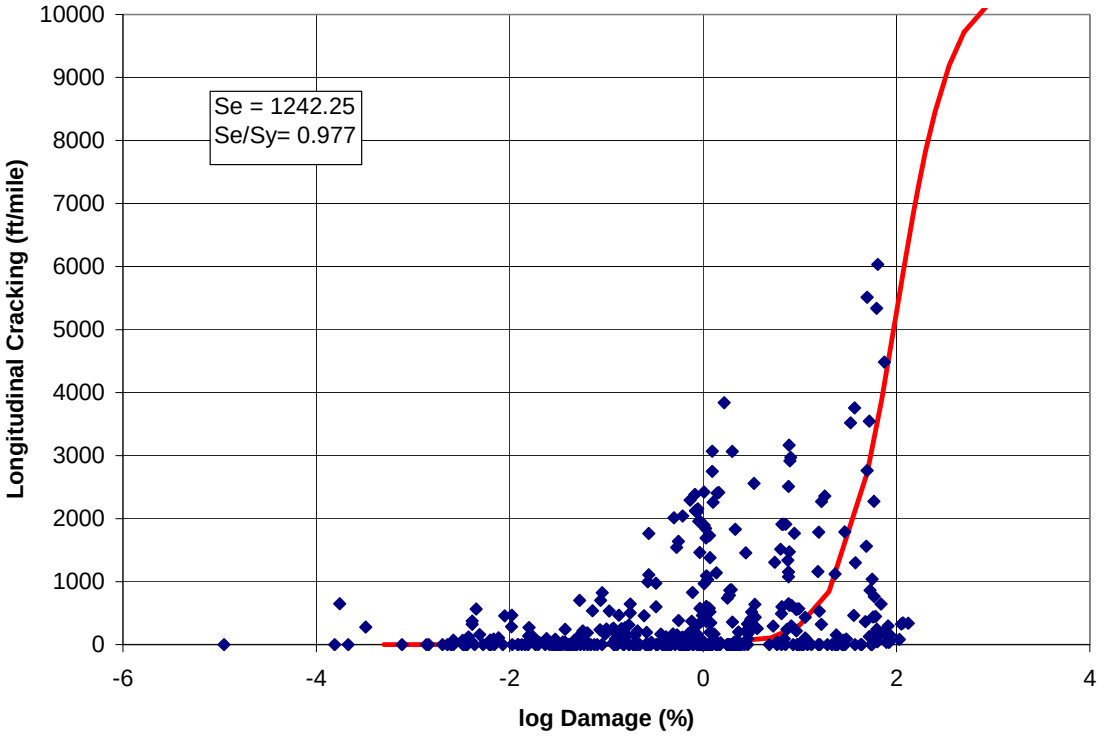

Figure 3.3.21. Top-Down cracking versus fatigue damage at surface of HMA layer.

Factors Affecting Fatigue Cracking in Flexible Pavements

Many factors affect the fatigue cracking in the pavement layers. Some of these factors can be controlled or modified, while the rest are external factors that cannot be controlled. The following factors affect the amount of fatigue cracking within the asphalt layers of the pavement structure:

- HMA layer thickness.
- HMA layer dynamic modulus.
- Binder grade in the HMA mixture.
- Air voids in the asphalt layers.
- Effective binder content in the asphalt layers.
- Base thickness.
- Subgrade modulus.
- Traffic load configuration.
- Traffic load, contact area and tire pressure.
- Traffic load repetitions.
- Temperature and environmental conditions.

While many of these parameters are constant throughout the design period (e.g., layer thickness), others may vary seasonally, monthly, hourly, or with pavement age. For accurate results, all variables that produce significantly different pavement response parameters (stress, strain) must be evaluated separately. The fatigue cracking accumulation defined in this Guide was determined to account for those cases as follows:

- Pavement age – accounts for the changes in HMA dynamic modulus and hardening of the asphalt binder.
- Month – accounts for monthly variations in surface and pavement temperatures, which affects the HMA dynamic modulus, as well as, the moisture variation in the subgrade and base layers. It can be a semi-monthly period if freezing and thawing exists.
- Traffic speed (loading frequency) – affect on the dynamic modulus of the HMA mixture.
- Load configuration – Single, tandem, tridem, and quad
    - Load level –
        - Single axles – 3,000 to 41,000 lb in 1,000-lb increments.
        - Tandem axles – 6,000 to 82,000 lb in 2,000-lb increments.
        - Tridem axles – 12,000 to 102,000 lb in 3,000-lb increments.
        - Quad axles – 12,000 to 102,000 lb in 3,000-lb increments.
- Temperature and environmental conditions –
    - Temperature is an important factor affecting the asphalt stiffness and consequently the dynamic modulus of asphalt concrete mixes. Because the modulus of the asphalt layers within the pavement structure affect the overall pavement response, it is important to properly account for the temperature as a function of time and depth.
    - Environmental conditions in the unbound materials are principally represented by moisture changes in the subgrade and base / subbase layers. The moisture content change is an important factor for a given type of unbound materials. This is due to the fact that increasing the moisture content in an unbound layer will lead to a decrease in the resilient modulus of the layer. For all other conditions remaining the same, this will lead to a larger E_i/E_{i+1} ratio of successive layers, which, in turn will lead to a greater tensile stress/strain in the HMA layer and therefore a greater level of fatigue damage. During the freezing season, the moisture may freeze and the layer may actually increases in stiffness. This will result in (for all practical purpose) little to no fatigue damage to occur in the HMA layer.

HMA Thickness and Subgrade Modulus on Alligator Cracking

The relationship shown in the Figure 3.3.22 illustrates an extremely important fundamental fact regarding the distribution of alligator fatigue cracking for flexible pavement systems. First of all, for all levels of HMA thickness, it can be clearly observed that the magnitude of alligator cracking is increased as the subgrade support is decreased.

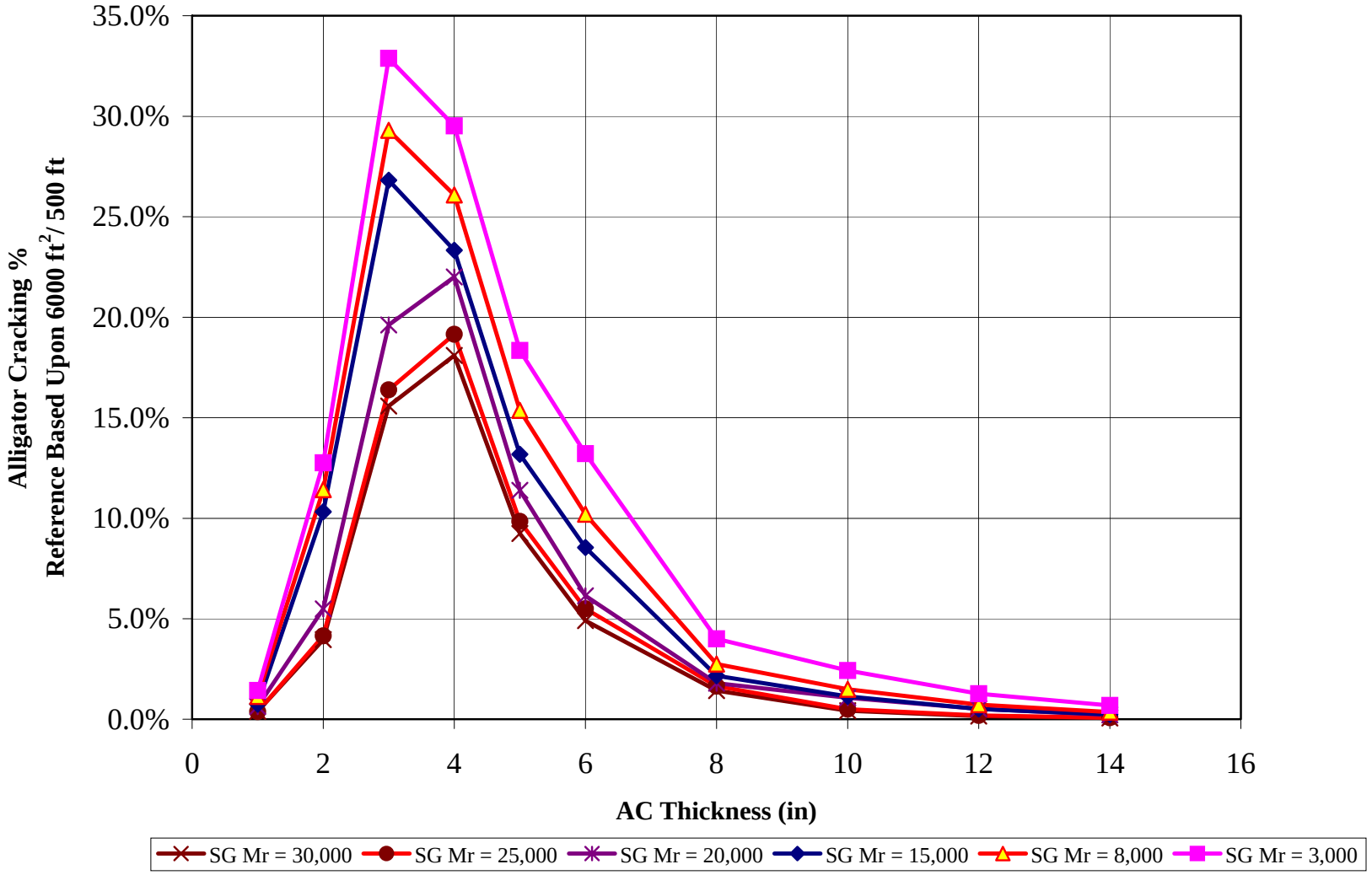

Figure 3.3.22. Effect of HMA layer thickness on alligator fatigue cracking

It can also be observed that the sensitivity, or impact of the subgrade support upon alligator cracking, is directly related to the thickness of the HMA layer.

Perhaps the most important fundamental conclusion that can be drawn from the figure is that for good performance, the proper thickness of HMA layers must be either as thin as practical or as thick as possible. It reinforces the adage of old time flexible pavement experts who inferred that " …if you build a pavement thin, it should be thin…if you build it thick, then it should be built thick". The figure clearly indicates that the greatest potential for fatigue fracture is really associated with HMA layers that are typically in the 3- to 5-in thickness range.

The fundamental reasoning behind the results shown in the figure is a powerful example of the utilization of a mechanistic approach to pavement design. It should be intuitive to the reader, that as the HMA thickness increases beyond 4 + inches, that the tensile strains generated at the bottom of the HMA layer are reduced with increasing HMA thickness. Thus, it is logical that as the HMA thickness is increased beyond a 4-inch layer, the fatigue life is directly increased due to a smaller tensile strain value occurring in the pavement system. Nonetheless, the real important fact that must be recognized is that the magnitude of the tensile strain does not necessarily increase proportionately to a decrease in HMA thickness. In fact, as the HMA thickness is reduced below the "maximum cracking level of 3- to 5-in", the tensile strains actually start to decrease and, in fact, may actually become compressive in nature. Thus, at very thin HMA layers, there is little to no tensile stresses or strains that may be found at the bottom of the HMA layer. This clearly explains why, fatigue behavior may improve with decreasing levels of HMA thickness.

While this is true, the reader must also recognize that, while thin HMA layers may not have significant fatigue problems; other major distress types, particularly, repetitive shear deformations, leading to permanent deformation or excessive rutting become the most salient design consideration for these pavement types. One disadvantage of a pavement system that has very small HMA layer thickness, is the fact that the stress state in the unbound layers (bases, subbases and subgrades) is greatly increased and hence increases the probability of rutting in these unbound layers, overlain by thin layers of HMA. These factors should be carefully weighted when trying to use thin HMA layers in design.

HMA Thickness and Subgrade Modulus on Longitudinal Cracking

A similar study indicating the influence of HMA thickness and subgrade modulus upon longitudinal cracking is shown in figure 3.3.23. An immediate comparison of the effect of HMA thickness and surface longitudinal cracking indicate similar effects, as compared to alligator cracking distress. In general, fatigue damage is maximum at the 3 in to 5 in HMA thickness level. Thus, both modes of fatigue distress are greatest for the intermediate (3- to 5-in) HMA thickness range.

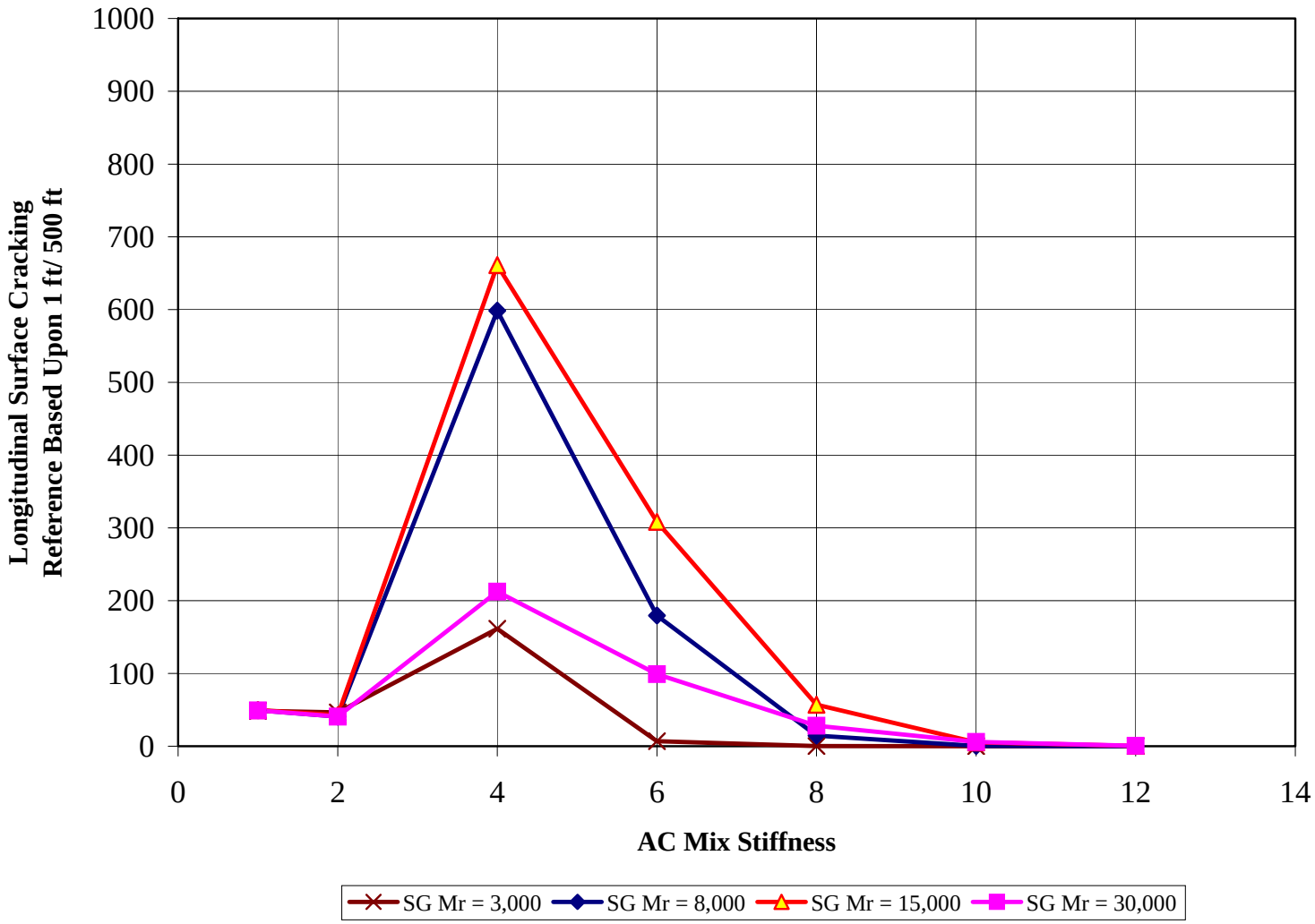

Figure 3.3.23. Effect of HMA layer thickness on longitudinal surface fatigue cracking (High E*).

However, it should be carefully observed that the influence of subgrade modulus is totally opposite to the damage trends shown for bottom-up alligator cracking. From the figure it can be seen that surface longitudinal cracking increases as the foundation support layer also increases. Thus, any variable that tends to increase the foundation support (stiffer subgrade, stabilized base/subbase, very low ground water table location, presence of bedrock near the surface) will tend to cause a larger tensile strain at the surface layer and tend to increase longitudinal surface cracking.

Fatigue Cracking Prediction Procedure

To predict load-associated fatigue cracking for flexible pavements, certain steps are needed to be followed. These steps are summarized below:

1. Tabulate input data – summarize all inputs needed for predicting cracking.
2. Process traffic data – the processed traffic data needs to be further processed to determine equivalent number of single, tandem, and tridem axles produced by the entire traffic load - axle spectra.
3. Process pavement temperature profile data – the hourly pavement temperature profiles generated using EICM (nonlinear distribution) need to be converted to the distribution of equivalent linear temperature differences by calendar month.
4. Process monthly moisture condition data – the effects of seasonal changes in moisture conditions on base / subgrade modulus must be determined.
5. Calculate stress and strain states – calculate tensile strains corresponding to each load, load level, load position, and temperature difference for each month within the design period at the surface and bottom of each asphalt layer of each layer. Using material modulus and Poisson's ratio; determine the elastic strains at each computational point. Calculate damage for each sub-season and sum to determine accumulated damage in each asphalt layer.
6. Calculate fatigue cracking – calculate the cracking for each layer from the damage calculated.

Step 1: Tabulate input data

All input data required for the prediction of fatigue cracking is explained in details in PART 2, Chapter 2.

Step 2: Process traffic data

The traffic inputs are first processed to determine the expected number of single, tandem, tridem, and quad axles in each month within the design period. This procedure is described in detail in PART 2, Chapter 4.

Step 3: Process temperature profile data

A base unit of one month is typically used for damage computations. In situations where the pavement is exposed to freezing and thawing cycles, the base unit of one month is changed to 15-days (half month) duration to account for rapid changes in the pavement material properties during the frost/thaw period. While damage computations are based

on a two-week or monthly average temperature; the influence of extreme temperatures, above and below the average, are directly accounted for in the design analysis. In order to include the extreme temperatures during a given month (or during 15 days for freeze/thaw period), the following approach is used in the analysis scheme.

The solution sequence from the EICM provides temperature data at intervals of 0.1 hours (6 minutes) over the analysis period. This temperature distribution for a given month (or 15-days) can be represented by a normal distribution with a certain mean value (μ) and the standard deviation (σ), $N(\mu,\sigma)$ as shown in figure 3.3.24.

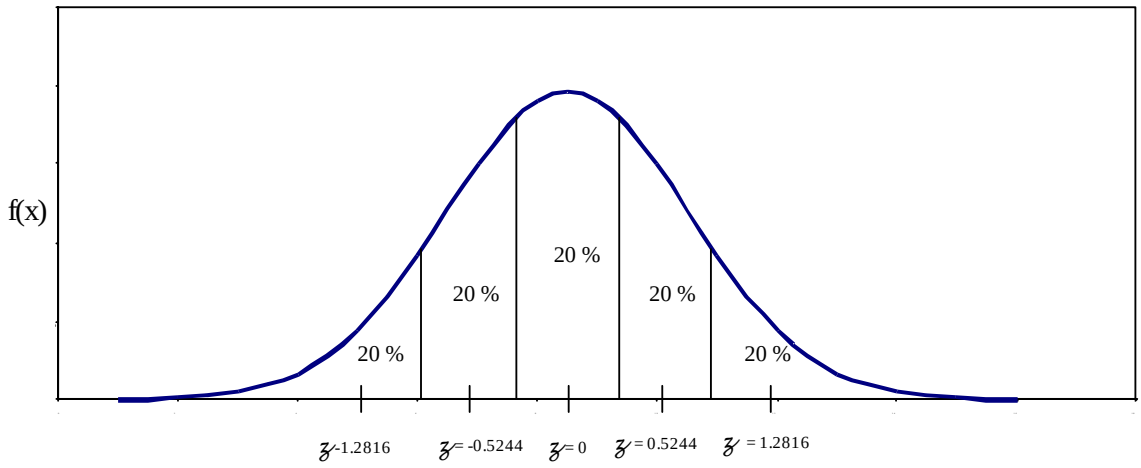

Figure 3.3.24. Temperature distribution for a given analysis period

The frequency distribution of temperature data obtained from the EICM is assumed to be normally distributed as depicted in figure 3.3.24. The frequency diagram obtained from the EICM represents the distribution at a specific depth and time. Temperatures in a given month (or bi-monthly for frost/thaw) may have extreme temperatures (even at a low frequency of occurrence) that could be significant for rutting.

It is obvious that the use of the average temperature value will not capture the damage caused by these extreme temperatures. In order to account for the extreme temperature, the temperatures over a given interval are divided into five different sub-seasons. For each sub-season the sub-layer temperature is defined by a temperature that represents 20 % of the frequency distribution of the pavement temperature. This sub-season will also represent those conditions when 20 percent of the monthly traffic will occur. This is accomplished by computing pavement temperatures corresponding to standard normal deviates of -1.2816, -0.5244, 0, 0.5244 and 1.2816. These values correspond to accumulated frequencies of 10-, 30-, 50-, 70-, and 90-percent within a given month.

Step 4: Process monthly moisture conditions data

EICM calculates the moisture content and corrects for the moisture change in the unbound layer. Refer to PART 2, Chapter 3 for detailed explanation of the method used to correct the unbound layer modulus.

Step 5: Calculate critical tensile strain

It is necessary to use the pavement response model for the layered pavement structure to calculate strains for all cases that need to be analyzed. The number of cases depends on the damage increment. The following increments are considered:

- Pavement age – by year.
- Season – by month or semi-month.
- Load configuration – axle type.
- Load level – discrete load levels in 1,000 to 3,000 lb increments, depending on axle type.
- Temperature – pavement temperature for the HMA dynamic modulus.

The damage increments and stress calculation are determined as follows.

Given a particular layered pavement cross section, critical elastic (resilient) strains are computed at each predefined pavement response computational point, by knowledge of the three-dimensional stress state and the elastic properties (modulus and Poisson's ratio) of the HMA layer in question from:

$$\varepsilon_{rx,y} = \frac{1}{E^*}(\sigma_{x,y} - \mu\sigma_{y,x} - \mu\sigma_z) \qquad (3.3.32)$$

The complex modulus of asphalt mixtures is employed in the Design Guide via a master curve. Thus, E^* is expressed as a function of the mix properties, temperature, and time of the load pulse.

Knowledge of the predicted horizontal tensile strain at any point, along with the layer dynamic modulus and N_f repetition relationship, allows for the direct calculation of the damage for any asphalt layer, after N repetitions of load, in the x and y direction to be computed.

The damage for each HMA layer is estimated using equation 3.3.33.

$$D_i = \frac{n_i}{N_{fi}} \qquad (3.3.33)$$

where:

n_i = actual traffic for period i.

N_{fi} = traffic allowed under conditions prevailing in i.

Step 6: Calculate fatigue cracking

From the accumulated damage calculated for each month (analysis period) for each asphalt layer, the fatigue cracking is predicted using the function described earlier in this section. The top-down cracking is calculated using the maximum damage accumulated at the surface of the top asphalt layer. The bottom-up cracking is calculated using the maximum damage accumulated at the bottom of the lowest asphalt layer.

Fatigue Cracking Reliability

The reliability design is obtained by determining the predicted load associated fatigue cracking at the desired level of reliability as follows:

$$FC\_P = (FC_i + Se_{FCi} \bullet Z_p) \quad (3.3.34)$$

where,

FC_*P*	=	predicted cracking at the reliability level P, % or ft/mile.
FC_i	=	predicted cracking based on mean inputs (corresponding to 50% reliability), % or ft/mile.
Se_{FCi}	=	standard error of cracking at the predicted level of mean cracking
Z_P	=	standard normal deviate.

$$Se_{FCBottom} = 0.5+12/(1+e^{1.308-2.949*logD}) \quad (3.3.35a)$$

$$Se_{FCTop} = 200+2300/(1+e^{1.072-2.1654*logD}) \quad (3.3.35b)$$

Appendix II describes how the expressions for standard error shown in equation 3.3.35 were developed.

Modification of Flexible Design to Reduce Fatigue Cracking

Alligator Cracking (Bottom Up)

From the LTPP database, it has been noted that the greatest degree of alligator cracking will generally occur in HMA layers between 3- to 5-in in thickness (see Appendix II). Thus one very logical way by which alligator fatigue cracking can be decreased is to simply increase the total thickness of the HMA layers.

The use of thin HMA layers can be used provided extreme care is taken in the stiffness (master curve) properties of the HMA layer used. In theory this is true. However, the use of thinner HMA layers (less than 3- to 4-in) may lead to a host of other potential distresses associated with permanent deformation (rutting) in the unbound base/subbase layers that more than affect any possible advantages with thin HMA layers.

It is important to recognize that the variable of HMA layer thickness and HMA mix stiffness are directly integrated together to achieve optimal mix fatigue resistance. If thin HMA layers are used, it is highly desirable to have a low stiffness (low E*) material. The presence of thin, very stiff HMA layer, are highly susceptible to alligator cracking. On contrast, as thicker HMA layers are used, the pavement engineer should try to utilize the highest stiffness (high E*) HMA possible. This will tend to decrease the critical tensile strains at the bottom of the HMA layer and enhance the structure's resistance to alligator cracking.

In addition to the general attributes of the overall mix stiffness (E*) in alligator cracking, it is very important to also appreciate that two mix volumetric properties also play an

important role in governing the fatigue damage. For any particular mix, the greater the V_{beff} (effective volume of bitumen) and the lower the V_a (air voids); will result in significant increase in HMA fatigue life.

While the previous discussion have focused primarily on properties / attributes of the HMA layers; the engineer should clearly understand that alligator cracking fatigue damage is fundamentally related to a large E_i/E_{i+1} ratio, relative to the stiffness of the HMA layer (E_i) and unbound sublayers (E_{i+1}) beneath the HMA layer. Thus any pavement structural changes that reduce the E_i/E_{i+1} ratio will significantly decrease the likelihood of fatigue damage. As a result, any changes that increase the foundation stiffness (i.e. by chemical stabilization; use of higher quality /stiffer layers; or increasing the thickness of high quality unbound base/subbase layers) will improve the bottom-up fatigue cracking resistance of the pavement system.

Finally, as unbound layer stiffness of base/subbase and subgrade materials may be significantly impacted by the presence of moisture; the use of positive Subdrainage design, lowering the GWT (Ground Water Table) and /or raising the grade away from the existing GWT will provide positive benefits to reducing / eliminating alligator fatigue cracking.

Longitudinal Cracking (Top Down)

The overall influence of longitudinal, surface down fatigue cracking, as a function of HMA thickness, is conceptually identical to the effect upon alligator cracking. In general, both forms of cracking appear to be most significantly at HMA layer thickness between 3" and 5". While lower mixture air voids (V_a) and higher amounts of asphalt cement (V_{beff}) will also increase the fatigue life for longitudinal cracking. The pavement / materials engineer must now carefully assess the mix design as a true compromise of wearing course distresses also caused by permanent deformation and possibly thermal fracture.

As a fundamental principle, longitudinal surface cracking may be increased with the use of lower stiffness wearing course mixtures. This is directly due to the fact that larger surficial tensile strains will occur in these lower stiffness HMA.

The differences in foundation support and its effect upon alligator (bottom up) cracking and longitudinal surface (top down) cracking are key issues that the engineer must appreciate and understand. In general, the presence of thick and /or stiff layers in the upper portion of the structural pavement cross section will tend to cause an increase in tensile surface strain and therefore longitudinal surface cracking. This is completely opposite trend for the alligator cracking. Softer HMA surface layers overlying stiff foundations will tend to cause large surface tensile strains and longitudinal cracking.

If longitudinal surface cracking is a possibility, the engineer must carefully evaluate the HMA layer properties and insure that all possible potential distress types are optimized (minimized) as best as possible.

Finally, the engineer should recognize that given a choice between surface longitudinal cracking and alligator cracking, it will normally be advisable to select the longitudinal surface cracking distress over alligator cracking. The reason for this is due to the fact that the eventual presence of surface (top down) cracks as well as permanent deformation in the upper HMA layers, can always be milled in future rehabilitations strategies. However, if alligator cracking is present, the chances of full "slab-layer" damage for the total HMA layer(s) are quite high. If this is the case, it is apparent that complete removals of the HMA layer or very thick overlays are the only preferred rehabilitation option.

Fatigue Cracking in Chemically Stabilized Mixtures

Accurate characterization of the fatigue behavior of chemically stabilized mixtures (CSM) is a very complex technical issue. The situation is further complicated by the fact that fatigue cracking in the material layer is not directly observed in the pavement surface. In essence, fatigue cracking of a CSM layer may result in several possible considerations:

- If the CSM layer lies directly underneath the HMA layers, any fatigue cracking in the chemically stabilized layer will result in a fraction of the cracking reflected through the HMA layer to be surface.
- If a crack relief layer (e.g. Unbound granular base/subbase layer) is placed between the HMA and CSM layers, it is possible that reflective cracking through the HMA layer may be greatly minimized or eliminated.
- As the CSM layer is subjected to increased levels of fatigue damage; the equivalent CSM layer modulus (E_{CSM}) may be significantly degraded. The foundation of these fatigue cracks will serve to reduce the CSM layer moduli, which in turn, will cause greater tensile strain in the HMA layer. This will cause an acceleration of bottoms up alligator cracking in the HMA layer itself.

While several literature models are available to characterize the fatigue behavior of CSM material, the relationship used in the Design Guide is a follows:

$$\log CTB\_Damage = \frac{(0.972\beta_{c1} - (\frac{\sigma_t}{MR})}{0.0825 * \beta_{c2}} \qquad (3.3.36)$$

where:

N_f = number of repetitions to fatigue cracking of the CSM layer.

σ_t = maximum traffic induced tensile stress at the bottom of the CSM layer (psi).

MR = 28 day Modulus of Rupture (Flexural Strength) (psi).

β_{c1}, β_{c2} = field calibration factors

The computational analysis of CSM fatigue cracking is conducted within the predefined 2-4 week analysis period. As a result, incremental damage per analysis period is

computed, and the following relationship is used to convert damage to the new (damaged) CSM moduli at the next analysis period.

$$E_{CSM}(t) = E_{CSM}(\min) + \frac{(E_{CSM}(\max) - E_{CSM}(\min))}{(1+e^{(-4+14*D)})} \quad (3.3.37)$$

where:

$E_{CSM}(t)$ = new CSM layer modulus at a damage level of D – psi.
$E_{CSM}(max)$ = maximum CSM layer modulus for intact layer – psi.
$E_{CSM}(min)$ = minimum CSM layer modulus after total layer destruction – psi.
D = CSM damage level – in decimal form (i.e. D = 0.60).

The empirical relationship used to relate CSM damage to cracking in the CSM layer is defined by:

$$C = \frac{1000}{(1+e^{(1-D)})} \quad (3.3.38)$$

where:

C = CSM layer cracking in units of feet of cracking per 500 feet long sections.
D = CSM damage level – in decimal form (i.e. D = 0.60).

At present, the CSM fatigue cracking and subsequent reflective cracking model have not been field calibrated due to the complexity and requirements of field section design input and performance data. As a result the field calibration factors for the fatigue life expression are defined to be:

$\beta_{c1} = 1.0$
$\beta_{c2} = 1.0$

In addition, because calibration –validation data is non- existent; no special reliability solution is available. The reliability data that is used is simply the standard deviation (variance) associated with normal HMA fatigue cracking.

CSM Fatigue Cracking Prediction Procedure

To predict load associated fatigue-cracking damage in CSM layers within semi-rigid asphalt pavement systems, certain steps arte needed to be followed. These steps are summarized below:

1. Tabulate input data – summarize all inputs needed for predicting the damaging effects of CSM layers.
2. Process traffic data – the processed traffic data needs to be further processed to determine equivalent number of single, tandem, tridem and quad axles produced by the entire traffic load- axle spectra.

3. Process Pavement temperature profile data – the hourly pavement temperatures profile generated using EICM (nonlinear distribution) need to be converted to the distribution of equivalent linear temperature differences by calendar month.
4. Process monthly moisture condition data – the effect of seasonal change in moisture conditions on base / subgrade modulus must be determined.
5. Calculate stress states – compute critical tensile stress corresponding to each load, load level, load position, and temperature difference for each month within the design period at the bottom of the CSM layer. Calculate damage for each sub-season and sum to determine accumulated damage in CSM layer. This new computed damage is the basis for ascertaining the damaged CSM modulus for the next analysis period.
6. Calculate fatigue cracking in CSM layer (if no crack relief layer present) - Use this to compute amount of reflected cracking into HMA layers. If crack relief layer present, use accumulated CSM damage to adjust (reduce) CSM modulus in next analysis interval to predict increased tensile strain state in HMA layer.

Step 1: Tabulate input data

All input data required for the prediction of CSM layer fatigue cracking is explained in details in PART 2, Chapter 2. The primary variable for CSM fracture is the 28-day flexural strength (MR – modulus of rupture) data. Another set of vital information in the CSM fatigue subsystem is to identify, whether or not, a crack relief layer is present, separating the HMA layer from the CSM layer. If no layer is present (crack relief), then the fatigue cracking predicted in the CSM layer is used directly in the HMA reflected crack subsystem. If a crack relief is present, then it is assumed that no CSM fatigue cracking will be reflected through the HMA layer. Finally, for either scenario, it should be recognized that the fatigue damage in the CSM layer would yield a reduced CSM moduli for the next analysis period. This reduced CSM moduli, will increase the E_i/E_{i+1} modular ratio in the HMA layer and subsequently increase the tensile stresses and strains to cause a greater level of HMA fatigue cracking.

Step 2: Process traffic data

The traffic inputs are first processed to determine the expected number of single, tandem, tridem, and quad axles in each month within the design period. This procedure is described in detail in PART 2, Chapter 4.

Step 3: Process temperature profile data

The pavement temperature data is processed in identical manner, as previously presented for the HMA fatigue cracking system. The Ultimate goal of this process is to establish the pavement temperature frequency distribution for a given (2 week r 1 month) analysis period. This temperature data, in turn, is used with the specific traffic spectrum operational speed to establish analysis period HMA dynamic modulus values. It is these values, along with other sublayers environmentally adjusted moisture moduli that determine the predicted state of tensile stress in the CSM layer within a given analysis period.

Step 4: Process monthly moisture conditions data

EICM calculates the moisture content and corrects the in-situ E_i (modulus) for the moisture changes in all unbound layer present in the structure. Refer to PART 2, Chapter 3 for detailed explanation of the methodology used to correct the unbound layer modulus.

Step 5: Calculate critical tensile strain

Knowledge of set of the preceding input, for a particular analysis season then allows for the prediction of the critical tensile stress at the bottom of the CSM layer. This is accomplished through use of the specific pavement response model employed. The number of tensile stress cases needed to be analyzed depends upon the following damage increments considered:

- Pavement age – by year.
- Season – by month or semi-month.
- Load configuration – axle type.
- Load level – discrete load levels in 1,000 to 3,000 lb increments, depending on axle type.
- Temperature – pavement temperature for the HMA dynamic modulus.

Within a given analysis period, the critical tensile stress (horizontal at bottom of layer)in the CSM layer is computed for a given set of HMA E* frequency values, for each axle type – load configuration.

Knowledge of the actual initial MR (CSM flexural strength) will allow for the computation of the actual N_f (number of repetitions to fatigue failure of the CSM layer) to be made. Knowing the actual traffic repetitions, occurring in a given analysis period of each load – axle type configuration, the CSM damage, D, can be determined and accumulated for each analysis period from

$$D_i = \frac{n_i}{N_{fi}} \qquad (3.3.39)$$

Given the computed CSM damage, in a given analysis period, a new (reduced) CSM modulus can be computed from the previous set of equations shown, for use in next analysis period damage computational cycle.

Step 6: Calculate fatigue cracking

From the accumulated damage calculated within a given analysis period, estimates of the CSM cracking can be made by the relationship presented between cracking and damage. When no crack relief layer is present; any cracking predicted in the CSM layer can then be reflected through the existing HMA layers. In addition, fatigue cracking in the HMA is also predicted, using the reduced level of CSM modulus caused by fatigue cracking within this layer.

Modification of Design to Reduce CSM Fatigue Cracking

There are several key considerations that must be made by the engineer when utilizing CSM base/subbase layers. The use of CSM layers affords several major advantages in pavement performance / analysis systems. First, the use of a high stiffness stabilized material, greatly lowers the E_i / E_{i+1} modular ratio in the HMA layers. The net effect of this is that tensile stress/ strain conditions at the bottom of the HMA layer become quite small (or in some cases, compressive in nature). This aspect greatly reduces the probability of direct, bottom- up alligator cracking to occur.

Another advantage of CSM layers is that they also, tend to reduce the states of stress/ strain within layers directly beneath them. This has the net effect of reducing the likelihood of permanent deformation (rutting) to occur in unbound subbases, and most importantly, subgrade layers.

While these attributes are theoretically possible, one major distress that is very common with CSM layers, particularly high stiffness layers, is that CSM fatigue cracking occurs and is generally reflected through any existing HMA layers. As a consequence, if an effective "crack relief" system can be utilized, the major advantages of the CSM will exist without the major potential disadvantage. Unbound crack relief layers (generally 3- to 4-in minimum) have been successfully used in many parts of the world. However, the key to success is 100 percent associated with the designer's ability to keep all moisture from being "pended" in the crack relief layer. If poor drainage occurs the crack relief layer quickly becomes saturated, effective soil stress go to zero due to saturation and shear failures will be widespread in the system.

Another significant design aspect relates to the need to maintain the high initial stiffness level of the CSM layer as long as possible during the design life. While the elimination of is-situ hydration / curing cracking is highly remote or possible; the key factor the engineer must recognize is that any design change that decreases CSM structural damage, will tend to maintain the longevity of the CSM moduli. This can only be accomplished by minimizing the factors that increase the CSM tensile stress and maximizing the factors that increases the flexural strength of the CSM layer. For a given CSM material, having a MR value constant; damage can only be minimized by increasing the CSM layer thickness or having the depth of the bottom CSM layer placed deeper in the pavement system. Both of these activities will tend to decrease the tensile stress and hence, decrease the load-associated damage of the CSM layer.

Thermal Fracture (Transverse Cracking)

The thermal cracking model in the Design Guide is an enhanced version of the approach originally developed under the SHRP A-005 research contract. Recently, a study was completed under the NCHRP 9-19 "Superpave Models" project to facilitate the incorporation of this thermal cracking model (TCMODEL) and related software for use in the Design Guide.

Several major updates have been made to the original TCMODEL and software. These enhancements included the incorporation of an improved analysis technique for converting raw data from the Superpave Indirect Tensile Test (IDT) into fundamental viscoelastic properties of the asphalt mixture, recalibration of the TCMODEL to reflect updated analysis procedures and additional new field data, and the development of comprehensive documentation for the TCMODEL approach.

Thermal Cracking Model

The amount of transverse cracking expected in the pavement system is predicted by relating the crack depth to an amount of cracking (crack frequency) by the following expression:

$$C_f = \beta_1 * N\left(\frac{\log C / h_{ac}}{\sigma}\right) \tag{3.3.40}$$

where:

C_f	=	Observed amount of thermal cracking.
β_1	=	Regression coefficient determined through field calibration.
N (z)	=	Standard normal distribution evaluated at (z).
σ	=	Standard deviation of the log of the depth of cracks in the pavement.
C	=	Crack depth.
h_{ac}	=	Thickness of asphalt layer.

The amount of crack propagation induced by a given thermal cooling cycle is predicted using the Paris law of crack propagation:

$$\Delta C = A\Delta K^n \tag{3.3.41}$$

where:

ΔC	=	Change in the crack depth due to a cooling cycle.
ΔK	=	Change in the stress intensity factor due to a cooling cycle.
A, n	=	Fracture parameters for the asphalt mixture.

The approach used to evaluate the A and n parameters is based, in part, upon previous work (*14*,*15*,*16*). Recalling that the master creep compliance curve can be expressed by the power function to yield:

$$D(\xi) = D_0 + D_1 \xi^m \tag{3.3.42}$$

The m value, derived from the compliance curve is used to compute the n fracture parameter through the equation:

$$n = 0.8\left(1 + \frac{1}{m}\right) \tag{3.3.43}$$

Once the *n* value is known, the *A* fracture parameter is computed from the equation:

$$A = 10^{\left(\beta*(4.389 - 2.52*\log(E*\sigma_m*n)\right)} \quad (3.3.44)$$

where:

E = Mixture stiffness.
σ_m = Undamaged mixture tensile strength.
β = Calibration parameter.

For national calibration, the parameters recommended for the three hierarchical levels based upon available data are summarized in table 3.3.2. Details on calibration parameters and database used at each level can be found in Appendix HH.

Table 3.3.2. National Calibration parameters for thermal cracking model.

Hierarchical Level	β_1	σ	E	β
1	400	0.769	10,000	5.0
2	400	0.769	10,000	1.5
3	400	0.769	10,000	3

For all hierarchical levels, in addition to the original field specimens and thermal cracking observations from 22 SHRP General Pavement Sections (GPS) used in the original SHRP calibration study of the TCMODEL, 14 Canadian SHRP (C-SHRP) and 5 MnROAD sections were used in the re-calibration of the TCMODEL used in the Guide. Although the recalibration included several analysis modifications and nearly twice as many field sections; the newly calibrated model parameters were found to be quite similar to parameters developed in the original SHRP study.

Structural Response Modeling for Thermal Cracking

The following factors affect the magnitude of the thermal cracking prediction in the HMA layer:

- Temperature-depth profile within the asphalt layer
- Creep compliance
- Creep compliance test temperature
- Tensile strength
- Mixture VMA
- Aggregate coefficient of thermal contraction
- Mix coefficient of thermal contraction
- HMA layer thickness
- Air voids
- Voids filled with asphalt, VFA
- Intercept of binder viscosity-temperature relationship at RTFO condition
- Penetration at 77^{o}F

While most of the parameters above remain constant throughout the design period (e.g., layer thickness), others vary seasonally or with pavement age. For accurate thermal analysis results, all cases that produce significantly different stresses must be evaluated separately. The thermal cracking increment defined in this Guide was determined equal to one month to account for those cases as follows:

- Temperature-depth profile within the asphalt layer - The general approach methodology used in the thermal cracking distress prediction model utilizes the EICM as the climatic algorithm to determine the temperature-depth profile within the asphalt layer at hourly time intervals over the entire analysis period (20 to 30 years). It allows for the prediction of the thermal stress at any given depth and time within the asphalt layer.
- Creep compliance – Evaluated at temperatures of 0, -10, and -20 °C (32,14, and -4 °F). It accounts for the linear visco-elastic properties on which the thermal cracking analysis is based on. It allows obtaining the fracture parameters used to compute the growth of the thermal crack length.
- Tensile strength – Indirect measure that also accounts for the linear visco-elastic properties on which the thermal cracking analysis is based on. It allows obtaining the fracture parameters used to compute the growth of the thermal crack length.

Thermal Cracking Prediction Procedure

To determine the amount of thermal cracking the next step-by-step procedure is followed:

1. Gathering input data – summarize all inputs needed for predicting thermal cracking.
2. Development of the master creep compliance curve – An enhanced data analysis technique is provided in the program MASTER.
3. Prediction of thermal stresses - Using visco-elastic transformation theory, the compliance can be related to the relaxation modulus of the asphalt mix. Knowledge of this parameter, coupled with the temperature data obtained from the EICM model, allows for the prediction of the thermal stress at any given depth and time within the asphalt layer. This is accomplished by the TCMODEL program.
4. Growth of the thermal crack length computation - Paris' Law is used to compute the growth of the thermal crack length within the asphalt layer.
5. Length of thermal cracks computation

Step 1: Gathering input data

The thermal cracking approach developed requires characterization of asphalt mixes in Indirect Tensile (IDT) mode. Because the thermal fracture analysis is based upon linear visco-elasticity, key visco-elastic properties of the asphalt mixture are measured. These measured properties are the creep compliance, using indirect tensile tests at one or three

temperatures, depending upon the level of analysis (0, -10, and -20 °C or 32, 14, and -4 °F); and the indirect tensile strength evaluated at only one temperature (-10°C).

For level 1 analysis, the inputs required are creep compliance values at three temperatures, whereas level 2 requires compliance values at only one temperature (-10 °C). For level 3, no testing is required and typical compliance values are hard coded for typical asphalt mix properties. These typical values are the result of hundreds of tests carried out on different mixes in the past several years. In this situation, the Design Guide software only requires asphalt mix properties such as Air voids, VMA, VFA, and Pen_{77F}. The process is further described in Appendix HH.

The specific lab testing requirements for the implementation of the TCMODEL must carefully follow the protocols developed by Roque et al. using the Indirect Tensile Strength system (*17*). The recommended testing approach uses several specific testing-data analysis concepts that must be observed. The indirect testing approach is based upon the use of on-specimen LVDT 's mounted in both the horizontal and vertical axis of the specimen. This system is placed on both sides (faces) of the test specimen.

One very important aspect of the process developed is related to the fact that a series of correction factors have been developed for the set of equations normally used to measure (compute) stresses, strains, compliance, strength and even the Poisson's ratio. These correction factors have been developed from a 3D FEM analysis of the indirect tensile test. They are necessary and justified to account for the real departure of the specimen response from the assumed, idealized 2D plane stress case that has classically been used to interpret Indirect Test results.

While the creep compliance, *D(t)*, for an idealized biaxial stress state condition is obtained through Hooke's Law and is:

$$D(t) = \frac{\varepsilon_x}{\sigma_x - \mu \sigma_y} \tag{3.3.45}$$

The 3D FEM correction factor developed by Roque et al. is given by:

$$D(t) = \frac{\varepsilon(t)}{\sigma} = \frac{H_m(t) * D * t}{P * GL}(C_{cmpl}) \tag{3.3.46}$$

where:

$$C_{CMPL} = \frac{1.071 * \pi * C_{BX}}{2(C_{SX} + 3\mu C_{SY})} \tag{3.3.47}$$

$D(t)$	=	Creep compliance response at time t.
$H_m(t)$	=	Measured horizontal deflection at time t.
GL	=	Gage length (=25.4 mm for 101.6 mm dia., =38.1 mm for 152.4 mm dia.).

P	=	Creep load.
t	=	Specimen thickness.
D	=	Specimen diameter.
μ	=	Poisson's ratio.
C_{cmpl}, C_{SX}, C_{SY}, C_{BX}	=	Correction factors for non-dimensional creep compliance, horizontal stress correction factor, vertical stress correction factor, and horizontal bulging factor, respectively.

The equations for the correction factors are:

$$C_{CMPL} = 0.6354\left(\frac{X}{Y}\right)^{-1} - 0.332 \tag{3.3.48}$$

With the factor restricted to the limits of:

$$0.20 \le \frac{t}{D} \le 0.65 \tag{3.3.49}$$

$$\left[0.704 - 0.213\left(\frac{t}{D}\right)\right] \le C_{CMPL} \le \left[1.566 - 0.195\left(\frac{t}{D}\right)\right] \tag{3.3.50}$$

$$C_{SX} = 0.948 - 0.01114(t/D) - 0.2693(\mu) + 1.436(t/D)(\mu) \tag{3.3.51}$$

$$C_{SY} = 0.901 + 0.138(\mu) + 0.287(t/D) - 0.251(\mu)(t/D) - 0.264(t/D)^2 \tag{3.352}$$

and

$$C_{BX} = 1.03 - 0.189(t/D) - 0.081(\mu) + 0.089(t/D)^2 \tag{3.3.53}$$

The value of (X/Y) represents the absolute value of the ratio of measured horizontal deflection to vertical deflection. As such, it is also used to compute the Poisson's ratio of the material during the test by:

$$\mu = -0.10 + 1.480\left(\frac{X}{Y}\right)^2 - 0.778\left(\frac{t}{D}\right)^2\left(\frac{X}{Y}\right)^2 \tag{3.3.54}$$

with

$$0.05 \le \mu \le 0.50$$

The newly revised protocol for the creep compliance testing is based on the use of a 100-second creep test. In general, three replicate specimens are tested at the three temperatures previously noted for Level 1 and at one temperature for Level 2. For Level 3 analysis, the creep compliance is obtained based on correlations with volumetric and mixture properties.

The creep compliance response at time t, can be written as:

$$D(t) = D_1 t^m \tag{3.3.55}$$

where:

D_1, m = Fracture coefficients.

t = Loading time in seconds.

The correlation used for the D_1 fracture parameter is:

$$\log(D_1) = -8.5241 + 0.01306T + 0.7957\log(V_a) + 2.0103\log(VFA) - 1.923\log(A_{RTFO}) \quad (3.3.56)$$

where:

T = Test temperature (^{o}C) (i.e., 0, -10, and –20 ^{o}C)

V_a = Air voids (%)

VFA = Void filled with asphalt (%) = $\frac{V_{beff}}{V_{beff} + V_a} \times 100$

V_{beff} = effective binder content, %

A_{RTFO} = Intercept of binder Viscosity-Temperature relationship for the RTFO condition

For the m parameter, the correlation used is:

$$m = 1.1628 - 0.00185T - 0.04596V_a - 0.01126VFA + 0.00247Pen_{77} + 0.001683Pen_{77}^{0.4605}T \quad (3.3.57)$$

where:

T = Test temperature (^{o}C) (i.e., 0, -10, and –20 ^{o}C)

V_a = Air voids (%)

VFA = Void filled with asphalt (%)

Pen_{77} = Penetration at 77 ^{o}F = $10^{290.5013-\sqrt{81177.288+257.0694*10^{(A+2.72973*VTS)}}}$

A = Intercept of binder Viscosity-Temperature relationship

VTS = Slope of binder Viscosity-Temperature relationship

The outcome of the m value has been set to a lower limit of 0.01.

For all three levels of data input, the Design Guide procedure requires tensile strength at –10^{o}C. Level 1 and 2 requires actual test data for tensile strength, whereas, level 3 has built in typical values based upon the asphalt mix properties, similar to creep compliance values.

For Levels 1 and 2, the strength test is conducted on the same test specimen that is used to establish the 100 second creep test. After the creep test is completed, failure is evaluated using a load rate of 51 mm per minute. The reported tensile strengths are the average of the three replicates used.

In the recommended test protocol, a special procedure is utilized to determine the "failure load" achieved during the indirect tensile test. This is again an important modification because the failure load has been found to be less than the maximum load that the

specimen can undergo. Thus, once the instant of failure is found (approach uses the deflection measurement difference), the failure load can be defined and the tensile strength computed from:

$$S_t = \frac{2P_f C_{sx}}{\pi D i} \tag{3.3.58}$$

where:

P_f = Failure load.
C_{sx} = Correction factor (previously defined).
t = Specimen thickness.
D = Specimen diameter.

For Level 3 analysis, the tensile strength at –10 ^{o}C was also correlated with mixture properties as with the creep compliance fracture parameters. The best indicators were the air voids, the void filled with asphalt content, the Penetration at 77 ^{o}F, and the *A* intercept of the binder temperature-viscosity relationship for the RTFO condition. The following correlation is used in the analysis:

$$\begin{aligned} S_t = {} & 7416.712 - 114.016V_a - 0.304V_a^{\,2} - 122.592VFA + 0.704VFA^2 \\ & + 405.71\log(Pen_{77}) - 2039.296\log(A_{RTFO}) \end{aligned} \tag{3.3.59}$$

where, the tensile strength (S_t) is given in psi. The outcome of the equation was set to a lower limit of 100 psi.

Based on the above correlations for Level 3 analysis, default values for creep compliance and tensile strength for several binders used in this analysis were calculated. A summary of the results is presented in Appendix HH.

Other inputs required are test duration, thickness of the asphalt layer, and coefficient of thermal contraction. For the coefficient of thermal contraction, the program has two options. In one instance, mixture VMA, aggregate thermal contraction and asphalt thermal contraction values are required for estimating the mix coefficient of thermal contraction or the user can directly enter the value for the mix thermal coefficient.

Step 2: Development of the master creep compliance curve

Enhanced data analysis techniques (through the new program MASTER are claimed to provide accurate evaluations of the time-temperature shift factor (a_T) and creep compliance model statistical fitting techniques through Prony and Power Model forms, as well as the development of the creep compliance master curve (CCMC).

In this analysis, a special data "trimming" technique is used to provide the best estimate of the mix response parameters. If three specimen replicates are used, each having measurements on both faces, a total of six strain (compliance) versus time curves can be developed. The trimming approach recommends elimination of the extreme high and low readings and then utilization of the averaging of the remaining four measurement strain-time responses.

Finally, the new procedure no longer requires the binder stiffness to extend the mixture creep compliance results to longer loading time for the construction of the CCMC. The results of the CCMC analysis are fit to a Prony series defined by:

$$D(\xi) = D(0) + \sum_{i=1}^{N} D_i\left(1 - e^{-\xi/\tau_i}\right) + \frac{\xi}{\eta_v} \qquad (3.3.60)$$

with

$$\xi = \frac{t}{a_T} \qquad (3.3.61)$$

and

ξ	=	reduced time.
t	=	real time.
a_T	=	temperature shift factor.
$D(\xi)$	=	creep compliance at reduced time ξ.
$D(0), D_i, \tau_i, \eta_v$	=	prony series parameters.

The results of the master creep compliance curve are also fit to a Power Model defined by:

$$D(\xi) = D_0 + D_1\xi^m \qquad (3.3.62)$$

The reason for determining an additional model is due to the fact that the Power slope parameter, *m*, is eventually used to compute several fracture (crack propagation) parameters in the fracture model.

Step 3: Prediction of thermal stresses

Using viscoelastic transformation theory, the compliance, *D(t)*, can be related to the relaxation modulus, E_r, of the asphalt mix. Knowledge of this parameter, coupled with the temperature data obtained from the EICM model, allows for the prediction of the thermal stress at any given depth and time within the asphalt layer.

The relaxation modulus function is obtained by transforming the creep compliance function. The relaxation modulus is represented by a generalized Maxwell model and expressed by a Prony series relationship:

$$E(\xi) = \sum_{i=1}^{N+1} E_i e^{-\xi/\lambda_i} \qquad (3.3.63)$$

where:

$E(\xi)$	=	Relaxation modulus at reduced time ξ.
E_i, λ_I	=	Prony series parameters for master relaxation modulus curve (spring constants or moduli and relaxation times for the Maxwell elements).

The knowledge of the relaxation modulus function allows for the computation of the thermal stresses in the pavement according to the following constitutive equation:

$$\sigma(\xi) = \int_0^{\xi} E(\xi - \xi') \frac{d\varepsilon}{d\xi'} d\xi' \qquad (3.3.64)$$

where:

$\sigma(\xi)$ = Stress at reduced time ξ.
$E(\xi-\xi')$ = Relaxation modulus at reduced time $\xi-\xi'$.
ε = Strain at reduced time ξ (= $\alpha(T(\xi') - T_0)$).
α = Linear coefficient of thermal contraction.
$T(\xi')$ = Pavement temperature at reduced time ξ'.
T_0 = Pavement temperature when $\sigma = 0$.
ξ' = Variable of integration.

Step 4: Growth of the thermal crack length computation

Fracture mechanics (Paris' Law) is used to compute the growth of the thermal crack length within the asphalt layer. This is accomplished by knowledge of the stress intensity factor, *K*, as well as the *A* and *n* fracture parameters obtained from the creep compliance and strength of the mixture.

TCMODEL is used to predict the amount of transverse cracking expected in the pavement system. As previously noted, the climatic input and viscoelastic properties (compliance-relaxation modulus) allow for the computation of the thermal stress, at any given time and location within the asphalt layer. Once this is accomplished, fracture mechanics, based upon Paris' Law, is used to compute the stress intensity and fracture properties of the material.

The stress intensity parameter, *K*, has been formulated by developing a simplified equation based upon theoretical FEM studies and results. From this analysis, it was determined that *K* could be estimated from:

$$K = \sigma(0.45 + 1.99 C_o^{0.56}) \qquad (3.3.65)$$

where:

K = Stress intensity factor.
σ = Far-field stress from pavement response model at depth of crack tip.
C_o = Current crack length, feet.

The crack propagation model used in the thermal fracture model is:

$$\Delta C = A \Delta K^n \qquad (3.3.66)$$

where:

ΔC = Change in the crack depth due to a cooling cycle.
ΔK = Change in the stress intensity factor due to a cooling cycle.

A, n = Fracture parameters for the asphalt mixture.

The approach used to evaluate the *A* and *n* parameters is based, in part, upon previous work (*14,15,16*). Recalling that the master creep compliance curve can be expressed by the power function to yield:

$$D(\xi) = D_0 + D_1 \xi^m \tag{3.3.67}$$

The *m* value, derived from the compliance curve is used to compute the *n* fracture parameter through the equation:

$$n = 0.8\left(1 + \frac{1}{m}\right) \tag{3.3.68}$$

Once the *n* value is known, the *A* fracture parameter is computed from the equation:

$$A = 10^{\left(\beta*(4.389 - 2.52*\log(E*\sigma_m*n)\right)} \tag{3.3.69}$$

where:

E = Mixture stiffness, psi.
σ_m = Undamaged mixture tensile strength, psi.
β = Calibration parameter.

Step 5: Length of thermal cracks computation

The degree of cracking (expressed as the length of thermal-transverse cracks occurring in a pavement length of 500 ft) is predicted from an assumed relationship between the probability distribution of the log of the crack depth to HMA layer thickness ratio and the percent of cracking.

The relation of the computed crack depth to an amount of cracking (crack frequency) is represented by the following expression:

$$C_f = \beta_1 * P_R \,(\log C > \log h_{ac}) \tag{3.3.70}$$

$$C_f = \beta_1 * N\left(\frac{\log C / h_{ac}}{\sigma}\right) \tag{3.3.71}$$

where:

C_f = Observed amount of thermal cracking.
β_1 = Regression coefficient determined through field calibration.
$N()$ = Standard normal distribution evaluated at ().
σ = Standard deviation of the log of the depth of cracks in the pavement.
C = Crack depth.
h_{ac} = Thickness of asphalt layer.

Thermal Cracking Model Assumptions

The maximum amount of thermal cracking assumed in the approach is:

$$C_{fmax} = 400 \text{ ft per } 500 \text{ ft of pavement length.}$$

This translates into a crack spacing of one crack (full 12-ft lane width) per 15 ft of pavement length. While this is the maximum assumed value; the model cannot predict more than 50 percent of this maximum value because failure occurs when the average crack depth equals (reaches) the thickness of the asphalt layer.

Thermal Cracking Reliability

The calibration of the thermal cracking model was accomplished at three hierarchical levels of analysis. Forty two PTI pavement sections were used for the calibration: 22 GPS sections from the LTPP database, 14 sections from the Canadian C-SHRP program, one section from Peoria, IL, and 5 MnROAD cells from the Minnesota DOT. Details and location of the sections are found in Appendix HH.

The reliability of the thermal cracking prediction was evaluated in two different ways: by using the actual historic pavement temperatures during the design period, and by using estimated temperatures based on average of historic records. The predicted thermal cracking was compared to the measured thermal cracking and the prediction errors were found.

The error analyses for Level are shown in figure 3.3.25 and 3.3.26. The average prediction errors were found to be –9.0 ft and 16.2 ft. for the first and second approaches, respectively. This comparison illustrates the power and the importance of inputting actual historic climatic data for the design period instead of estimated data.

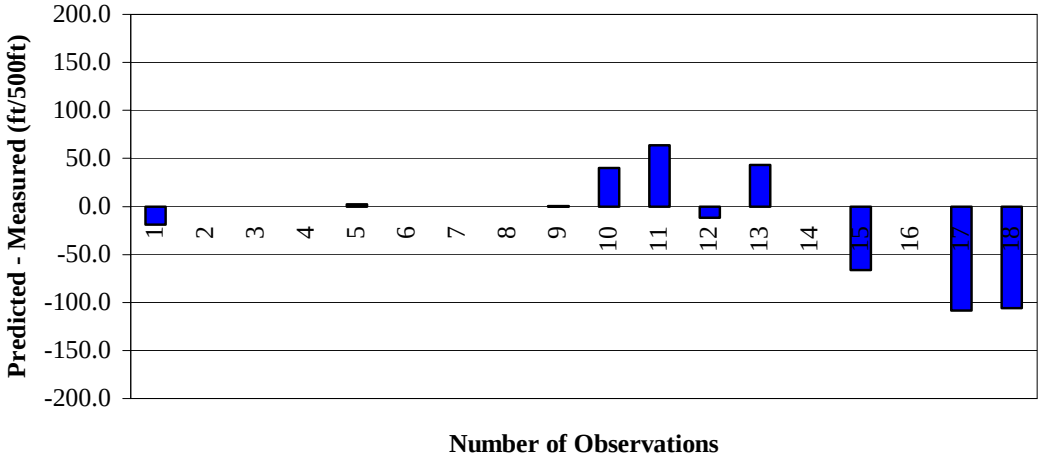

Figure 3.3.25. Level 1 prediction errors (actual pavement temperature).

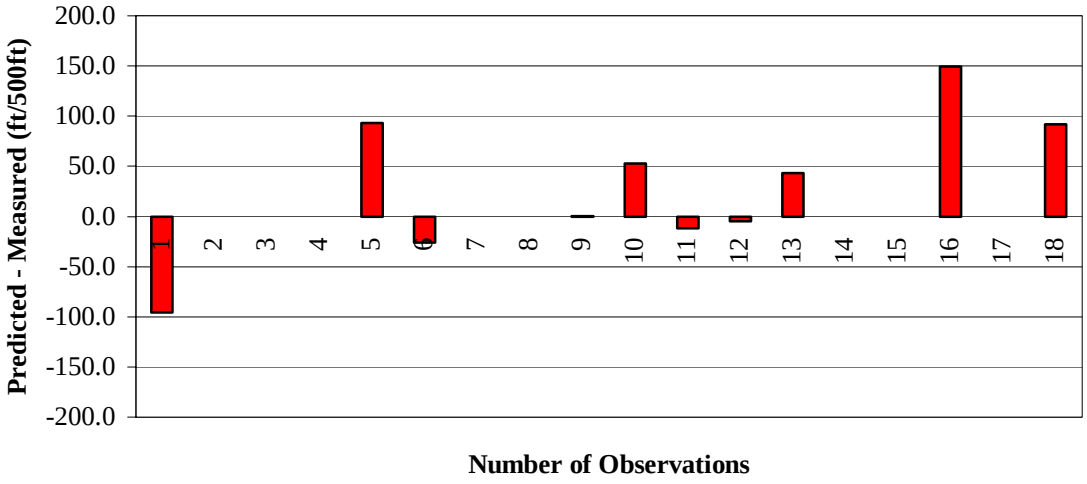

Figure 3.3.26. Level 1 prediction errors (estimated pavement temperatures based on historic data)

For Level 2 analysis, predicted thermal cracking values were obtained using the same analyses described for Level 1. The predicted and the measured thermal cracking were compared and the prediction errors are shown in figures 3.3.27 and 3.3.28. The average prediction errors were found to be 30.1 ft and 49.7 ft. for the first and second approaches, respectively. The difference in errors highlights the importance of having accurate and actual input pavement temperatures.

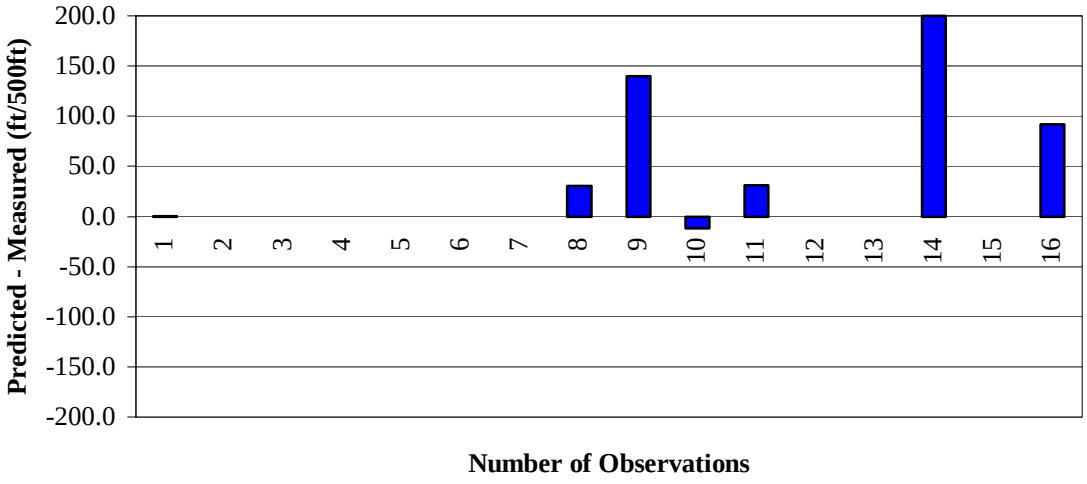

Figure 3.3.27. Level 2 prediction errors (actual pavement temperature)

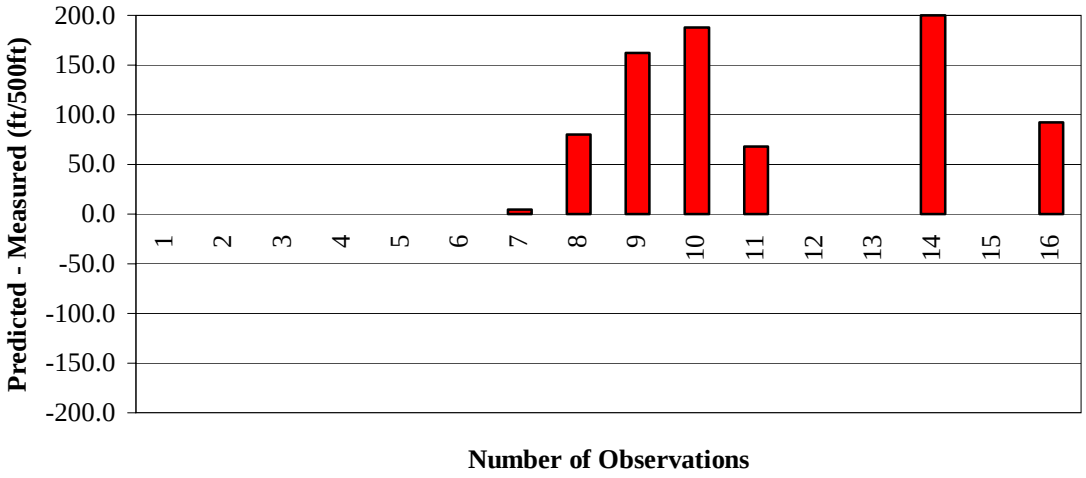

Figure 3.3.28. Level 2 prediction errors (estimated pavement temperatures based on historic data)

Data for 36 LTPP sections (156 observations) was collected and the Level 3 analysis was performed using twelve different combinations: three values for the adjustment factor on the fracture parameter *A* on the Paris Law (β=1.0, 3.0, and 5.0), and four different ways to determine the measured thermal cracking: Sum of Low, Medium, and High Severity Cracking (3a); Summation of Medium and High (3b); High Values Only (3c); and the use of the Weighted Average of the three severity levels as shown below (3d):

$$Total\ Measured\ Cracking = \frac{Low\_Severity + 3\ Medium\_Severity + 5\ High\_Severity}{9} \quad (3.3.72)$$

The summary of statistics found for all the combinations is given in tables 3.3.3 through 3.3.5.

Table 3.3.3. Statistical summary for validation of the TC Model with LTPP sites β = 1.0.

Statistical Parameter	Analysis Level					
	1	2	3a	3b	3c	3d
Average Prediction Error	NA	NA	-70.64	-2.83	32.42	18.86
Standard Deviation	NA	NA	137.1	103.3	81.92	80.08

Table 3.3.4. Statistical Summary for Validation of the TC Model with LTPP Sites β = 3.0

Statistical Parameter	Analysis Level					
	1	2	3a	3b	3c	3d
Average Prediction Error	NA	NA	-2.97	64.84	100.1	86.53
Standard Deviation	NA	NA	119.6	101.8	95.14	86.97

Table 3.3.5. Statistical Summary for Validation of the TC Model with LTPP Sites
$\beta = 5.0$

Statistical Parameter	Analysis Level					
	1	2	3a	3b	3c	3d
Average Prediction Error	NA	NA	13.20	81.00	116.3	102.7
Standard Deviation	NA	NA	129.7	105.7	94.67	88.80

The frequency distribution of errors was plotted associated with each of the combinations mentioned above, and the plots are shown in figures 3.3.29 through 3.3.31.

Best estimates and lower variances were found using a Paris law adjustment factor (β) equal to 1.0 (no adjustment) and using the weighted average of the three different severity levels, being the results using β equal to 3.0 quite close. As shown in tables 3.3.3 and 3.3.4, the average and standard error of estimate were lower than that found by the original Level 3 analysis model using the PTI data.

However, a sensitivity analysis performed on the Level 3 Analysis yielded that the model provides the best predictions when a β factor of 3.0 is being used. Therefore, this factor was decided to go with the models developed. The average prediction error and the standard deviation are shown in Table 3.3.4. The details of the sensitivity analysis for Level 3 calibration of the thermal cracking model can be found in Appendix HH - Annex C

Based on the data obtained for each level of analysis, the following relationships were developed for the standard error of the thermal cracking reliability:

Level 1: $Se_{TC\_1} = 0.2474 * THERMAL + 10.619$ (3.3.73a)

Level 2: $Se_{TC\_2} = 0.3371 * THERMAL + 14.468$ (3.3.73b)

Level 3: $Se_{TC\_3} = 0.6803 * THERMAL + 29.197$ (3.3.73c)

where

Se_{TC_i} = standard error of estimate for thermal cracking (ft/500ft) for level i analysis

THERMAL = predicted thermal cracking in ft/500ft

Modification of Design to Reduce Thermal Cracking

The most important factor affecting thermal cracking is the stiffness of the mix. In order to reduce the predicted thermal cracking, the design needs to be modified by decreasing the stiffness of the mix and run the analysis again. Generally, this is most efficiently implemented by use of a lower PG Grade that the one initially used.

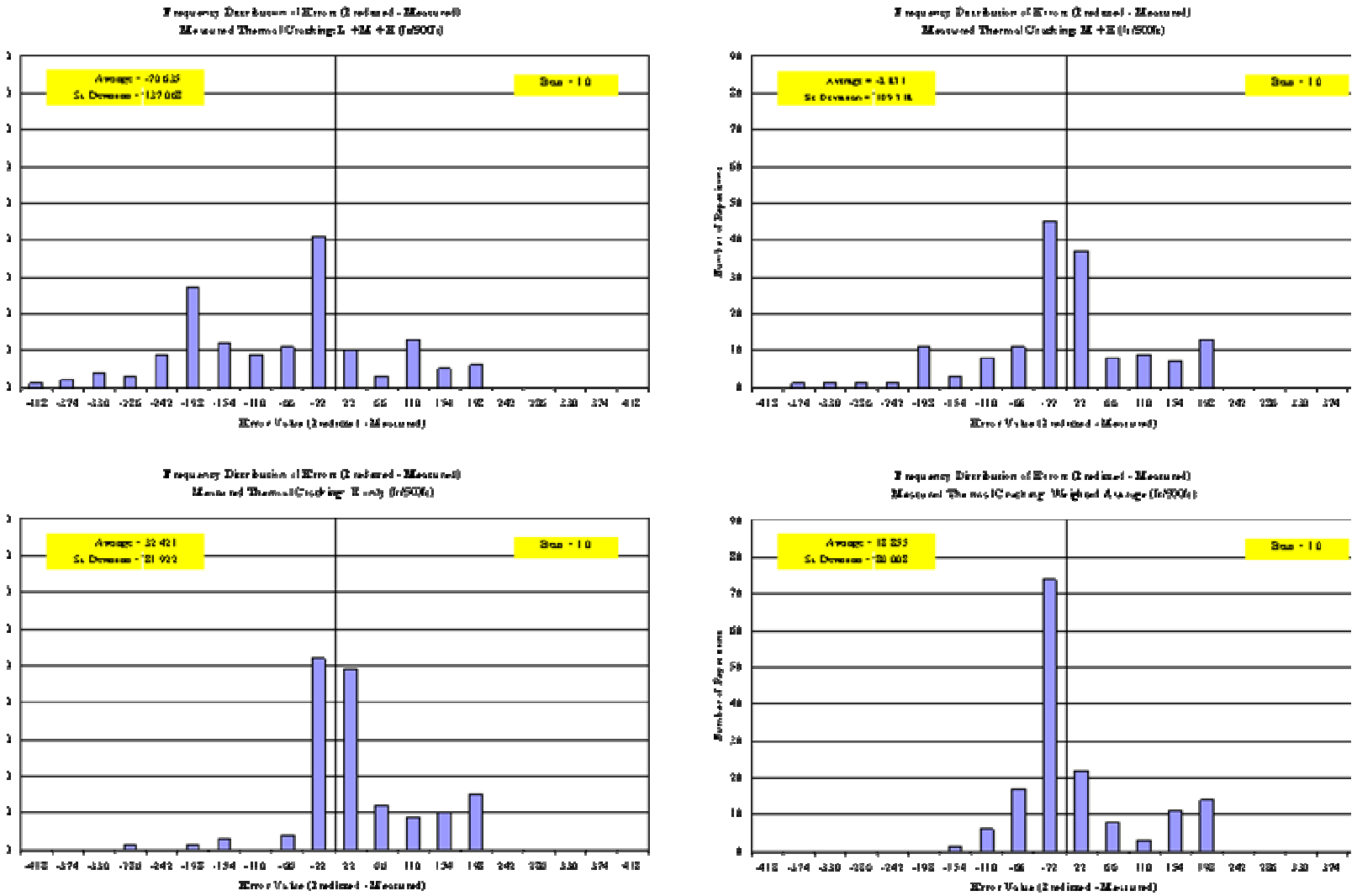

Figure 3.3.29. Summary of frequency distribution for Level 3 analysis with beta factor = 1.0.

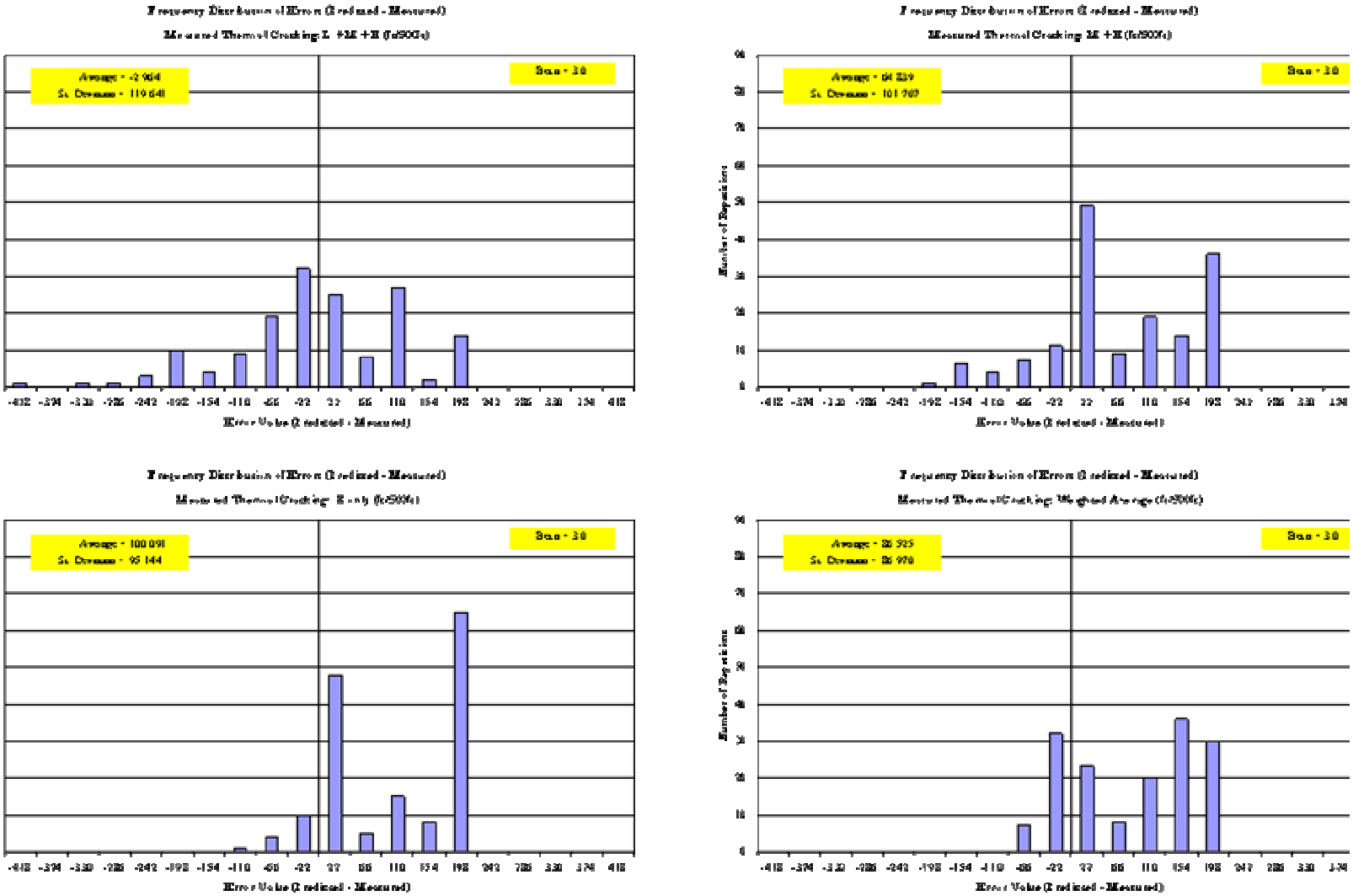

Figure 3.3.27. Summary of frequency distribution for Level 3 analysis with beta factor = 3.0

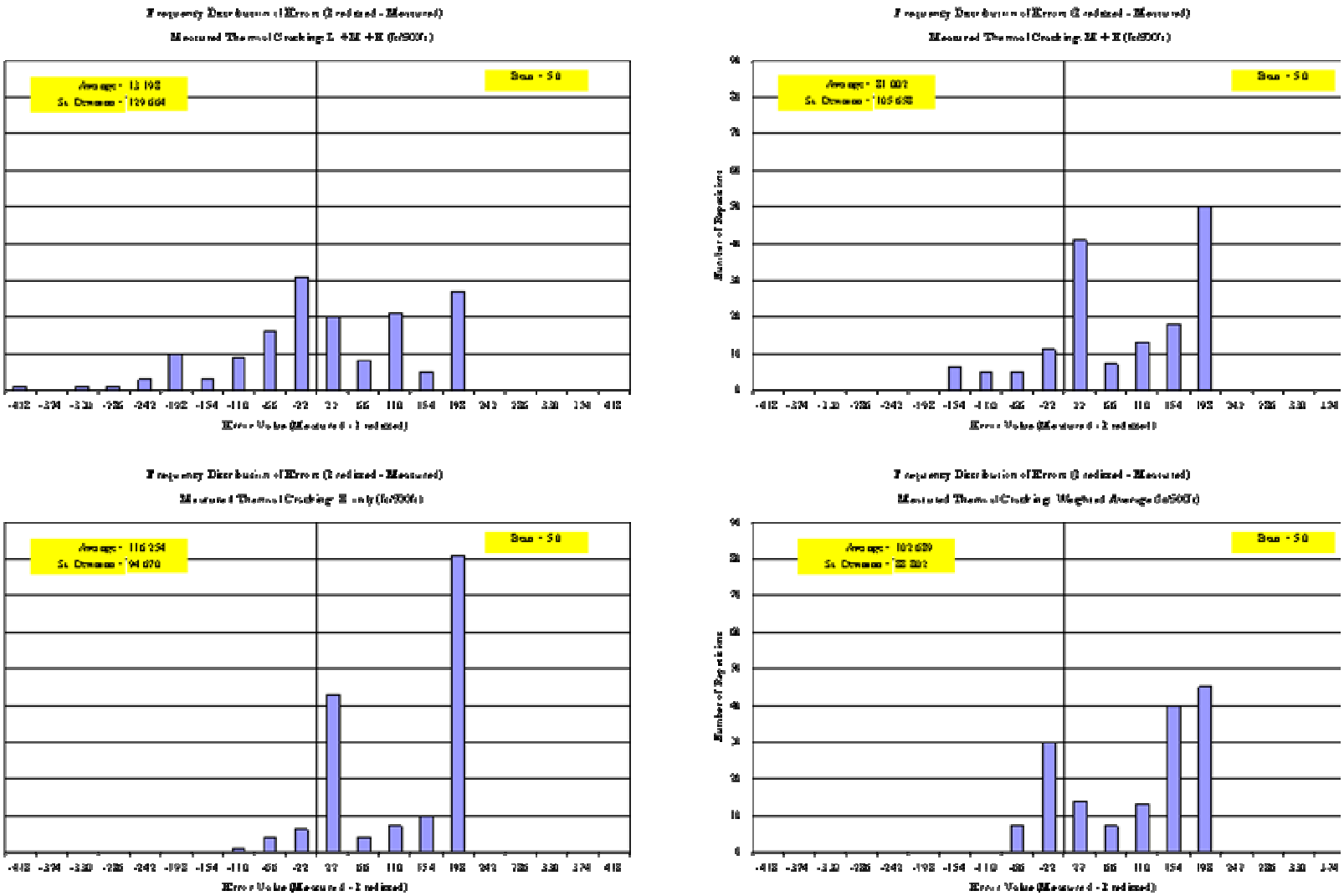

Figure 3.3.28. Summary of frequency distribution for Level 3 analysis with beta factor = 5.0

The second factor that can be considered is the asphalt thickness. Based on the mechanistic methodology used in the thermal cracking predictive module (also see Appendix HH), the thicker the pavement, the longer the crack will take to propagate with depth.

Smoothness Models (IRI)

Several research studies have successfully modeled smoothness using key pavement distress types (*8,12,19*). These studies have found that flexible pavement smoothness can be affected significantly by rutting, rut depth variance, and fatigue cracking.

Many of the distresses that have been correlated to smoothness are load and climate related and are predicted by mechanistic-empirical modeling techniques as outlined in the preceding sections of this chapter (fatigue cracking, permanent deformation, and thermal cracking). Other distresses such as potholes, block cracking, and longitudinal cracking also affect smoothness. However, since current practice does not allow us to model these distresses using mechanistic-empirical principles, in the Design Guide procedure, designers are given the option of directly entering the potential of the occurrence of such distresses while modeling smoothness. In addition, smoothness loss due to soil movements and other climatic factors (depressions, frost heave, and settlement) are also considered in the prediction of smoothness through the use of a "site factor" term (represented by a cluster based on foundation and climatic properties).

The models for predicting IRI for use in new and reconstruction flexible pavement design are a function of the base type as described below. Appendix OO provides a detailed discussion on the development of these models.

Unbound Aggregate Bases and Subbases

$$IRI = IRI_O + 0.0463\left[SF\left(e^{\frac{age}{20}} - 1\right)\right] + 0.00119\left(TC_L\right)_T + 0.1834\left(COV_{RD}\right) + 0.00384\left(FC\right)_T + 0.00736\left(BC\right)_T + 0.00115\left(LC_{SNWP}\right)_{MH} \quad (3.3.74a)$$

where:

IRI	=	IRI at any given time, m/km.
IRI_O	=	Initial IRI, m/km.
SF	=	Site factor (see equation 3.3.74b).
$e^{age/20} - 1$	=	Age term (where *age* is expressed in years).
COV_{RD}	=	Coefficient of variation of the rut depths, percent (assumed to be 20 percent).
$(TC_L)_T$	=	Total length of transverse cracks (low, medium, and high severity levels), m/km).
$(FC)_T$	=	Fatigue cracking in wheel path, percent total lane area
$(BC)_T$	=	Area of block cracking as a percent of total lane area (user input).
$(LC_{SNWP})_{MH}$	=	Length of moderate and high severity sealed longitudinal cracks outside wheel path, m/km (user input).

$$SF = \left(\frac{(R_{SD})(P_{.075}+1)(PI)}{2*10^4} \right) + \left(\frac{\ln(FI+1)(P_{02}+1)\left[\ln\left(R_m+1\right)\right]}{10} \right) \quad (3.3.74b)$$

where:

R_{sd}	=	Standard deviation of the monthly rainfall, mm.
P_{075}	=	Percent passing the 0.075 mm sieve.
PI	=	Percent plasticity index of the soil.
FI	=	Average annual freezing index, ^{o}C-days.
P_{02}	=	Percent passing the 0.02 mm sieve.
R_m	=	Average annual rainfall, mm.

Model statistics:

N	=	353 observations
R^2	=	0.620
$RMSE$	=	0.387 m/km
S_e/S_y	=	0.747

The predicted IRI for HMA pavements over unbound granular bases and subbases at the desired level of reliability is obtained as follows:

$$IRI\_P = IRI + STD_{IRI} \bullet Z_P \quad (3.3.75)$$

$$IRI\_P \leq 100\ \%$$

where,

IRI_P	=	predicted IRI at the reliability level P, m/km.
IRI	=	predicted IRI based on mean inputs (corresponding to 50% reliability), m/km.
STD_{IRI}	=	standard deviation of IRI at the predicted level of mean IRI.
Z_P	=	standard normal deviate.

The standard deviation of IRI for HMA pavements with granular bases and subbases is derived from the variance expression below by taking a square root of the computed variance from individual variances of the terms.

$$\begin{aligned} Var[IRI] &= Var[IRI_0] + \{(0.0367(e^{age/20}) - 0.0367)\}^2 Var[SF] \\ &+ 1.05625\times10^{-5} Var[(FC)_T] + 1.67445\times10^{-5} Var[COV_{RD}] \\ &+ 1.1236\times10^{-6} Var[(TC_L)_T] + 4.9562\times10^{-5} Var[(BC)_T] \\ &+ 2.4336\times10^{-6} Var[(LC_{SNWP})_{MH}] + S_e^2 \end{aligned} \quad (3.3.76)$$

where,

$Var[IRI]$	=	Variance of IRI at the predicted level of mean IRI.
$Var[IRI_0]$	=	Variance of the initial IRI.
$Var[SF]$	=	Variance of the site factor term (estimated using typical values).
$Var[(FC)_T]$	=	Variance of fatigue cracking in wheel path (estimated from fatigue cracking standard deviation model).

$Var[COV_{RD}]$ = Variance of coefficient of variation of the rut depth (estimated using typical values).

$Var(TC_L)_T$ = Variance of total length of transverse cracks (at all severity levels).

$Var[(BC)_T]$ = Variance of area of block cracking (estimated).

$Var[(LC_{SNWP})_{MH}]$ = Variance of length of moderate and high severity sealed longitudinal cracks outside wheel path (estimated using typical values).

S_e^2 = Variance of overall model error = 0.15 $(m/km)^2$.

Asphalt Treated Bases

$$IRI = IRI_O + 0.0099947(Age) + 0.0005183(FI) + 0.00235(FC)_T + 18.36\left[\frac{1}{(TC_S)_H}\right] + 0.9694(P)_H \quad (3.3.77)$$

where:

$(TC_S)_H$ = Average spacing of high severity transverse cracks, m (estimated from thermal cracking model).

$(P)_H$ = Area of high severity patches, percent of total lane area, % (user input).

All other variables are as previously defined.

Model statistics:

N = 428 observations

R^2 = 0.499

RMSE = 0.292 m/km

S_e/S_y = 0.775

The predicted IRI for HMA pavements over asphalt treated bases at the desired level of reliability is obtained in accordance with equation 3.3.75. The standard deviation of IRI for HMA pavements with asphalt treated bases required for equation 3.3.75 is derived from the variance expression below by taking a square root of the computed variance from individual variances of the terms.

$$Var[IRI] = Var[IRI_0] + 3.047 \times 10^{-5} Var[(FC)_T] + \left[\frac{-33.59}{(\overline{TC_S})_H + 1)^2}\right]^2 Var[(TC_S)_H] + 0.90802 Var[P_H] + S_e^2 \quad (3.3.78)$$

where:

$Var[(TC_S)_H]$ = Variance of average spacing of high severity transverse cracks (estimated from thermal cracking model).

$Var[(P)_H]$ = Variance of area of high severity patches (estimated from typical values).

All other variables are as explained previously.

Chemically Stabilized Bases

$$IRI = IRI_o + 0.00732(FC)_T + 0.07647(SD_{RD}) + 0.0001449(TC_L)_T + 0.00842(BC)_T + 0.0002115(LC_{NWP})_{MH} \quad (3.3.79)$$

Where, all the variables are as previously defined.

Model statistics:

N = 50 observations
R^2 = 0.83
RMSE = 0.229 m/km
S_e/S_y = 0.436

The predicted IRI for HMA pavements over chemically stabilized bases at the desired level of reliability is obtained in accordance with equation 3.3.75. The standard deviation of IRI for HMA pavements with chemically stabilized bases required for equation 3.3.75 is derived from the variance expression below by taking a square root of the computed variance from individual variances of the terms.

$$Var[IRI] = Var[IRI_0] + 5.358\times10^{-5}Var[(FC)_T] + 5.848\times10^{-3}Var[SD_{RD}] + 2.0996\times10^{-8}Var[(TC_L)_T] + 7.0896\times10^{-5}Var[(BC)_T] + 4.473\times10^{-8}Var[(LC_{NWP})_{MH}] + S_e^2 \quad (3.3.80)$$

All the variables are as previously defined.

In the Design Guide approach, the mean rut depth is predicted using mechanistic principles over time rather than the variation in rut depth (i.e., COV_{RD} and SD_{RD}), which is used in the smoothness models, discussed above. The models to estimate SD_{RD} of predicted rutting is:

$$SD_{RD} = 0.665 + 0.2126(RD) \quad (3.3.81)$$

where:

SD_{RD} = Standard deviation of rut depths, mm
RD = Mean rut depth, mm

Model statistics:

N = 824 observations
R^2 = 0.404
RMSE = 0.914

IRI Prediction Procedure

The IRI prediction is simple once the distress potential inputs (block cracking and patching) are configured and pavement distress predictions have been completed. The steps for predicting IRI are as follows:

Step1: Predict pavement distresses

- Follow the procedure explained in section 3.3.4.3 to obtain HMA fatigue cracking prediction.
- Follow the procedure explained in section 3.3.4.3 to obtain mean values of total permanent deformation. Obtain standard deviation and coefficient of variation estimates from the predicted mean value as explained previously.
- Follow the procedure explained in section 3.3.4.3 to obtain HMA thermal cracking prediction.

Step 2: Select initial IRI and estimate distress potential

The initial IRI depends on the project smoothness specifications. Typical values of initial IRI range from 50 to 100 in/mi.

Estimate the potential from the following distresses to occur:

- Medium and high severity longitudinal cracking outside the wheel path.
- High severity patching.

Section 3.3.3.6 provides guidance on how to estimate these quantities.

Use the empirical model given in equation 3.4.43 to determine joint spalling.

Step3: Predict IRI

Use the respective IRI models given in equation 3.3.74 through 3.3.81 to predict IRI over the project life.

3.3.5 SPECIAL AXLE CONFIGURATION

In addition to the usual general traffic analysis (mix of single, tandem, tridem, and quad axle vehicles), the flexible pavement design procedure has an alternative traffic procedure for analyzing special axle configuration. The primary intended function of the special axle analysis routine is to structurally analyze the pavement performance due to special, heavy, non-conventional off-road vehicle systems that are often subject to special permitting requirements. This is a very important feature of the Guide because it provides the designer information on the amount of damage that could be caused by single or multiple passes of the special vehicle to the pavement structure. Special vehicles cannot be analyzed along with the general traffic.

The necessary characteristics of the design vehicle that will be needed for the analysis are described below.

Vehicle Designation: Name of design vehicle/gear, used for information purposes only.

Tire Load: Represents the load on a single tire within the gear assembly. It is assumed that the remaining tires in the design gear will have the same load. Only one tire load can be specified for the analysis.

Tire Pressure: Only one tire pressure is used for all tires in the special gear configuration. This will result in the same area of contact for all the tires within the gear.

Annual Average Traffic: Average number of repetition for the initial year. The analysis period and the growth rate are then used to obtain the total number of repetitions. The growth rate is the next input on this screen. The total repetitions over a period of time are used for damage estimation as a function of time. If the user only intends to study the effect of one repetition, 12 repetitions needs to be entered, which will result in one repetition per month. In addition, the user needs to define design life as one month.

Tire Location: In the general traffic analysis, the user does not have a lot of flexibility in terms of wheel locations. But for a special gear, the user can specify up to 10 wheels in the x-y plane.

Analysis Location: For the general traffic analysis, the analysis locations are determined by the Design Guide software internally and are discussed earlier. The user does not have the flexibility to modify the analysis locations. In the case of a special gear configuration, the user can specify up to 10 analysis computation points. The program requires a minimum of one location for analysis. Once the points are specified, a graphical schematic layout of the points can be viewed within the program.

The selection of the analysis points is a function of the distress type. For a rutting analysis, the user might only be interested in the computational points under and between the wheels. No analysis points are needed outside the gear configuration, since the maximum rutting is likely to occur under or between the wheels. This is also true for analyzing bottom-up fatigue cracking. However, in the case of top-down fatigue cracking, the user may be interested in looking at the surface tensile strains outside the gear configuration. The user has the full flexibility to define the analysis locations in contrast to general traffic, whereas for the general traffic analysis locations are internally defined internally by the Design Guide software.

3.3.6 CALIBRATION TO LOCAL CONDITIONS

Any agency interested in adopting the design procedure described in this Guide should prepare a practical implementation plan. The plan should include training of staff, acquiring of needed equipment, acquiring of needed computer hardware, and calibration/validation to local conditions.

The mechanistic-empirical design procedure in this guide represents a major improvement and paradigm shift from existing empirical design procedures (e.g., AASHTO 1993), both in design approach and in complexity. The use of mechanistic principles to both structurally and climatically (temperature and moisture) model the pavement/subgrade structure requires much more comprehensive input data to run such a model (including axle load distributions, improved material characterization, construction factors, and hourly climatic data such as ambient temperatures, precipitations, solar radiation, cloud cover, and relative humidity). Thus, a significant effort will be required to evaluate and tailor the procedure to the highway agency. This will make the new design procedure far more capable of producing more reliable and cost-effective designs, even for design conditions that deviate significantly from previously experienced (e.g., much heavier traffic).

It is important to realize that even the original (relatively simple) AASHTO design procedures, originally issued in 1962 and updated several times since, required many years of implementation by state highway agencies. The agencies focused on obtaining appropriate inputs, applying calibration values for parameters like the "regional" or climatic factor, subgrade support and its correlation with common lab tests, traffic inputs to calculate equivalent single axle loads, and many other factors. In addition, many agencies set up test sections that were monitored for 10 or more years to further calibrate the design procedure to local conditions. Even for this relative simple procedure by today's standards, many years were required for successful implementation by many state highway agencies.

3.3.6.1 Need for Calibration to Local Conditions

Clearly, the Design Guide's mechanistic-empirical procedure will require an even greater effort to successfully implement a useful design procedure. Without calibration, the results of mechanistic calculations (fatigue damage) cannot be used to predict rutting, fatigue cracking, and thermal cracking with any degree of confidence. For fatigue cracking, none of the direct pavement responses (deflection, stress, or strain) can be used directly to predict the rate of crack development because a complex algorithm is required to model the cracking mechanism that produces "damage." This damage must be correlated with actual cracking in the field. The distress mechanisms are far more complex than can be practically modeled; therefore, the use of empirical factors and calibration is necessary to obtain realistic performance predictions.

The design procedure described in the Guide is largely based on mechanistic engineering principles that provide a fundamental basis for the structural design of pavement structures. The flexible pavement design procedures have been calibrated using design inputs and performance data largely from the national LTPP database which includes sections located throughout significant parts of North America. The distress models specifically calibrated included:

- Rutting (asphalt and unbound layers).
- Fatigue cracking (bottom-up and top-down).

- Thermal cracking.

This calibration effort was a major iterative work effort that resulted in distress prediction models with national calibration constants. The calibration curves generally represent "national" performance of flexible pavements in the LTPP database. Whatever bias included in this calibration data is naturally incorporated into the distress prediction models. The initial calibration was based on 80 percent of the data. The models were then "validated" using the remaining 20 percent of the data. Since both models showed reasonable validation, all data was combined to obtain the final comprehensive national calibration models. However, this national calibration may not be entirely adequate for specific regions of the country and a more local or regional calibration may be needed.

The IRI models for flexible pavements are empirical in nature and were developed directly from the available LTPP data. Further validation for a local agency may not be needed, but could be accomplished if desired as described in this section.

3.3.6.2 Approach to Calibration

Because this design procedure is based on mechanistic principles the procedures should work reasonably well within the inference space of the analytical procedure and the performance data from which the procedure was calibrated. However, this is a very complex design procedure and it must be carefully evaluated by highway agencies wishing to implement. The following is the recommended calibration/validation effort required to implement the Design Guide for flexible pavements:

1. Review all input data.
2. Conduct sensitivity analysis.
3. Conduct comparative studies.
4. Conduct validation/calibration studies.
5. Modify input defaults and calibration coefficients as needed.

<u>Review All Input data</u>

All inputs to the Design Guide software should be reviewed with five major goals in mind.

- Determine the desired level for obtaining each input on various types of design projects (low volume as compared to high volume where achieving an adequate design is more critical). The Design Guide allows three levels of inputs and each level has different procedures.
    - Level 1—site-specific testing data such as laboratory testing of soils and materials, FWD testing and backcalculation, and ATC and WIM testing on site.

- Level 2—regional factors and material properties from available testing procedures or correlation equations (e.g., use of CBR to estimate resilient modulus).
- Level 3— typical local values (if known) or default values.

Note that the LTPP data available for the calibration under NCHRP Project 1-37A was a mixture of all levels. Several inputs are very critical but are not well defined and these are the ones where the agency should conduct sensitivity analysis as described below.

- Determine if defaults provided with the Design Guide software are appropriate for the agency and modify if needed.
- Select allowable ranges for inputs for various types of projects within the geographical area of the agency (low volume, high volume, different geographic areas within the state).
- Select procedures to obtain these inputs for regular design projects (e.g., traffic volume and weight inputs). Determine the effects of the accuracy of input values on the resulting design.
- Conduct necessary testing to establish specific inputs (e.g., asphalt concrete dynamic modulus, axle load distributions), acquire needed equipment for any testing required.

Sensitivity Analysis

Each agency should conduct sensitivity analysis of the new design procedure. This is accomplished by selecting a typical design situation with all design inputs. The software is run and the mean distresses and IRI predicted over the design period. Then individual inputs are varied, normally one at a time (unless two or more are correlated and then two or more are varied in unison as would occur in nature) and the change in all outputs observed. Appropriate tables and plots are prepared and the results evaluated. Inputs can be divided into three groups for example:

1. Those that have very significant effect on one or more outputs.
2. Those that have a moderate effect on one or more outputs.
3. Those that have only minor effect on one or more outputs.

Those inputs that belong to group No. 1 must be more carefully selected than No. 3 as they will have a very significant effect on design. The above sensitivity may be repeated for low, medium and high traffic project designs to see if that has an effect on inputs.

Comparative Studies

Conduct comparisons of designs from the Guide procedure with those of the existing procedure. Select typical design situations (previous designs would be ideal) and obtain the design inputs for the Design Guide. Run the Design Guide software and determine the distresses and IRI over the analysis period. Evaluate the adequacy of the design based on the results and agency performance experience. If deficiencies exist in the Design Guide predictions, determine the reasons if possible.

Calibration to Local Conditions

The national calibration-validation process was been successfully completed. Although this effort was very comprehensive, further validation study is highly recommended as a prudent step in implementing a new design procedure that is so different from current procedures. A validation database should be developed to confirm that the national calibration factors or functions are adequate and appropriate for the construction, materials, climate, traffic, and other conditions that are encountered within the agencies highway system.

Prepare a database of agency performance data and compare the new design procedure results with the performance of these "local" sections. This will require the selection of at least 20 flexible pavement sections around the state. If the state has very distinct climates this should be done in each climate.

The goal of the calibration-validation process is to confirm that the performance models accurately predict pavement distress and ride quality on a national basis. For any specific geographic area, adjustments to the national models may be needed to obtain reliable pavement designs.

Modify the Calibrations/Inputs

If significant differences are found between the predicted and measured distresses and IRI for the agencies highways, appropriate adjustments must be made to the performance models. This study will also establish the level of accuracy desirable for key input parameters and default input values. Make modifications to the new procedure as needed based on all of the above results and findings.

REFERENCES

1. Mallela, J., H. Von Quintus, L.Titus-Glover, M.E. Ayers, A.E. Eltahan, S.P. Rao, W.O. Tam. "Introduction to Mechanistic-Empirical Pavement Design," *Reference Manual*, NHI Course 131064, Publication No. NHI-02-048, National Highway Institute, Federal Highway Administration, Washington, D.C., March 2002.
2. Barksdale, R., "Laboratory Determination of Resilient Modulus for Flexible Pavement Design: Final Report", NCHRP Web Doc 14, National Cooperative Highway Research Program, Washington DC, 1997.
3. HRB (1962) *The AASHO Road Test*, Report 5: Pavement Research; Report 6*: Special Studies* and Report 7: Summary Report, Highway Research Board.
4. Shell, 1978. Shell Pavement Design Manual – Asphalt Pavements and Overlays for Road Traffic, Shell International Petroleum. London.
5. Huang, Y.H. (1993) *Pavement Analysis and Design*, Prentice-Hall, Inc., Englewood Cliffs, NY.
6. Asphalt Institute (1991) *DAMA (CP-1/1991 Revision)—Pavement Structural Analysis Using Muli-Layered Elastic Theory*, Lexington, KY.
7. Leahy, R.B., *Permanent Deformation Characteristics of Asphalt Concrete*, Ph.D. Dissertation, University of Maryland, College Park, 1989.
8. Ayres, M. and Witczak, M. (1998) "AYMA – A Mechanistic Probabilistic System to Evaluate Flexible Pavement Performance", Transportation Research Board, 77th Annual Meeting, Paper No.980738, Washington, D.C.
9. Kaloush, K. E. and Witczak, M. W. (2000). "Development of a Permanent to Elastic Strain Ratio Model for Asphalt Mixtures". *Development of the 2002 Guide for the Design of New and Rehabilitated Pavement Structures. NCHRP 1-37 A.* Inter Team Technical Report. Sept. 2000.
10. Tseng, K. and Lytton, R. (1989) *Prediction of Permanent Deformation in Flexible Pavement Materials.* Implication of Aggregates in the Design, Construction, and Performance of Flexible Pavements, ASTM STP 1016, ASTM, pp. 154-172.
11. Ayres, M. (1997) *Development of a Rational Probabilistic Approach for Flexible Pavement Analysis*, Ph.D. Dissertation, University of Maryland, College Park, MD.
12. Carey, W.N. and P.E. Irick (1990) *The Pavement Serviceability–Performance Concept*. Highway Research Bulletin 250. Washington, DC: Highway Research Board.
13. Asphalt Institute. 1991. Thickness Design – Asphalt Pavements for Highways and Streets. Manual Series No.1 (MS-1), Lexington, KY.
14. Schapery, R. A., "A Theory of Crack Growth in Viscoelastic Media," ONR Contract No. N00014-68-A-0308-003, Technical Report No. 2, MM 2764-73-1, Mechanics and Materials Research Center, Texas A&M University, College Station, Texas, March 1973.
15. Lytton, R. L., Shanmugham, U., and B. D. Garrett, "Design of Asphalt Pavements for Thermal Fatigue Cracking, Research Report No. FHWA/TX-83/06+284-4, Texas Transportation Institute, Texas A&M University, College Station, Texas, January 1983.

16. Molenaar, A.A.A., "Fatigue and Reflection Cracking Due to Traffic Loads," Proceedings of the Association of Asphalt Paving Technologists, Vol. 53, pp. 440-474, 1984.
17. Roque, R. and W.G. Buttlar, "Development of a Measurement and Analysis System to Accurately Determine Asphalt Concrete Properties Using the Indirect Tensile Test," Journal of the Association of Asphalt Paving Technologists, Vol. 61, pp. 304-332, 1992.
18. Paterson, W. D. O. (1989) "A Transferable Causal Model for Predicting Roughness Progression in Flexible Pavements." *Transportation Research Record 1215*. Washington, DC: Transportation Research Board.
19. *ILLI-PAVE PC Version User's Manual* (1990), NCHRP Project 1-26, Transportation Facilities Group, University of Illinois, Urbana-Champaign, IL.
20. Schwartz, C.W. (2000) "Implementation of a Nonlinear Resilient Modulus Constitutive Model for Unbound Pavement Materials," *Proceedings, 10th International Conference on Computer Methods and Advances in Geomechanics*, Tucson, AZ, January, 2001 (in press).
21. Schwartz, C.W. (2000) "Effect of Stress-Dependent Base Layer on the Superposition of Two-Dimensional Flexible Pavement Solutions," *Proceedings, 2nd International Conference on 3D Finite Elements for Pavement Analysis, Design, and Research*, Charleston, WV, October (in press).
22. Ullidtz, P., and Peattie, K.R. (1980) "Pavement Analysis by Programmable Calculators," *Transportation Engineering Journal*, ASCE, Vol. 106, No. TE5.
23. Thompson, M. R. and E. J. Barenberg, "Calibrated Mechanistic Structural Analysis Procedures for Pavements, Final Report, NCHRP Project 1-26, National Cooperative Highway Research Program, Washington DC, 1990.
24. Ullidtz, P. (1998) *Modelling Flexible Pavement Response and Performance*, Polyteknisk Forlag, Denmark.
25. Burmister, D.M. (1943) "The Theory of Stresses and Displacements In Layered Systems and Applications to the Design of Airport Runways," *Proceedings, Highway Research Board*, Vol. 23.
26. Zienkiewicz, O.C. (1977) *The Finite Element Method*, McGraw-Hill, New York.
27. Al-Omari, B. and M.I. Darter (1992) Relationships Between IRI and PSR. Report Number UILU-ENG-92-2013. Springfield, IL: Illinois Department of Transportation.
28. Smith, K.L., K. D. Smith, L.D. Evans, T.E. Hoerner, and M.I. Darter (1997) *Smoothness Specifications for Pavements*. Final Report. NCHRP 1-31, Washington, DC: Transportation Research Board.
29. Darter, M.I. and E.J. Barenberg (1976) *Zero-Maintenance Pavements: Results of Field Studies on the Performance Requirements and Capabilities of Conventional Pavement.* Report No. FHWA-RD-76-105, Washington, DC: Federal Highway Administration.
30. Owusu-Antwi, E.B., L. Titus-Glover, L. Khazanovich, and J. R. Roesler (1997) "Development and Calibration of Mechanistic-Empirical Distress Models for Cost Allocation." Final Report, Washington, DC: Federal Highway Administration.
31. Kajner, L., M. Kirlanda, and G. Sparks (1990) "Development of Bayesian Regression Model to Predict Hot-Mix Asphalt Concrete Overlay Roughness." *Transportation Research Record 1539*. Washington, DC: Transportation Research Board.